UNIVERSITY OF CALIFORNIA

Santa Barbara

# Economic and Environmental Implications of Low-carbon Transition in Energy System: Case Studies on Lighting Technologies, Electricity System, and Direct Air Capture

A dissertation submitted in partial satisfaction of the

requirements for the degree Doctor of Philosophy

in Environmental Science and Management

By

Yang Qiu

Committee in Charge:

Professor Sarah Anderson, Chair

Professor Eric Masanet

Professor Ranjit Deshmukh

September 2022

The dissertation of Yang Qiu is approved.

_____

Eric Masanet

_____

Ranjit Deshmukh

_____

Sarah Anderson, Committee Chair

September 2022

Economic and Environmental Implications of Low-carbon Transition in Energy System:

Case Studies on Lighting Technologies, Electricity System, and Direct Air Capture



by

Yang Qiu

ACKNOWLEDGEMENTS

My five-year PhD journey is almost at the end. Standing at this turning point of my life and reflecting the past five years, I feel very grateful for the helps I received from many people. Firstly, I would like to thank my faculty advisor Prof. Sangwon Suh, who inspired me to think big scientific questions, gave me hard times to make me grows, and guided me to be an independent researcher. I also thank my committee members, Prof. Sarah Anderson, Prof. Eric Masanet, and Prof. Ranjit Deshmukh, who generously provided constructive feedback on my research and opportunities to improve my teaching skills. My gratitude further extends to Dr. Patrick Lamers, Dr. Vassilis Daioglou, Prof. André Bardow, and Dr. Stuart Cohen and all other collaborators, who helped me tremendously and made my PhD journey more diverse.

I want to give thanks to my lab mates, Jiajia Zheng, Haozhe Yang, Mengya Tao, Yuwei Qin, Runsheng Song and Jessica Vieira, for providing a competitive and enjoyable office vibe in which we all grow and share joyful moments together. I also appreciate the inclusive environment and valuable resources offered by the whole Bren community that allowed me to conduct interdisciplinary research and interact with smart people from different backgrounds.

Last but not least, I would like to give my special thanks to my beloved parents and other family members in China. It was your care, support, and love that made me thrive and achieve important milestones in my life. I also thank my wife, Dr. Ran An, who has been sharing the happiness and hardships with me along the way and giving me encouragement and support.

All the technical skills and lessons I have learned during my PhD journey have made me prepared to enter the next stage of my life. As a scientific researcher, I will keep dedicating myself to the mission of using science to better understand the environmental issues we are facing and how human beings can move to a more sustainable and environmental-friendly world.

VITA OF YANG QIU
May 2022

## EDUCATION

Ph.D., Environmental Science & Management Jun 2022
*University of California, Santa Barbara*

M.S., Environmental Science May 2017
*State University of New York, College of Environmental Science and Forestry (SUNY-ESF)*

M.S., Applied Statistics May 2017
*Syracuse University*

B.S., Forestry Resources Conservation and Recreation Jul 2013
*Beijing Forestry University*

## PUBLICATIONS

- **Yang Qiu**, Stuart Cohen, Sangwon Suh. "Decarbonization scenarios of the U.S. electricity system and their costs." (In Review)
- **Yang Qiu**, Patrick Lamers, Vassilis Daioglou, Noah McQueen, Harmen-Sytze de Boer, Mathijs Harmsen, Jennifer Wilcox, André Bardow, Sangwon Suh. "Environmental trade-offs of direct air capture in climate change mitigation toward 2100." (Accepted by *Nature Communication*)
- Shoki Kosai, Arnidah Binti Badin, **Yang Qiu**, Kazuyo Matsubae, Sangwon Suh, and Eiji Yamasue. "Evaluation of resource use in the household lighting sector in Malaysia considering land disturbances through mining activities." *Resources, Conservation and Recycling* 166 (2021): 105343.
- Qiao-Chu Wang, Peng Wang, **Yang Qiu**, Tao Dai, and Wei-Qiang Chen. "Byproduct Surplus: Lighting the Depreciative Europium in China's Rare Earth Boom." *Environmental Science & Technology* 54, no. 22 (2020): 14686-14693.
- Ali Chamas, Hyunjin Moon, Jiajia Zheng, **Yang Qiu**, Tarnuma Tabassum, Jun Hee Jang, Mahdi Abu-Omar, Susannah L. Scott, and Sangwon Suh. "Degradation rates of plastics in the environment." *ACS Sustainable Chemistry & Engineering* 8, no. 9 (2020): 3494-3511.
- **Yang Qiu**, and Sangwon Suh. "Economic feasibility of recycling rare earth oxides from end-of-life lighting technologies." *Resources, Conservation and Recycling* 150 (2019): 104432.
- **Yang Qiu**, Timothy Volk. Nutrient Status of Willow Growing on a Former Industrial Site Amended with Organic Materials. Master Thesis. 2017. State University of New York College of Environmental Science and Forestry.

- Xue Zhang, Lu-Shuang Gao, **Yang Qiu**, Jing Guo. Characteristics of Korean Pine (Pinus koraiensis) Radial Growth at Different Heights and Its Response to Climate Change on Changbai Mountain. *Acta Ecologica Sinica*, 35, no. 9 (2015): 2978-2984.
- **Yang Qiu**, Lu-Shuang Gao, Xue Zhang, Jing Guo, and Zhi-Yuan Ma. Effect of Climate Change on Net Primary Productivity of Korean Pine (Pinus koraiensis) at Different Successional Stages of Broad-leaved Korean Pine Forest. *The Journal of Applied Ecology*, 25(7). (2014): 1870-1878.

## RESEARCH EXPERIENCE

Graduate Student Researcher Sep 2017 – Present
*University of California, Santa Barbara, USA*

Graduate Intern Jun – Dec, 2020
*National Renewable Energy Laboratory (NREL), USA*

Visiting PhD Student Jun – Sep, 2019
*RWTH Aachen University, Germany*

Graduate Research Assistant Sep 2014 – May 2017
*SUNY-ESF, USA*

## TEACHING AND MENTORING EXPERIENCE

Teaching Assistant Jan 2021 – Present
*University of California, Santa Barbara, USA*

Graduate Mentor May 2021– Present
*University of California, Santa Barbara, USA*

Teaching Assistant Aug – Dec, 2016
*SUNY-ESF, USA*

## ACADEMIC CONFERENCE

- Oral Presentation – Environmental trade-offs of direct air capture in climate change mitigation toward 2100. The Fourteenth IAMC Annual Meeting, 12/2021.

- Oral Presentation – Environmental trade-offs of applying direct air capture technologies in industrial and transportation sectors. American Center for Life Cycle Assessment 2020 Virtual Conference, 09/2020.
- Oral Presentation – Economic feasibility of recycling rare earth oxides from end-of-life lighting technologies. 10th International Conference on Industrial Ecology. 08/2019. Beijing, China.
- Oral Presentation – Economic feasibility of recycling rare earth oxides from end-of-life lighting technologies. 13th Society and Materials International Conference. 05/2019. Pisa, Italy.
- Poster – Rare earth elements demand and recycling in efficient lighting technologies. Gordon Research Conference on Industrial Ecology. 05/2018. Les Diablerets, Switzerland.

ABSTRACT

Economic and Environmental Implications of Low-carbon Transition in Energy System: Case Studies on Lighting Technologies, Electricity System, and Direct Air Capture

by

Yang Qiu

The decarbonization of energy system plays a fundamental role in global climate change mitigation efforts, and it entails unprecedented infrastructural transformations across the whole energy supply chain and the end uses as well as large scale deployment of emerging low-carbon technologies. In addition to the carbon mitigation potential, it is also critical to comprehensively assess other sustainability dimensions of the decarbonization actions.

Techno-economic analysis (TEA) and life cycle assessment (LCA) are two main methods that are used to quantify the economic and environmental performances for energy system technologies, respectively. However, applying these methods at technology-level is limited to capture the dynamic system contexts and their effect on the technology performances. The main contribution and novelty of this dissertation is that it evaluated the economic and/or environmental implications of decarbonization actions in the energy system by linking the relevant methods with scenario analysis and/or system modeling approaches. This methodology integration makes it possible to capture the effects of system interaction and evolution on the performance of decarbonization actions.

A transition to energy-efficient lighting technologies (e.g., fluorescent and light-emitting diode (LED) lightbulbs) assist climate change mitigation by reducing energy consumption. In Chapter II, I studied the uses and recycling of critical rare earth oxides (REOs) in the efficient lighting technologies. The demand for REOs in the lighting sector shows a rapid increase during 1990 and 2014 driven by the global adoption of fluorescent lightbulbs, but this increasing trend decreases after the peak as more efficient LED lightbulbs (that requires significant less REO consumption than fluorescent lightbulbs) penetrated the market and replaced fluorescent lightbulbs. The REO recycling from end-of-life lighting technologies are not economically feasible under 2018 REO prices, even though economy of scale can reduce recycling cost by two third as plant capacity increases from 100 t/yr to 1,500 t/yr, highlighting that the improvement of REO recycling rate may need higher REO prices or commensurate policy interventions.

In Chapter III, I quantified the total system cost of the U.S. electric power system under different decarbonization scenarios based on the capacity expansion and dispatch outputs from an electricity system optimization model. I found pursuing zero $CO_2$ emission by replacing fossil fuel with renewable and other low-carbon energy sources would incur $335–$494 billion additional cost (5% discount rate, 2020 US$) to the U.S. electricity system during 2020–2050 (compared to a reference scenario). Additionally, the marginal costs of mitigating the last few percent $CO_2$ emission from the U.S. electricity system could exceed the costs of some carbon dioxide removal (CDR) solutions, such as bioenergy with carbon capture and storage (BECCS) and direct air carbon capture and storage (DACCS), indicating their potential opportunity to decarbonize the electricity system.

In Chapter IV, I evaluated the prospective environmental performance of DACCS which is a CDR solution that deliberatrely removes carbon dioxide ($CO_2$) from atmosphere. I found decarbonizing the electricity sector leads to environmental trade-offs for DACCS by increasing its terrestrial ecotoxicity and metal depletion levels both by an average of 56% from 2020 to 2100, but these increases can be reduced by improving the material and energy use efficiencies of DACCS as it scales up. Also, DACCS deployment aids the achievement of long-term climate targets, its environmental and climate performance however depend on sectoral mitigation actions, and thus DACCS deployment should not suggest a relaxation of sectoral decarbonization targets.

This dissertation provides robust and reliable insights for the low-carbon transition in energy system by evaluating the economic and environmental performances of decarbonization actions in dynamic system contexts. Decarbonization actions in the energy system could lead to economic and environmental trade-offs which should be carefully studied and considered in policy decisions. Future studies and policies may also rely on multi-criterion decision analysis to decide how to implement a variaty of decarbonization actions in energy system based on the optimization of different sustainability dimensions.

TABLE OF CONTENTS

# I. Introduction

## *A. Background*

The increasing anthropogenic greenhouse gas (GHG) emission has been the dominant cause of global average temperature rise since the pre-industrial time. To avoid severe and irreversible impacts of global warming on human and nature systems, international consensus has been formed to limit global temperature rise (relative to pre-industrial levels) to well below 2 °C and pursue efforts to meet a 1.5 °C target by 2100 under the Paris Agreement[1]. These ambitious climate targets require rapid reduction of GHG emissions from a wide range of social-economic sectors and even deliberate carbon dioxide removal (CDR) from the atmosphere[2,3].

The energy system (including energy supply and end uses) is the single largest contributor to global GHG emission, with its $CO_2$ emission reaching 38 Gt $CO_2$/yr in 2019 and accounting for approximately two-thirds of annual global anthropogenic GHG emissions (59 Gt $CO_2$ eq in 2019)[4]. Therefore, a rapid and sweeping transition of energy system to net-zero GHG emission by mid-century plays a fundamental role for achieving the stringent climate targets[5]. Decarbonizing the energy system requires unprecedented infrastructural transformations across the whole energy supply chain and the end uses, including: (1) Adoption of variable renewable and low-carbon energy sources in the power sector; (2) Improvements in energy generation and use efficiency, (3) Electrification of energy end uses, and (4) Application of carbon management with CDR solutions[6,7].

Although climate mitigation actions alleviate global warming, they also face other economic or non-climate environmental challenges. For example, the cost of energy generation of renewable solar and wind have reduced dramatically in recent year[8], leading to their rapid-

growing deployment worldwide to decarbonize the electricity system[9]. But, due to the temporal variability and unpredictability of renewable solar and wind resources, further increase of their penetrations in the electricity system may lead to higher fluctuation of energy output and higher forecasting errors. These challenges require the electricity system to add more back-up capacity and balancing services to maintain the system reliability and stability, which impose additional integration cost on the electricity system[10,11]. In the energy demand side, low-carbon transition in the lighting sector is driven by the application of more energy-efficient lighting technologies, such as fluorescent and light-emitting diode (LED) lightbulbs. Compared to inefficient incandescent lightbulbs, fluorescent and LED lightbulbs need a wider variety of metals in their components to achieve high performance, but the increased material complexity can potentially cause adverse environmental impacts[12] and pose challenges for sustainable waste management[13] at the products' end of life. CDR solutions contribute to climate mitigation by removing carbon dioxide from the atmosphere. However, BECCS is likely to cause competition for natural and agriculture land[14], pose risks for food production[15,16] and biodiversity[17]. DACCS, which separate highly dilute carbon dioxide from air through chemical or physical processes, may requires substantial amount of energy and material inputs for its operation, leading to possible adverse environmental impacts[18–20]. Due to these potential concerns and risks, large-scale deployment of these CDR solutions still remains uncertain.

Given the wide variety of economic and environmental challenges related to decarbonization actions, it is critical to comprehensively evaluate other sustainability dimensions (beyond the goal of carbon mitigation) of these actions, especially for those emerging technologies that are not yet commercialized.

Techno-economic analysis (TEA) and life cycle assessment (LCA) are two main methods that are used to quantify the economic and environmental performances of technologies in energy system, respectively[21]. At the technology level, TEA evaluates the cost and revenue based on economic data and input parameters under specific technical and financial assumptions. Such analysis can provide useful information about average economic performance of the technology or support project-specific policy and investment decisions that are restricted to the parameter assumptions[21]. In the energy system, levelized cost of energy (LCOE) is a common metric that is used to estimate and compare the energy generation costs of different technologies in TEA. LCOE is calculated by averaging the life-cycle total costs (present value) of an energy generating technology by its life-cycle energy outputs[22]. In the literature, many studies that report the rapid cost reductions of renewable energy technologies and their economic advantages compared conventional fossil fuels are mostly based on the evaluation of their LCOE[8,23,24]. Some studies incorporate the variability of economic data and input parameters to capture the uncertainty of LCOE under different technological, financial, and geographical contexts[8,25]. However, LCOE still faces some limitations, with one main being that the calculation of LCOE is based on static technical parameters (e.g., capacity factor and energy efficiency) and focuses on technology level, so it does not capture the effects of system operation dynamics and system integration on the energy cost. In the power system, the electricity demand is not homogenous in time, instead, it fluctuates widely on time scales of minutes up to season, so some generation technologies (also called dispatchable generation sources), such as coal, natural gas, hydropower, etc., need to adjust their power outputs to maintain electricity supply-demand balance all time. In addition, the electricity generation from variable renewable solar and wind are driven by weather and the diurnal cycle of the sun, so as these VRE sources increase their shares in power grid mix, the

power output variations of dispatchable sources become even more drastic, causing the so-called the "Duck Curve"[26]. The variation of power outputs (depending on the demand and supply situation) affects the value of the generated energy, which however, is not considered in the LCOE[27]. Second, the power system transition does not simply imply a one-to-one replacement of VRE sources and conventional fossil fuel sources. Due to the intermittency of VRE, additional dispatchable capacity is needed as operating or backup reserve, which is made available either on-line or on-standby so that it can be called on to generate electricity when supply-demand balance is interrupted due to unpredictability or variability of the conditions[28]. The costs of installing, maintaining, and operating these backup reserve are not considered in the LCOE either[29]. Given the limitation of LCOE, it is insufficient to evaluate the economic competitiveness of energy system technologies and it also falls short of evaluating the real potential and economic implication of adopting renewable energy technologies in the power system transition.

LCA, on the other hand, quantifies the potential environmental impacts of the product or service throughout its entire life cycle which spans from raw material extraction through production, transportation, use, end-of-life treatment. A traditional LCA (also called attributional LCA, or ALCA) focuses on the immediate physical flows within the technology-specific system boundary, and the environmental impacts are typically estimated based on average physical flow data of each unit process and a linear relationship between the inputs and outputs of the system[30]. Generally speaking, ALCA approach catches a "snapshot" of the average environmental impacts of a technology system based on an existing and static supply chain and identifies the environmental hotspot throughout life cycle stages, but they are limited in revealing how environmental impacts of the studied object may change in a future-oriented manner. The real

world is a dynamic and interacting system. A technology at different deployment scales and technology readiness level (TRL) could have different material and energy use efficiencies due to learning and economy of scale[31–33], and technology transition and innovation may also occur in the upstream and downstream supply chains over time[34,35]. All these factors could potential change the environmental impacts of the studied object by following non-linear projections with material and energy inputs over long-term period[36].

Given the limitations of technology-level TEA and LCA mentioned above, there is a need to link these economic and environmental assessment methods with scenario analysis or system-level modeling approach to evaluate the performance of decarbonization actions in a dynamic system context.

Energy system models are mathematical models that provide holistic analysis and evaluations on energy system planning and operations by integrating energy system characteristics with economic parameters, environmental regulations, and policy targets[37,38]. In the past decade, a variety of energy system models has been developed to serve different purposes. For example, some models focus on long term evolution of energy system and support investment decision and planning, and this type of model typically covers a time span of several decades, but with coarse temporal resolution in each year (i.e., a year is typically represented by several so-called “time slices”), while others only cover one or several years with high intra-annual resolution (e.g., minutes or hours), enabling the model to analyze the operational decision and unit commitment of different energy system technologies under dynamic situations. Also, the geographical coverage of these models varies from analyzing single projects or individual buildings to modelling the energy system at the national or global level. Additionally, depending on the methodology, energy system models are also divided into optimization, simulation, and

equilibrium models. Optimization models are expected to identify the optimal solution through a pre-defined objective function (e.g., minimizing total system cost) based on a set of constraints that consists of energy system operation characteristics, resources availability, and environmental regulations, etc. One the other hand, the purpose of simulations models is to estimate and analyze a variety of possible scenarios or pathways of energy system as a result of different combinations of key parameters related to cost, emission, energy demand, and technologies options, etc. Instead of finding an optimal solution, simulation models provide several alternative routes and end states with dissimilar strengths and weaknesses, leaving it to the users to make decisions on the basis of a variety of considerations. Equilibrium models take an economic approach, and they model the energy sector as a part of the whole economy and study how it relates to and interacts with the rest of the economy. Such models, therefore, can be used to evaluate the policy implications on energy system development in a broader context of the whole economy[39,40].

A growing number of energy system models nowadays incorporate economic metrics, to understand the economic implication of energy system transition[10,41–44]. Compared to technology-level TEA, the economic analysis based on energy system models takes into account a broader range of technological, economic, environmental, and policy aspects of the energy system and also captures the complex interactions within the energy system as well as between the system and the rest of the economy, such a comprehensive modeling approach allows for more robust and reliable analysis to assist policy decisions on future energy system transition.

LCA has also been improved to capture the change of environmental impacts based prospective LCA frameworks. Prospective LCA deals with changes of environmental impacts incurred by the technological improvement and transition that happens both in the studied object itself or along its supply chain over long-term time period. Prospective LCA typically consider

and evaluate a broad ranges of technology alternatives that can provide a similar function, and it also incorporates the predictive scenarios that informs how technological improvement (e.g., change of material and energy use efficiency due to technology learning and economy of scale) and transition (e.g., low-carbon transition in the energy system) occurs over long term period[45]. Recently, a growing number of prospective LCA studies have incorporated scenarios from integrated assessment model (IAM)[35,46–48], and these scenarios projects technical and economic characteristics of the industrial metabolism that considers natural resources constraints, existing infrastructure, and climate policy targets. Hence, these methodological improvements in LCA provide the basis for more realistic and robust assessment for the environmental impacts of emerging technologies under specific long-term climate change mitigation pathways.

### *B. Objective and organization of this dissertation*

In this dissertation, the main objective is to assess and reveal the economic and environmental implications of low-carbon transition in the energy system. To achieve this objective, I have linked material flow analysis, TEA, and LCA with scenario analysis and/or system modeling approaches to study different decarbonization actions in the energy system, including energy-efficient transition of lighting technologies, decarbonization of electric power sector, and DACCS. This methodology integration makes it possible to capture the effects of system interaction and evolution on the performance of decarbonization actions. This dissertation includes the following three chapters and is then concluded with a summary:

The Chapter II focuses on the uses and recycling of critical rare earth elements in the lighting sector as it transitions towards more energy-efficient lighting technologies (e.g., fluorescent and LED lightbulbs). In this chapter, I quantified demand and end-of-life flows of rare earth oxides (REO) in the lighting sector by linking a dynamic material flow analysis with future projections

of lighting technologies under different scenarios. Then, I further assessed how economy of scale affects the cost-and-benefit of REO recycling in the lighting sector based on our estimated end-of-life REO flows and technology learning curve approaches.

In Chapter III, the capacity expansion and dispatch of the U.S. electric power system were modelled under different decarbonization scenarios using an electricity system optimization model. Based on the model outputs, I quantified the total system cost of decarbonizing the U.S. electric power system from 2020 to 2050. The electricity technologies that contribute to the system cost and its regional variation were also identified. I further converted the system costs and $CO_2$ emissions into $CO_2$ abatement costs for the decarbonization scenarios, and compared them with social cost of carbon and levelized cost of two CDR solutions (BECCS and DACCS). The comparison provides insights for the cost-benefit of reaching zero-carbon electricity system and the potential opportunity of adopting CDRs to mitigate the $CO_2$ emission from the U.S. electricity system.

The Chapter IV evaluated the environmental trade-offs of DACCS technologies under climate change mitigation contexts based on a prospective LCA framework. This framework is linked with a IAM that provides the future transition pathways of electricity system and the projections of DACCS deployment at four global regions (U.S., China, Russia, and Western Europe) and the overall world under the 1.5°C climate targets. This linkage makes it possible to study the prospective environmental impacts of DACCS by considering the effects of electricity system transition and the economy of scale and learning of DACCS. In addition, I also quantified the prospective environmental impacts of electricity generation under the scenarios with and without DACCS deployment to assess the effect of DACCS on the decarbonization pathway of electricity system.

This dissertation is ended with a summary of the main findings from the three chapters and a higher level conclusion of the whole dissertation.

## II. Economic feasibility of recycling rare earth oxides from end-of-life lighting technologies

Material from:

Qiu, Y., & Suh, S. (2019). Economic feasibility of recycling rare earth oxides from end-of-life lighting technologies. *Resources, Conservation and Recycling*, 150, 104432.

https://doi.org/10.1016/j.resconrec.2019.104432



**Abstract.** Transition to efficient lighting technologies, such as fluorescent and LED lamps, is an important strategy to mitigate climate change. However, it also increases the demand for critical materials such as rare earth oxides (REOs). While recycling can alleviate the dependence on primary REOs, recycling these materials from lighting technologies is currently economically infeasible, limiting its adoption. As more REOs will become available for recycling, the economy of scale is expected to reduce the cost, therefore improving their circularity. Here we analyze the effects that the scale of recycling operation and REO prices have on the economic feasibility of REO recycling using dynamic material flow analysis and technology learning curve approaches. Our results show that end-of-life REOs from lighting technologies are expected to peak between 2020 and 2027. Increasing recycling plant capacity can reduce cost from about $7,200/t REO phosphors at 100 t/yr capacity to about $2,500/t REO phosphors at 1,500 t/yr capacity. Nevertheless, we found that REO recycling would not be economically feasible under 2018 REO prices, irrespective of scale. For a plant at 800 t/yr capacity, recycling becomes profitable only after a threefold increase from 2018 REO prices. The break-even point can be further reduced at a larger scale. Our results suggest that scaling-up recycling plants in the course

of growing volume of end-of-life lighting technologies alone will not automatically increase REO recycling under current market conditions. Significant improvement of REO recycling rate in lighting technologies would therefore require substantially higher REO prices or commensurate policy interventions.

### *A. Introduction*

Lighting technologies are undergoing an energy-efficiency transition[49,50]. Transition from incandescent lightbulbs to fluorescent lamps (FLs), including compact fluorescent lamps (CFLs) and linear fluorescent lamps (LFLs), started in the 1990s, thanks to their high energy efficiency, long lifetime, affordable prices, and the worldwide phase-out of incandescent lightbulbs[51,52]. Globally, FLs accounted for 60% of newly installed lamps in 2015[53]. In recent years, as light-emitting diodes (LEDs) have become affordable enough for general lighting, LEDs are expected to replace FLs and become the dominant lighting technology[53–55]. Compared to incandescent lightbulbs, FLs usually have higher luminous efficacy of 60 to 95 lm/W, and longer lifetime of 8,000 to 10,000 hours, and LEDs even show better performance compared to FLs, with the luminous efficacy of 90 to 120 lm/W and lifetime over 15,000 hours[50,51]. Lighting is responsible for about 15% of global electricity consumption (3300 TWh/yr) and 4.6% of greenhouse gas (GHG) emissions (1400 Mt $CO_2$ eq/yr)[56]. According to a recent UNEP report, the transition to more efficient LEDs would lead to an electricity consumption reduction of 800TWh/yr and GHG emission reduction of 390 Mt $CO_2$ eq/yr by 2030[50].

Despite the energy and environmental benefits of efficient lighting technologies, they increase the consumption of a variety of metals including aluminum, barium, copper, gallium iron, lead, nickel, zinc, and rare earth elements (REE). FLs contains higher amount of copper, lead, zinc and REEs, while LED contains higher amount of aluminum, barium gallium and silver[12]. Within these metals, the REEs are considered as critical materials worldwide, and the US Department of Energy ranked several rare earth elements (Yttrium, Europium, Terbium, Neodymium, and Dysprosium) as critical metals, indicating their high importance to clean energy and the high supply risk[57]. In the efficient lighting technologies, rare earth oxides (REOs)

are used to produce phosphors of FLs and LEDs[58]. The type and amount of REOs required by FLs and LEDs vary among different technologies. FLs use a thin layer of trichromatic phosphors coating inside the glass tube, which converts ultraviolet lights to visible white light[59,60]. For LEDs, a yellow phosphor is often used to convert blue LED light into white light, while other combinations are also in use[61,62]. The use of REOs in phosphors for lighting technologies accounted for 10% of total market demand and 18% economic value in the rare earth market in 2013[63].

Currently, supply security of rare earth elements (REEs) is uncertain. China dominates global REE mining, processing and refining, raising concerns on potential supply interruptions[61,63]. The global shortage of REE supply and corresponding price hikes during 2009 to 2011, for example, was ignited by the Chinese restriction of REE export quotas[59,64,65]. The "balance problem" is another reason causing REE supply tensions; the elementary compositions of REEs found in natural deposits vary significantly, and they usually do not match with the proportion of REEs demanded by the market, causing surpluses of some REEs while shortages of others, which is reflected in the drastic disparity of their prices[66,67].

Recycling is considered as a strategy to mitigate the supply risk of critical materials, especially for the countries that depend heavily on imported resources[68]. Recycling REOs from end-of-life (EoL) lighting technologies as a secondary supply requires the characterization of future REOs demand and EoL streams from lighting technologies. In the literature, few studies have traced the stock and flow of REOs from lighting technologies. Machacek et al. estimated the global demand and potential secondary supply of yttrium, europium and terbium in the lighting sector, focusing on the period from 2015 to 2020[63]. Ciacci et al. analyzed the europium cycle and the potential for recycling focusing on 28 EU countries[58]. Global scale prospective

assessment on the recyclability of REOs from lighting technologies, however, has been lacking in the literature.

Economic feasibility plays a key role in understanding market-based recycling practice[69]. Industrial REOs recycling from EoL lighting technologies, for example, is scarcely practiced today as REOs recycling can hardly make any profit since the REO price collapse after 2013[58]; Solvay-Rhodia opened two industrial-scale facilities in France in 2011, which respectively focused on the upstream and downstream processes of REOs recovery from EoL fluorescent lightbulbs[63,70], but these two plants had to shut down in 2016 following the demand drop of rare earth in the lighting sector and the global REE price collapse[71]. According to Innocenzi et al., recycling REOs from EoL FLs is not economically feasible under the 2016 REO market prices[72,73]. Amato et al. also analyzed the profitability of a recycling plant that recovers rare earth elements from EoL fluid catalytic cracking catalysts (FCCC), fluorescent powders and permanent magnets[74]. The result showed that the profitability indexes (defined as the division of net present value over capital investment) of recycling FCCC, fluorescent powder and permanent magnets are 1.26, 0.03 and 1.75, indicating extremely low profitability of the recycling operation of fluorescent powder. These studies, however, focused on the costs of recycling based on the current volume of EoL lighting technologies, which may be reduced in the future given the growing volume of EoL REOs and technology learning.

Our study aims to answer the following questions: First, what are the future trajectories of REO flows from EoL lighting technologies? Second, would the higher volume of REOs from EoL lighting technologies and associated learning enable profitable REOs recycling? If not, what would be the REO price floor needed for profitable recycling of REOs from efficient lighting technologies?

### *B. Methods and data*

In this study, we conducted a dynamic material flow analysis to estimate the global trajectories of REOs demand and EoL flow from efficient lighting technologies (FLs and LEDs) for the time period of 1990 – 2050. Then, based on the volume of REOs EoL flow that are available for recycling, we incorporated the learning curve approach to estimate the possible change of REO recycling cost by considering the effect of economy of scale.

1. Dynamic Material flow analysis

Stock and flow model is widely used in the field of industrial ecology to quantify the accumulation, depletion, or flows of materials in a system[75–81]. It has been adopted to quantify industrial emission[82], nanomaterial release[83], waste streams[84]. In this study, we conducted a dynamic material flow analysis which incorporated the stock model to estimate the waste stream generation of REOs from the lighting sector between 1990 and 2050 based on the annual demands and lifetime distributions of different lighting technologies.

The global CFL and LFL demand data were collected from the IEA and US DOE reports[51,57], and data were presented in the appendix (Table A1 and A2) . Due to the limited time frames of the original data (CFL is 1990-2030, LFL is 2007 - 2025), projections were made based on the historical growth trends of these two types of lighting technologies to generate a homogeneous time frame from 1990 to 2050. We assumed that the LED technology started to penetrate general lighting market from 2010 by replacing the demand for FLs. CFL was replaced by LED bulbs, and LFL was replaced by linear LED lamps (Linear LED). Three scenarios were set up to represent different LED penetration speeds: low, medium and high. Under the three scenarios, LED started to penetrate general lighting market in 2010 by replacing FLs. The replacement

rates increased linearly from 0% at 2010, and reached 100% by 2050, 2040, and 2030 respectively.

The lifetimes of different lighting technologies were collected, and each lighting technology was considered for both residential and non-residential (including outdoor, commercial and industrial) applications due to the different daily operational times in these two sectors. The average operational times for residential and non-residential lighting are about 2.3 and 11.2 hours/day respectively [85,86]. For CFLs and LEDs bulbs, we assume 70% of them are used in residential sector, and 30% of them are used in non-residential sector. For LFLs and linear LEDs, 20% of them are used in residential sector, and 80% of them are used in non-residential sector [87]. The lifetimes by year of different lighting technologies within the two application sectors were calculated based on their respective lifetimes by hour and daily operational times (Table 1).

The Weibull distribution has been verified to have better analytical tractability and generate higher goodness-of-fit in estimating a product's lifetime [75,88,89]. Therefore, the two-parameter Weibull distribution was chosen to approximate the lifetime distributions of lighting technologies, and the probability density distribution function is shown as follows:

$$P(l) = \frac{\alpha}{\beta} \times (\frac{l}{\beta})^{\alpha-1} \times \exp\left(-\left(\frac{l}{\beta}\right)^{\alpha}\right) \quad (1)$$

$\alpha$ is the shape parameter, and $\beta$ is the scale parameter. $l$ is the product's lifetime by year. $P(l)$ quantifies the proportion of inflow that will be disposed at $l_{th}$ year. The shape parameter $\alpha$ of different lighting technologies were collected from literatures, and scale parameter $\beta$ of different lighting technologies were calculated based on the lifetime by year $l$ using the following formula:

$$\beta = \frac{l}{\exp\left(\Gamma(1+\frac{1}{\alpha})\right)} \quad (2)$$

Where Γ is a gamma function:

$$\Gamma(\alpha) = \int_0^{\infty} x^{\alpha-1} \times \exp(-x)\, dx \quad (3)$$

The shape and scale parameters of four types of lighting technologies are also presented in Table 1.

**Table 1. Lifetime and Weibull distribution parameters for four lighting technologies**

| | CFL | LFL | LED bulb | Linear LED |
|---|---|---|---|---|
| Lifetime by hour (hr)[a] | 8,000 | 10,000 | 15,000 | 20,000 |
| Lifetime by year residential (yr) | 10 | 12 | 18 | 24 |
| Lifetime by year non-residential (yr) | 2 | 3 | 4 | 5 |
| Shape parameter ($\alpha$)[b] | 2.1 | 1.9 | 2 | 2 |
| Scale parameter for residential ($\beta$) | 11.3 | 13.5 | 20.3 | 27.1 |
| Scale parameter for non-residential ($\beta$) | 2.3 | 3.4 | 4.5 | 5.6 |

Note:
[a] Data collected from Waide (2010) [51]; UNEP (2017) [50]
[b] Data collected from Heidari et al. (2018) [81]; Wang et al. (2013)[89]

In the stock model, inflow represents the amount of new lighting technology that is installed for service at a given year. We assumed that the amount of new installed lighting technology each year was equal to the annual demand for that lighting technology. The outflow $O_a(n)$ is the total amount of EoL lighting technology *a* that enters waste stream at $n_{th}$ year, which is calculated by:

$$O_a(n) = \sum_{t=1}^{n-1} I_a(t) \times P_a(n-t) \qquad n > t \quad (4)$$

$I_a(t)$ is the inflow of lighting technology *a* that is installed in the $t_{th}$ year. $P(n-t)$ is the stochastic Weibull distribution which determines the proportion of lighting technology *a* that is installed in the $t_{th}$ year and has the lifetime of *n-t*. The EoL outflow $O_a(n)$ is the sum of the outflows of lighting technology *a* that were installed in previous years and reached the EoL at the $n_{th}$ year.

**Table 2. Phosphors and REO content of different efficient light technologies**

| | Phosphors (g/unit) | $Y_2O_3$ (g/unit) | $Eu_2O_3$ (g/unit) | $Tb_4O_7$ (g/unit) | $CeO_2$ (g/unit) | $La_2O_3$ (g/unit) |
|---|---|---|---|---|---|---|
| CFL[a] | 1.3 | 0.61 | 0.04 | 0.05 | 0.19 | 0.08 |
| LFL (T5)[a, c] | 2.4 | 0.75 | 0.05 | 0.06 | 0.08 | 0.25 |
| LFL (T8)[a, c] | 5.8 | 1.79 | 0.12 | 0.13 | 0.18 | 0.59 |
| LED bulb[b] | 0.0100 | 0.0049 | 0.0004 | NA | 0.0013 | NA |
| Linear LED[b, d] | 0.1200 | 0.0588 | 0.0048 | NA | 0.0156 | NA |

Note:
[a] Data collected from Bauer et al. (2011)[57]
[b] Data collected from Machacek et al. (2015)[63] , Lim et al. (2011)[55]
[c] The two types of LFL are differentiated based on the diameter: LFL (T5) has 5/8 inch diameter. LFL (T8) has 8/8 (1) inch diameter. The overall LFL is reported in the final result.
[d] The average phosphors coating area of a linear LED was assumed to be 12 times of a LED bulb according to [90] therefore the phosphors and REOs contents of linear LED were estimated by multiplying the phosphors and REOs contents of LED bulb by a factor of 12.

The phosphors and REO contents in FLs and LEDs were collected from literatures (Table 2). The annual inflow and outflow of REOs in lighting sector were determined by multiplying the contents of REOs to the amount of lighting technologies:

$$I_{r,\ a}(n) = C_{r,\ a} \times I_a(t) \quad (5)$$

$$O_{r,\ a}(n) = C_{r,\ a} \times O_a(n) \quad (6)$$

$$I_r(t) = I_{r,\ a}(t) + I_{r,\ b}(t) + I_{r,\ c}(t) + \cdots \quad (7)$$

$$O_r(n) = O_{r,\ a}(n) + O_{r,\ b}(n) + O_{r,\ c}(n) + \cdots \quad (8)$$

$I_{r,\ a}(t)$ and $O_{r,\ a}(n)$ are the inflow and outflow of REO *r* in lighting technology *a* at the year of *n*; $I_r(t)$ and $O_r(n)$ are the inflow and outflow of REO *r* in all lighting technologies (*a*, *b*, *c* ...) at the year of *n*; $C_{r,\ a}$ is the content of REO *r* in one unit of lighting technology *a*.

2. Learning curve

The unit cost of production has been found to decrease at a rate as the cumulative production increases for a wide range of manufacturing and service sectors, which is referred as the learning curve or "learning by doing"[91]. The learning effect can be characterized by a number of

mechanisms, such as technology advancement, increased labor productivity, economy of scale and improved material and energy efficiency[92–94]. The learning effect was first described by Theodore Wright, who found that the unit labor costs of airplane production declined as a power law function of cumulative production[95], and it has also been widely observed in other industries, such as semiconductor[96–98] and energy[99,100] technologies. As for the electronic waste recycling, Zeng et al., found that technological learning significantly reduced the recycling cost for bulk and precious metals (Cu, Fe, Al, Pb and Au) in waste cathode-ray tube TV due to progressive automation of demanufacturing[101]. In this study, the learning curve empirical method was applied to estimate the possible cost reduction of the REO recycling process by considering the recycling scale. The learning curve function is shown as follows:

$$\frac{C_t}{C_1} = \left(\frac{X_t}{X_1}\right)^a \quad (9)$$

$C_t$ is the recycling cost at time t; $C_1$ is the original recycling cost; $X_t$ is the plant capacity at time t; $X_1$ is the original plant capacity; $a$ is the scale factor.

Industrial scale REO recycling from the lighting sector has been conducted through hydrometallurgical processes including leaching, precipitation, filtration and calcination[63,70,102]. The data of capital and operative costs were collected from literatures for two types of recycling plants: mobile and fixed plant (Table 3). A mobile plant has limited capacity but better mobility, and it is considered a solution for small regions with limited volume of waste stream, while a field plant usually has a higher capacity and is able to manage higher volumes of waste[69]. The recycling cost is the sum of capital and operative costs. Given the data availability, the boundary of recycling process in this study starts from waste phosphor powders, and the end-product is saleable REOs mixture containing $Y_2O_3$, $Eu_2O_3$, $Tb_4O_7$, $CeO_2$ and $La_2O_3$. The cost of purchasing

the phosphor powders ($1,000/t) is collected from literature and included in the operative cost calculation in this study[63].

**Table 3. Capacity and cost of recycling facilities.**

| Plant type | Capacity (t/yr)[c] | Capital cost ($/t)[d] | Operative cost ($/t) | Recycling cost ($/t) |
|---|---|---|---|---|
| Mobile[a] | 93 | 1,972 | 5,460 | 7,432 |
| | 185 | 991 | 4,345 | 5,336 |
| | 277 | 662 | 3,971 | 4,633 |
| | 370 | 496 | 3,773 | 4,268 |
| Field[b] | 1200 | 168 | 2,675 | 2,842 |

Note:
[a] Data collected from Innocenzi et al. (2016, 2017)[72,73]. Recycling cost data of mobile plants in these references were collected in 2014 and originally presented as EURO per metric ton (€/t), and we converted them into USD per metric ton ($/t) by the average 2014 rate of USD:EURO = 0.753:1 (www.macrotrends.net)
[b] Data collected from Strauss et al. (2016)[103]
[c] The unit of plant capacity is "metric ton of REO phosphor powders can be treated per year".
[d] Capital cost is reported by amortizing total capital cost over six (mobile plant) and seven (field plant) years.

3. Uncertainty analysis

The profit was calculated by subtracting recycling cost from revenue of selling recycled REOs to the market. The 2018 average REO market prices were collected for $Y_2O_3$, $Eu_2O_3$, $Tb_4O_7$, $La_2O_3$ and $CeO_2$, and they are $3.0/kg, $56.0/kg, $461.0/kg, $2.1/kg and $2.0/kg respectively[104]. The revenue was calculated by multiplying the amount of recycled REOs to their respective market prices. The revenue was subjected to uncertainty caused by the recycling process efficiency rate, REO compositions in the end-product and a discount rate. The recycling process efficiency rate was defined as the ratio of the amount of recycled REOs mixture (end-product leaving the recycling process) to the amount of phosphor powders collected for recycling. The discount rate was defined as the depreciation of the market price of each REO given the end-product being REOs mixture[72]. Monte Carlo Simulation is a method that can be used to assess model uncertainty[105]. In this study, 1000 iterations of Monte Carlo Simulation were conducted to estimate the range of revenue, and the 90% quartile range of revenue was

reported. The model parameters are assumed to follow the triangular distribution, and their uncertainty ranges were reported in Table 4. A sensitivity analysis was also conducted to analyze the effect of different parameters on the revenue by selling the recycled REO mixture under 2018 market prices.

**Table 4. Uncertainty ranges of recycling process efficiency rate, REO composition in the end-product and discount rate.**

| | | |
|---|---|---|
| Recycling process efficiency rate (%)[a, b] | | 12.1 – 32.3 |
| REO compositions in the end-product (%)[a] | $Y_2O_3$ | 80.0 – 88.0 |
| | $Eu_2O_3$ | 4.0 – 5.8 |
| | $Tb_4O_7$ | 0.5 – 1.1 |
| | $CeO_2$ | 0.4 – 1.3 |
| | $La_2O_3$ | 0.01 |
| Discount rate (%)[a, b] | | 60 – 70 |

Note:
[a] Data collected from Innocenzi et al. (2016)[72]
[b] Data collected from Strauss et al. (2016)[103]

### *C. Results*

1. Demand for lighting technologies

The result illustrates that demand for FLs experienced a significant increase from 1990 to 2010, but this increasing trend slowed down since 2010 and reached the peak at around 2014 given the LED penetration in the general lighting market (Figure. 1). The LED penetration speed showed significant effect on the demand for FLs. Under the low LED penetration scenario, total demand for FLs remains stable from 2015 to 2025, with a total amount being around 6,500 million units (CFL and LFL account for around 70% and 30% respectively). After 2025, the demand for FLs will rapidly decease. Under medium and high LED penetration, the demand for FLs at peak year of 2014 were about 6,700 and 6,200 million units respectively at the global level (CFL and LFL account for around 70% and 30% respectively). The total demand rapidly declined after the peak year of 2014.

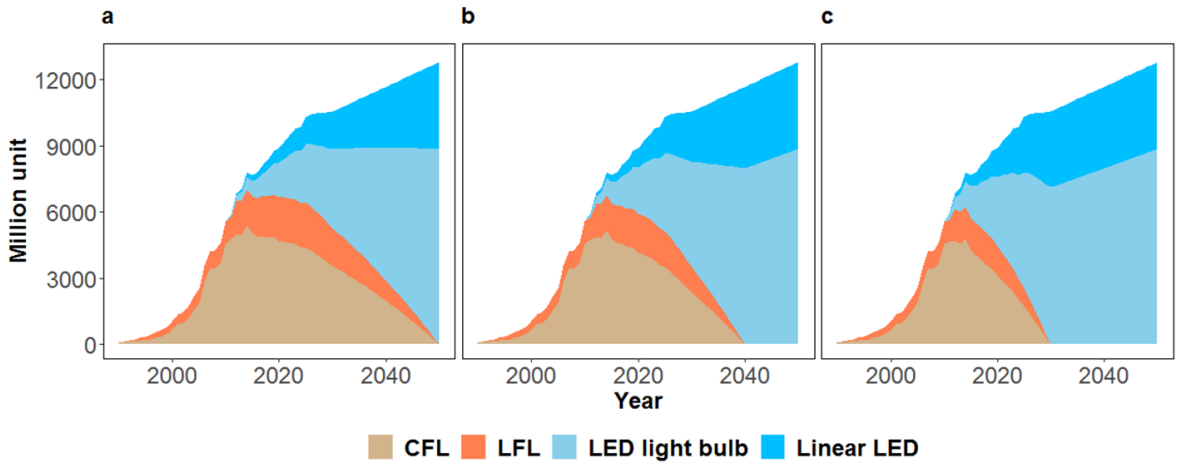


**Figure 1. Demand for different lighting technologies under low (a), medium (b) and high (c) LED penetration scenarios**

2. REO demand and waste stream

The demand for REOs in the lighting sector dramatically increased between 1990 and 2010 following the global adoption of FLs. Under the low LED penetration scenario, the increase in demand for REOs slowed down after 2010 when LEDs started to expand their market shares, and the peak year is at 2019, with the total amount of REOs being around 9,700 t/yr. Under the medium and high LED penetration scenarios, the peak REO demand from lighting technologies is at 2014, with the total amount being around 8,400 to 9,000 t/yr. After 2014, the REO demand rapidly declined under these two scenarios. REO flow from EoL lighting technologies is expected to follow a similar trend but with a few years of delay; the peak year is likely to be around 2020 to 2027 depending on the LED penetration speed, and the total amount of peak REO EoL flow will be around 9,300 t/yr, 8,200 t/yr, and 6,800 t/yr for low, medium, and high LED penetration scenario respectively. After the peak year, the amount of REOs from EoL lighting technologies is expected to exceed the amount of REOs required to meet the demand for lighting technologies. In other words, the annual secondary supply of REOs from lighting sector will be theoretically sufficient to satisfy its demand after the peak year if REOs can be recycled

without loss (Figure 2). The estimated demand and waste of REOs from lighting sector between 2010 and 2050 can be found in Table A3.

We also estimated the contribution of different lighting technologies to total REO waste stream (Supplementary Table 3). The result shows that FLs will be the dominant source of REO secondary supply in the lighting sector until 2030, with more than 95% of share in the waste stream under all the three LED penetration scenarios. After 2030, the contribution to total REO waste stream will vary depending on the LED penetration speed. Under the low LED penetration scenario, the FLs will still account for more than 90% of the REO waste stream until 2050, but under high LED penetration scenario, the LEDs will contribute 85% of the REO waste stream by 2050.

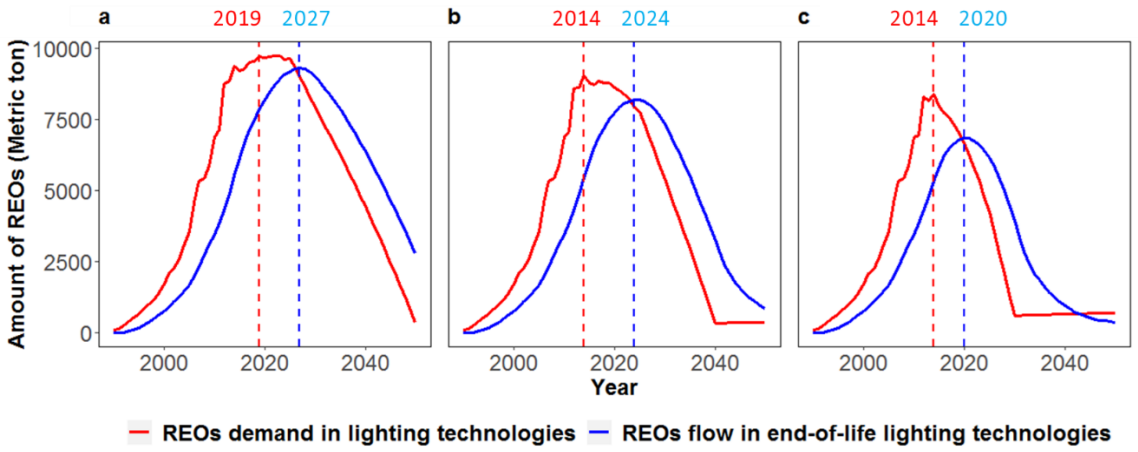


**Figure 2. Total REO demand and waste stream in lighting sector under low (a), medium (b) and high (c) LED penetration scenarios (dash lines showing the year when REO demand in lighting technologies equals to REO flow in EoL lighting technologies)**

3. Recycling cost and profit analysis

The projected REO recycling cost from the lighting sector is presented in Figure 3. By inputting the plant capacity data and corresponding recycling cost data into a regression analysis, the scale factor *a* is estimated to be -0.39 for the REO recycling process considered in this study. Model result shows that, to recycle 1 metric ton of phosphor powders from EoL FLs, plant

capacity increase can reduce the recycling cost from $7,223/t (plant capacity of 100 t/yr) to $2,496/t (plant capacity of 1,500 t/yr). The profit of REO recycling process was calculated by subtracting the cost from revenue based on the 2018 REO prices and three other break-even price scenarios that allow profitable recycling for three capacity levels (Figure 4). The results show that REO recycling is hardly profitable under the 2018 REO prices regardless of the plant capacity. The break-even REO prices that lead to profitable recycling varies depending on the plant capacity. The break-even REO prices at 100, 800 and 1,500 t/yr of capacities, were 6.3, 2.8 and 2.2 times that of 2018 REO prices, respectively.

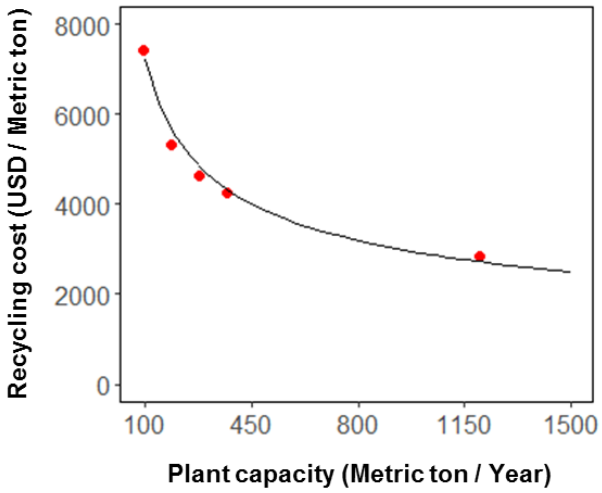


**Figure 3. Recycling cost projection under different plant capacities (red dots represent the empirical data collected from literature, black line represents the estimated recycling cost projection).**

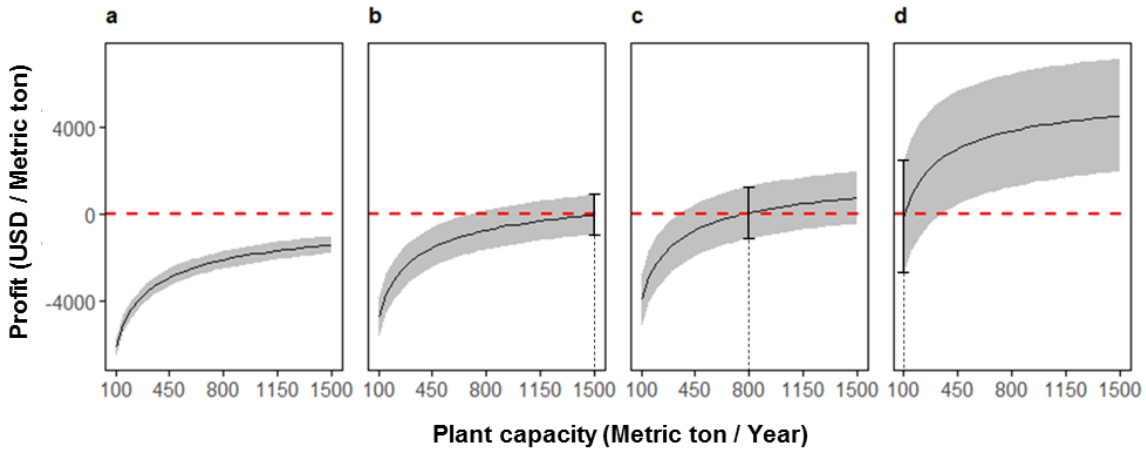


**Figure 4. Profitability of REOs recycling process with different plant capacities under 2018 REO prices level (a) and three other break-even prices of plant scale at 1,500 (b), 800 (c) and 100 t/yr (d).**

The sensitivity analysis shows that by selling the amount of REO mixture recycled from 1 metric ton of phosphors powder under 2018 REO market prices, the baseline revenue is $1,294. The recycling process efficiency rate has the highest impact on revenue, because it can change the baseline revenue by ±45%. The $Tb_4O_7$ composition can change the baseline revenue by ±15.4%, which has the most significant impact on the revenue among the five REOs (Figure. 5).

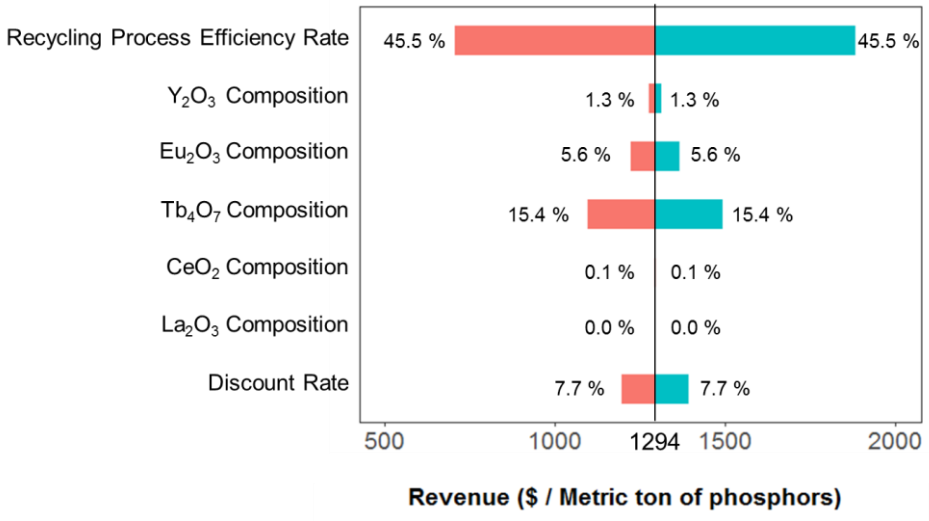


**Figure 5. Sensitivity analysis on the effects of different parameters on the revenue of selling the recycled REO mixture under 2018 market prices.**

### *D. Discussion*

The result of this study shows that the demand for REOs in the lighting sector has reached the peak at around 2014 to 2019 depending on different LED penetration scenarios. Among the five rare earth elements we analyzed, yttrium, europium and terbium have been considered critical materials by both the US and European Union due to their importance for clean energy and relatively high supply risk[57,106]. As the demand for REOs in the lighting sector will experience decline after the peak year, the criticality of these REOs is likely to decrease in the near future. On the other hand, the amount of REOs from EoL lighting technologies will increase for the next one to eight years, allowing potentially increasing volume of secondary supply of REOs if recycling becomes economically feasible. Exploiting the secondary supply of REOs from EoL lamps through recycling could also counter the supply security concerns over these critical natural resources.

The changes in the market share of lighting technologies and the overall demand for REOs are expected to affect the future supply and demand structure of $Y_2O_3$, $Eu_2O_3$, $Tb_4O_7$, of which 53.7%, 100% and 88.7% have been used for the phosphors manufacturing[107]. For instance, $Eu_2O_3$ is currently used exclusively for phosphors. As FLs are replaced by LEDs in the future, it is expected that the overall demand for $Eu_2O_3$ will decrease, and so will its criticality and market price. A potential oversupply of europium is also likely to occur as its demand starts to decline after the peak year, therefore recycling will not be a favorable option for $Eu_2O_3$[58,108]. However, yttrium and terbium have relatively diverse applications. Currently, 34% of yttrium is used as additives in ceramics and glass, and 11% of terbium is added to the NdFeB magnets as a substitute for dysprosium. As the lighting sector uses less $Y_2O_3$ and $Tb_4O_7$, their supply can be possibly absorbed by other applications. For example, terbium is reported to have a better effect

in improving the temperature resistance of NdFeB compared to dysprosium, and an increasing amount of this material could be applied in magnets as its future demand in lamp phosphors decreases. Therefore, recycling could become feasible at a meaningful scale for these two types of REOs if demands for other sectors expand[67].

A lack of economic feasibility, however, still is a major challenge in achieving the circularity of REOs. Although our results indicate that the increase of plant capacity has a potential to reduce cost, recycling of REOs is not profitable given the low REO prices at the moment regardless of the plant capacity. As for a recycling plant at 1,500 t/yr of capacity, the REO prices need to increase by a factor of 2.2 in order to cover the cost of recycling, and for the mobile plant, which usually has smaller capacity, the REO prices need to increase even more to break even. When studying the same REO recycling operation based on mobile plant with the capacity of 184.0 t/yr, Innocenzi et al. found that the recycling process could be profitable if the final REO mixture could be sold at 15.0 €/kg, which was about 2.8 times of the value of the recycled REO mixture (5.4 €/kg) reported in that study[72]. Using the technology learning curve model, we also estimated that, for a plant with the capacity of 184 t/yr, the break-even REO prices for profitable recycling is 4.0 times that of 2018 REO prices. This value is higher than 2.8, and the reason can be that the REO market prices have been further decreased after 2016, therefore the 2018 REO prices need to increase even more to break even. The sensitivity analysis shows that the recycling process efficiency rate and the $Tb_4O_7$ composition in the end-product (REO mixture) have the major effects on the revenue. Therefore, technologies that can further increase these two parameters will significantly improve the economic feasibility of the recycling operation.

In the future, it is unclear whether the REO prices would increase sufficiently high enough for the market to recycle REOs on its own, therefore, we suggest that the government can also play a critical role to improve the recycling of REOs from EoL lighting technologies. Currently, the few FLs being recycled have been relying on the extended producer responsibility (EPR) policy, under which government places the responsibility for treatment and disposal of post-consumer products on the manufacturers[63,109]. Under the EPR, the government either allows manufacturers to charge customers recycling fees at the time of purchase and fund the recycling process[110], or levies advanced recycling fees from manufacturers and uses it to subsidize the third-party recycling facility[111]. However, the current EPR policy aims to manage mercury, not REOs[112]. Therefore, should REOs recycling be a policy objective, current EPR policy can be expanded to bear the cost of REOs recycling. Besides, Machacek et al. also mentioned that the recyclers usually make the decision on recycling or landfilling the waste lamp phosphors depending on the cost comparison between these management approaches, therefore, increasing the cost or restricting the policy regulation of landfilling the waste lamp phosphors could be another option to improve the REO recycling[63].

Additionally, our study shows that more than 95% of the potential secondary supply of REOs will be available through EoL FLs before 2030, so we highlight the importance of increasing the collection rate of EoL FLs, which is necessary to enable the economy of scale in REOs recycling. High collection rates of FLs have been observed in only limited countries and regions, such as the EU countries with the average collection rate of FLs being 40%, and Taiwan with a collection rate over 80%[113], mainly thanks to the mandatory EPR legislation. Other than that, the convenient collection system, developed recycling technology, and other infrastructures that allow adequate rule enforcement, effective information provision, stable financial management

are also important factors for the high collection rates in these countries[114]. However, in other major consumers of the world, such as China, US, Japan and Australia, the EoL FLs collection rates are generally below 15%[63]. Therefore, it is necessary to further investigate how to improve the lamp collection rates in these countries.

The comprehensive recycling operation by Solvay-Rhodia started from the dissembling of the waste light bulb, and ended with separated REEs[70]. However, due to the data availability, the recycling operation we considered in this research started from collected waste phosphors powder, with the end-product being REO mixture. Therefore, we applied the discount rate to account for the depreciation of the market price of each REO given the end-product being REO mixture. We recommend that future study focus on the economic feasibility analysis of a comprehensive recycling operation for individual REE, for example terbium, which has much higher economic value and can be used in other technologies. This type of research will better inform the recyclers with their decision-making on recycling the REEs.

Although economic feasibility is an important factor in determine the recyclability of REOs, Machacek et al. also discussed the externalities related to the REO recycling operation (avoided environmental and health impact, creation of jobs opportunities, R&D and innovation, and broader social value), which need to be considered comprehensively when making decision on establishing the recycling facilities[63]. Therefore, future research that studies these externalities will also provide valuable information.

In this study, we present a dynamic material flow analysis of REOs in lighting technologies from 1990 to 2050. The result shows, as LEDs penetrate the market, the demand for REOs in the lighting technologies reached the peak at around 2014 to 2019 depending on the LED penetration speed. The amount of REOs available from EoL lamps is expected to increase for the next one to

eight years with the peak year at around 2020 to 2027, allowing recycling operations to take advantage of the economy of scale. Increasing recycling plant capacity can reduce cost from about $7,200/t REO phosphors at 100 t/yr capacity to about $2,500/t REO phosphors at 1,500 t/yr capacity, we find that the rate to which the cost of recycling is reduced may not be sufficient to break even under the 2018 REO market prices, irrespective of the scale of recycling operation. Significant improvement of REO recycling rate in lighting technologies would therefore require substantially higher REO prices, policy support, and improvement of recycling technology.

## *E. Appendix*

**Supplementary Table 1. The data of CFL demand from 1990 to 2030**

| Year | CFL (million unit) | Year | CFL (million unit) | Year | CFL (million unit) |
|---|---|---|---|---|---|
| 1990 | 91.8 | 2004 | 1539.2 | 2018 | 6035.8 |
| 1991 | 116.4 | 2005 | 1897.6 | 2019 | 6263.7 |
| 1992 | 133.8 | 2006 | 2812.0 | 2020 | 6275.7 |
| 1993 | 155.2 | 2007 | 3450.4 | 2021 | 6443.1 |
| 1994 | 176.5 | 2008 | 3412.2 | 2022 | 6583.9 |
| 1995 | 204.3 | 2009 | 3702.7 | 2023 | 6750.4 |
| 1996 | 236.0 | 2010 | 4584.2 | 2024 | 6726.2 |
| 1997 | 309.7 | 2011 | 4891.6 | 2025 | 7007.4 |
| 1998 | 362.7 | 2012 | 5214.4 | 2026 | 7101.7 |
| 1999 | 479.1 | 2013 | 5370.8 | 2027 | 7122.5 |
| 2000 | 685.3 | 2014 | 5992.3 | 2028 | 7126.5 |
| 2001 | 941.3 | 2015 | 5752.6 | 2029 | 7127.8 |
| 2002 | 970.9 | 2016 | 5743.5 | 2030 | 7131.8 |
| 2003 | 1202.6 | 2017 | 5934.3 | | |

Note:
Data source collected from Waide (2010)[51]

**Supplementary Table 2. The data of LFL demand from 2007 to 2025**

| Year | LFL-T5 (million unit) | LFL-T8 (million unit) |
|---|---|---|
| 2007 | 129.1 | 656.7 |
| 2008 | 148.0 | 694.7 |
| 2009 | 170.8 | 740.2 |
| 2010 | 189.8 | 782.0 |
| 2011 | 224.0 | 820.0 |
| 2012 | 235.4 | 1375.1 |
| 2013 | 254.3 | 1437.4 |
| 2014 | 280.9 | 1518.8 |
| 2015 | 292.3 | 1627.4 |
| 2016 | 326.5 | 1748.3 |
| 2017 | 345.4 | 1892.6 |
| 2018 | 360.6 | 1997.5 |
| 2019 | 383.4 | 2112.3 |
| 2020 | 406.2 | 2220.9 |
| 2021 | 425.2 | 2331.1 |
| 2022 | 440.3 | 2452.0 |
| 2023 | 455.5 | 2574.3 |
| 2024 | 470.7 | 2687.5 |
| 2025 | 493.5 | 2801.5 |

Note:
Data collected from Bauer et al. (2011)[57]

**Supplementary Table 3. REOs demand and waste from lighting sector and the contribution of different lighting technologies to total REOs waste**

| Year | $Y_2O_3$ (t/yr) | | $Eu_2O_3$ (t/yr) | | $Tb_4O_7$ (t/yr) | | $CeO_2$ (t/yr) | | $La_2O_3$ (t/yr) | | Total REOs (t/yr) | | Contribution to total REOs waste stream (%) | |
|---|---|---|---|---|---|---|---|---|---|---|---|---|---|---|
| | Demand | Waste | Demand | Waste | Demand | Waste | Demand | Waste | Demand | Waste | Demand | Waste | FLs | LEDs |
| Low LED penetration | | | | | | | | | | | | | | |
| 2010 | 4,358 | 2,188 | 288 | 145 | 326 | 163 | 1,035 | 449 | 862 | 501 | 6,869 | 3,445 | 100.0% | 0.0% |
| 2020 | 6,148 | 5,202 | 408 | 345 | 456 | 388 | 1,240 | 1,064 | 1,419 | 1,191 | 9,670 | 8,188 | 99.8% | 0.2% |
| 2030 | 5,061 | 5,743 | 337 | 381 | 369 | 424 | 944 | 1,157 | 1,180 | 1,322 | 7,941 | 9,028 | 99.0% | 1.0% |
| 2040 | 2,855 | 4,071 | 192 | 271 | 199 | 295 | 579 | 844 | 626 | 901 | 4,451 | 6,382 | 97.3% | 2.7% |
| 2050 | 276 | 1,801 | 23 | 122 | 0 | 120 | 773 | 408 | 0 | 341 | 372 | 2,792 | 90.4% | 9.6% |
| Medium LED penetration | | | | | | | | | | | | | | |
| 2010 | 4,358 | 2,188 | 288 | 145 | 326 | 163 | 1,035 | 449 | 862 | 501 | 6,869 | 3,445 | 100.0% | 0.0% |
| 2020 | 5,486 | 4,916 | 364 | 326 | 405 | 366 | 1,108 | 1,012 | 1,261 | 1,118 | 8,624 | 7,738 | 99.7% | 0.3% |
| 2030 | 3,453 | 4,670 | 231 | 310 | 246 | 342 | 684 | 962 | 786 | 1,050 | 5,400 | 7,334 | 98.4% | 1.6% |
| 2040 | 256 | 2,103 | 21 | 142 | 0 | 144 | 68 | 473 | 0 | 412 | 345 | 3,275 | 93.0% | 7.0% |
| 2050 | 276 | 574 | 23 | 42 | 0 | 26 | 73 | 141 | 0 | 69 | 372 | 852 | 63.3% | 36.7% |
| High LED penetration | | | | | | | | | | | | | | |
| 2010 | 4,358 | 2,188 | 288 | 145 | 326 | 163 | 1,035 | 449 | 862 | 501 | 6,869 | 3,445 | 100.0% | 0.0% |
| 2020 | 4,296 | 4,346 | 277 | 288 | 304 | 323 | 819 | 908 | 946 | 974 | 6,641 | 6,838 | 99.4% | 0.6% |
| 2030 | 589 | 2,523 | 19 | 169 | 0 | 179 | 1 | 570 | 0 | 504 | 609 | 3,946 | 95.5% | 4.5% |
| 2040 | 637 | 643 | 21 | 46 | 0 | 33 | 1 | 159 | 0 | 85 | 658 | 965 | 71.1% | 28.9% |
| 2050 | 684 | 279 | 23 | 22 | 0 | 3 | 1 | 71 | 0 | 10 | 708 | 384 | 15.5% | 84.5% |

# III. Decarbonization scenarios of the U.S. electricity system and their costs

Material from:

Qiu, Y., Cohen, S., & Suh, S. (2022). Decarbonization scenarios of the US Electricity system and their costs. Applied Energy, 325, 119679.

https://doi.org/10.1016/j.apenergy.2022.119679



**Abstract.** Decarbonizing the electricity system to zero-carbon emission is crucial for climate change mitigation. Previous studies have shown that such a transition in the United States (U.S.) may lead to higher system cost compared to a business-as-usual case, but it is not well-known how the cost of electricity generation varies at sub-regional level under the transition, and studies have rarely evaluated the trade-off between the cost and avoided climate damages, as well as the potential roles of negative emission technologies (NETs) in the electricity decarbonization. Here, we present a regionally resolved national model to quantify the cost of decarbonizing the U.S. electricity system under a set of possible scenarios. The result shows that, compared to the reference scenario without a decarbonization policy, reaching zero $CO_2$ emission by 2050 would incur, depending on the scenarios, 335–494 billion USD additional costs to the electric power sector during 2020–2050. The regional costs of electricity generation ranges from 2.4 to 4.7 cent/kWh, largely due to the generation profiles and renewable resources availability of the regions. The additional costs can be translated to average $CO_2$ abatement cost of 29–59 USD/tonne $CO_2$ (with 2%–7% discount rates), which are comparable to the social cost of carbon in the literature at around 4% discount rate. The results also show that the costs of mitigating the

last few percent $CO_2$ emission from the U.S. electricity system exceed the costs of NETs, indicating an opportunity for NETs to contribute to electricity decarbonization.

### *A. Introduction*

Decarbonization of the electricity system is crucial for climate change mitigation. To achieve the 2 °C climate target of Paris Agreement, the electric power sector needs to rapidly reduce its greenhouse gas (GHG) emissions to nearly zero by mid-century[2,115–117].

Literature confirms the technical feasibility of decarbonizing the electricity system to a large extent, or even reaching 100% carbon dioxide ($CO_2$) reduction. However, a stark difference in views persists as to the cost of such a transition. Some studies have shown that decarbonizing the electricity system via deployment of various low-carbon and renewable sources can substantially increase average cost of electricity[10,41,42,118–121], as additional investments are needed for reserve capacity and storage[27]. While others have found that such a transition will lower the average cost of electricity. The lower cost is partially due to the declining prices of photovoltaics (PV), wind turbines, and electricity storage systems[122–124]. In addition, several studies showed the combined effect of higher energy use efficiency, electrification, and demand response could potentially lower the cost of electricity. This is because electrification and demand response could create more flexible load and better matches demand with supply and storage. This mechanism, together with higher energy use efficiency, reduces overall energy demand and electricity curtailment, thus avoiding overbuilt capacity and the associated cost [125,126,43,127]. Furthermore, when externalities (health and environmental costs due to carbon emission and other air pollutions) are included, a deep decarbonization pathway will also have lower aggregated cost of electricity compared to a reference case[43,44,125,126].

In the United States (U.S.), previous studies have adopted various modeling approaches to explore the decarbonization pathways and their implications broadly for economy-wide energy-systems or the electric power sector specifically. Jacobson et al. studied the U.S. energy system

powered only by wind, water and solar (100% WWS) using a trial-and-error simulation model, and showed that such a 100% WWS system leads to energy cost saving [125,128]. This modeling approach only simulated the generation profiles on the target year based on supply-demand balance without modeling the progressive capacity expansion over time, which does not reflect the system dynamics and costs along the transition. Iyer et al. developed a state-level model of the U.S. energy system embedded within a global human-earth system model and used it to study the evolution of U.S. energy system in the national climate change mitigation context[129,130]. However, this model has relatively large temporal and spatial aggregations, making it challenging to capture the granularity of load and resource variations when high renewable deployment is involved. To overcome these limitations, recent studies have developed a hybrid modeling approach that linked a demand-side model (which estimates time-varying and economy-wide energy demand) and a linear programming model with high temporal resolution to determine the optimal capacity expansion and operations for a carbon-neutral U.S. energy system, and these studies projected multiple feasible pathways of achieving a carbon-neutral U.S. energy system but all had higher system cost[131,132].

For the electric power sector, previous studies have mainly adopted capacity expansion models or used them in a hybrid fashion to study the implication of power system transition to zero or net-zero carbon emission. To capture complex investment and high-resolution operating decisions, Cole et al. used a combined capacity expansion and production cost modeling framework to quantify the total system cost of transitioning to a 100% renewable energy (RE) power system in the U.S. They also observed that such a transition incurs higher system cost compared to a reference case, and the incremental costs increase nonlinearly as the transition target approaches to 100% RE[42]. Several other studies took further steps and evaluated the roles

of firm low-carbon energy resources (e.g., nuclear, carbon capture-equipped capacity)[10], negative emission technologies (NETs)[133], and inter-regional transmission networks[134] in the decarbonization of U.S. power sector. These all emphasized that adopting a broader technology portfolio to decarbonize the U.S. power sector could reduce system cost and maintain grid stability as compared to a system relying on 100% renewable energy sources.

This work contributes to the existing literature on zero carbon electricity systems at the national level, specifically building on the modelling capabilities and scenarios of Cole et al., 2021[42], with an in-depth look at two decarbonization pathways of the U.S. electricity system at the national and regional levels. In one pathway, the electricity system achieves zero $CO_2$ emission by 2050 with generation only from renewable sources, while the other pathway adopted the same $CO_2$ emission target and trajectory as the first one but allows the use of other low-carbon sources during the interim and target year of decarbonization. Our goal is to compare the dynamic capacity expansion and generation under the two pathways and evaluate how they affect the total system cost. Compared to previous works discussed above, we further explore the regional variability by looking at the cost of electricity generation across different sub-regions in the contiguous U.S. and investigate the contribution of various generation and storage technologies to the regional electricity cost. In another extension on prior work, we put the total system cost in context by calculating the CO2 abatement costs of the decarbonization pathways and comparing them with social costs of carbon and the costs of existing NETs, and this allows us to explore the cost-benefit trade-off of a fully decarbonized U.S. electricity system and the potential role of NETs as carbon mitigation options in such a transition.

### *B. Method*

In this study, we incorporate the future projections of electricity demand and technology costs into a sequential optimization model. We use the model to simulate the least-cost capacity expansion and dispatch of electricity system in the contiguous U.S. under various transition pathways. The total system cost estimated in this study includes both capital and operational costs, which depend on installed capacity and generation output, respectively, over the whole transition period from 2020 to 2050.

1. The electricity capacity expansion model

Regional Energy Deployment System (ReEDS) is a capacity expansion and dispatch model of the electric power sector[135,136]. By incorporating grid reliability requirements, technology resource constraints, and policy constraints, the model determines the least-cost mix of technologies that meets regional electricity demand requirements. The cost minimization is performed sequentially by solving a linear programming for each two-year period from 2010 to 2050. The core ReEDS optimization serves load and maintains operational reliability in 17 time-slices within each model year, which includes four seasons (Spring, Summer, Fall, and Winter), and each season has a representative day with four chronological time-slices (overnight, morning, afternoon, and evening), and the 17th time-slice is a "summer peak" representing the top 40 hours of summer load. In addition, a separate hourly dispatch model uses 7 years of hourly load and renewable resource data to inform the core optimization with time-varying estimates of renewable energy curtailment, capacity credit for renewables and storage, and hourly arbitrage value of storage. In the contiguous U.S., ReEDS simulates the generating capacity and balances supply and demand in 134 model balancing areas (BAs), allowing the

model to capture the geospatial complexity of resources and technology availability across the country.

In this study, the ReEDS model was applied to estimate the capacity expansion, electricity generation, system costs, and CO2 emission in the contiguous U.S. for four alternative electricity scenarios. The system costs include capital cost, operational and maintenance (O&M) cost, and fuel cost.

2. The electricity scenarios

We considered four electricity scenarios that represent different development pathways of the U.S. electricity system. We adopted the 2020 version of the ReEDS model developed in the study by Cole et al., 2021[42], focusing on two key decarbonization scenarios presented in that work as the base 100% Renewable Energy scenario and the Nuclear Counts scenario. The four electricity scenarios and their assumptions are shown as follows:

*Reference scenario*: We assumed the reference projections of electricity demand, technology and fuel costs derived from Annual Energy Outlook (AEO) 2020 and 2020 NREL Annual Technology Baseline (ATB)[137,138].

*Coal scenario*: We used almost the same reference projections of electricity demand, technology, and fuel costs as in the Reference scenarios except for fuel cost of coal. Instead, we used a low coal price projections based on delivered coal price for electric power sector under high oil and gas supply scenario from AEO 2020[137] (Supplementary Table 1).

*100% Renewable scenario*: 1. We used the same reference projections of electricity demand, technology, and fuel costs as in Reference scenario; 2. We assumed the shares of renewable energy sources increased from 20% at 2020 to 100% at 2050 by imposing a national renewable generation mandate constraint (The projection of annual deployment rate is provided in

Supplementary Table 2); 3. The definition of 100% renewable means that total generation of the electricity system, including transmission and distribution losses, are all from renewable sources (a list of renewable sources considered in this study is provided in Supplementary Table 4) in the target year of 2050.

*Zero Carbon scenario*: 1. We used the same reference projections of electricity demand, technology, and fuel costs as in the Reference scenario; 2. Compared to the prior study[42], we implemented a $CO_2$ constraint to limit the annual $CO_2$ emission from the electricity system such that the annual carbon emissions aligned with the annual $CO_2$ emissions under the 100% Renewable scenario (Supplementary Table 3). In this way, the Zero Carbon scenario had the same annual $CO_2$ emission as the 100% Renewable scenario, allowing us to compare their costs based on the same carbon reduction capability.

3. Cost calculation

The ReEDS simulated the annual cost every two years based on least cost optimization from 2010 to 2050. The annual cost included capital cost, O&M cost, and fuel cost for generation, storage, and transmission technologies. In this study, the initial (base) year was assumed to be 2020, and the final year was 2050. Therefore, we calculated the total cost of U.S. electricity system by summing up the amortized capital cost, operational and maintenance cost, and fuel cost that were incurred and paid off during 2020 and 2050. The capital cost of capacity being built before 2020 and the capital costs that would be paid off after 2050 were excluded. The total cost of U.S. electricity system from 2020 to 2050 were calculated as the present value (with discount rate of 5% and economic lifetime of 20 years) with the base year of 2020 and reported as 2020 U.S. dollar (2020$). More details about the cost calculation can be found in Supplementary Note 1.

4. Cost of electricity generation in sub-regions

To understand how cost of electricity generation varies among different sub-regions across the contiguous U.S. and the underlying technological contribution, we further divided the contiguous U.S. into 12 North American Electric Reliability Corporation (NERC) regions. We calculated the unit cost of electricity generation $C_{Unit\ cost,r,s}$ and its change from Reference scenario $C_{Unit\ cost\ change,r,s}$ for each NERC region $r$ and scenario $s$ as follows:

Unit cost of electricity generation $C_{Unit\ cost,r,s}$:

$$C_{Unit\ cost,r,s} = \frac{PV_{Total\ cost,r,s}}{PV_{Total\ generation,r,s}} \quad (1)$$

where $PV_{Total\ cost,r,s}$ represents total cost (present value) of electricity system in region $r$ under scenario $s$ from 2020 to 2050, and $PV_{Total\ generation,r,s}$ represents the total 30-year generation (present value) in region $r$ under scenario $s$, and it is calculated by discounting annual generation $G_{Total\ generation,t,r}$ and summing them up from 2020 to 2050.

$$PV_{Total\ generation,r,s} = \sum_{t_0}^{t_f}(G_{Total\ generation,t,r,s} \times \frac{1}{(1+d)^{t-t_0}}) \quad (2)$$

Change of unit cost $C_{Unit\ cost\ change,r,s}$:

$$C_{Unit\ cost\ change,r} = \frac{PV_{Total\ cost,r,s} - PV_{Total\ cost,r,Reference}}{PV_{Total\ generation,r,s}} \quad (3)$$

where the $PV_{Total\ cost,r,s}$ represents the total 30-year cost (present value) of one of the three electricity scenarios (Coal, Zero Carbon and 100% Renewable) and $PV_{Total\ cost,r,Reference}$ represents the total 30-year cost (present value) of the Reference scenario. The change of unit cost indicates the cost change per unit electricity generation for each region to transition from Reference scenario to the Coal, Zero Carbon and 100% Renewable scenario respectively. Both $C_{Unit\ cost,r,s}$ and $C_{Unit\ cost\ change,r,s}$ represent the cost related to electricity generation, rather than electricity consumed, in each region. They do not account for electricity import and export across

regions and the associated payment and revenue for each region. The geographical boundaries of the NERC regions were adopted from the ReEDS documentation[135].

5. Average and incremental $CO_2$ abatement cost

We also calculated both average and incremental $CO_2$ abatement cost (for both Zero Carbon and 100% Renewable scenarios) to quantify the cost of decarbonizing the U.S. electricity system in the context of $CO_2$ mitigation following the method developed in the study by Cole et al., 2021[42]. The average $CO_2$ abatement cost (calculated at four discount rates: 2%, 3%, 5% and 7%) represents the average cost of reducing 1 metric ton $CO_2$ emission under the scenario $s$, and it can be calculated as follow:

$$Average\ CO_2\ Abatement\ Cost_s = \frac{PV_{Total\ cost,s} - PV_{Total\ cost,Reference}}{PV_{Total\ CO_2,Reference} - PV_{Total\ CO_2,s}} \quad (4)$$

where $PV_{Total\ cost,s}$ is the total 30-year cost of U.S. electricity system (present value) under scenario $s$. $PV_{Total\ CO_2,s}$ is the total 30-year $CO_2$ emission (present value) under scenario $s$, and it is calculated by discounting annual $CO_2$ emission $E_{Total\ CO_2,t,s}$ and summing them up from 2020 to 2050.

$$PV_{Total\ CO_2,s} = \sum_{t_0}^{t_f}(E_{Total\ CO_2,t,s} \times \frac{1}{(1+d)^{t-t_0}}) \quad (5)$$

The incremental $CO_2$ abatement cost (reported only at discount rate of 5%) quantifies the cost of mitigating additional $CO_2$ emission by achieving a higher $CO_2$ reduction (or renewable share) target. Here, we first developed a group of renewable scenarios by using the same assumption as the 100% Renewable scenario, but setting different renewable share targets (80%, 90%, 95%, and 99%) by 2050 (Supplementary Table 2). The discounted cost and $CO_2$ emission results under these renewable scenarios (including the 100% Renewable scenario) were used to calculate the incremental $CO_2$ abatement cost of the 100% Renewable scenario. Then, we

developed a group of carbon reduction scenarios based on the same assumption as the Zero Carbon scenario but using different $CO_2$ emission constraints. These $CO_2$ emission constraints were based on the $CO_2$ emission results from the renewable scenarios, and they reach the $CO_2$ reduction targets (87%, 92%, 94%, and 99% reduction by 2050 relative to 2005 level) that are equal to the 2050 $CO_2$ reduction levels under those renewable scenarios (Supplementary Table 3). Similarly, the discounted cost and $CO_2$ emission results under these carbon reduction scenarios (including the Zero Carbon scenario) were used to calculate the incremental $CO_2$ abatement cost of the Zero Carbon scenario. The incremental $CO_2$ abatement cost under the carbon reduction (or renewable share) targets $T_1$ and scenario $s$ can be calculated as follow:

$$Incremental\ CO_2\ Abatement\ Cost_{s,T_1} = \frac{PV_{Total\ cost,s,T_1} - PV_{Total\ cost,s,T_0}}{PV_{Total\ CO_2,s,T_0} - PV_{Total\ CO_2,s,T_1}} \quad (6)$$

where $PV_{Total\ cost,s,T_1}$ and $PV_{Total\ CO_2,s,T_1}$ represent the total 30-year cost and $CO_2$ emission (both in present value) under the targets $T_1$ and scenario $s$, and $PV_{Total\ cost,s,T_0}$ and $PV_{Total\ CO_2,s,T_0}$ represent the same metrics under the previous targets $T_0$ and scenario $s$. While this metric is not a shadow price indicating the marginal $CO_2$ abatement cost, it provides a meaningful way to compare $CO_2$ costs across scenarios.

### *C. Results*

1. Total cost of electricity system from 2020 to 2050

Our results show that the Zero Carbon and Renewable scenarios achieve zero operational $CO_2$ emissions by 2050 while incurring $2,567 billion and $2,726 billion total costs (present value at 5% discount rate, 2020$), respectively, between 2020 and 2050, which is equivalent to 15% and 22% increases relative to the Reference scenario (Figure 1a). Cumulatively, they both emit around 15 Gt $CO_2$, saving a total 23 Gt $CO_2$ compared to Reference scenario over the 30 years (Figure 1b). The Coal scenario has the lowest total cost at $2,217 billion, which is $16 billion (or 0.7%) less than the Reference scenario, but it corresponds to the largest total $CO_2$ emissions (40 Gt) over the course of 30 years.

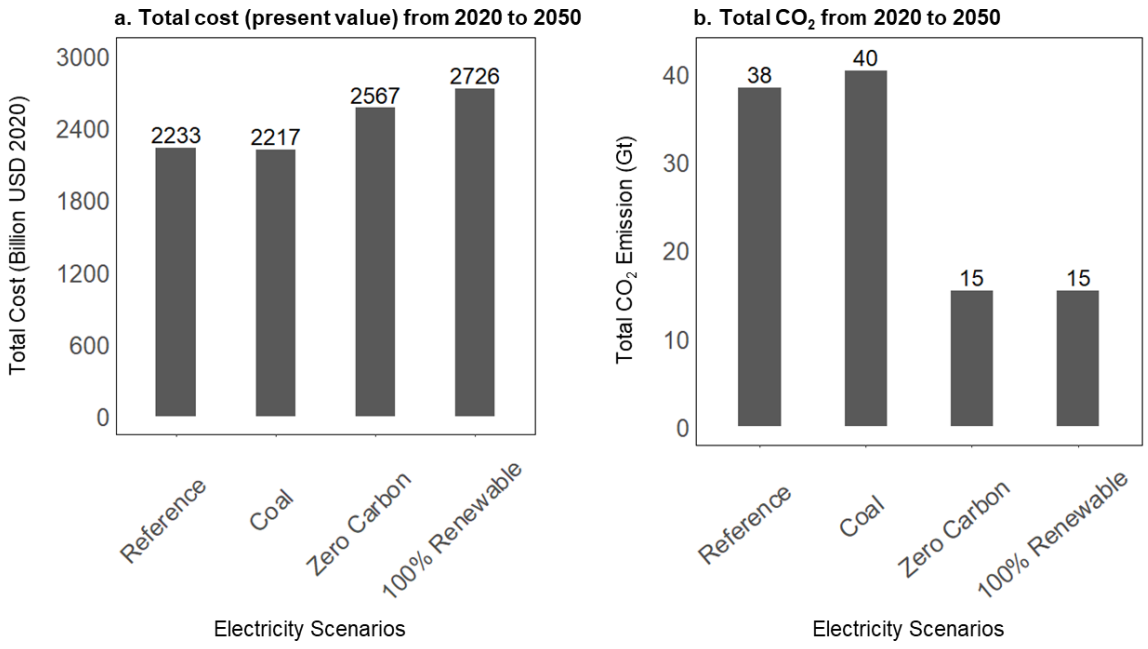


**Figure 1. Total cost (present value at 5% discount rate, 2020$) (a) and total $CO_2$ emission (b) of the U.S. electricity system from 2020 to 2050 under four electricity scenarios.**

The cost differences can be explained by the evolution of installed capacities and generation mixes under the four electricity scenarios. Compared to Reference scenario (2,020 GW total capacity in 2050), the Zero Carbon and 100% Renewable scenarios reach much higher total capacities (2,885 GW and 3,131 GW, respectively) by 2050, with the additional capacity mainly driven by the newly installed solar PV, land-based wind, and battery storage (Figure 2). In addition, combined cycle and combustion turbine gas power plants fired with renewable fuels (RE-CC and RE-CT) are installed or retrofitted from existing natural gas plants, and they also play important roles as renewable firm generation sources that can meet electricity demand when needed. RE-CC and RE-CT are nominally assumed to use hydrogen fuel produced from renewable electricity. The combined capacities of RE-CT and RE-CC are 485 GW and 506 GW in 2050 under the Zero Carbon and 100% Renewable scenarios, respectively, contributing to about 5% of annual electricity generation in 2050 for both scenarios. The capacity additions lead to higher capital and O&M costs from renewable sources, battery, and transmission for both the Zero Carbon (+$612 billion) and 100% Renewable (+$980 billion) scenarios (relative to the Reference), and these additional costs negate the cost savings due to less electricity generation from fossil (coal and Gas-CC, Gas-CT) and nuclear (only for the 100% Renewable scenario) sources. Overall, the Zero Carbon and 100% Renewable scenarios have $335 billion and $494 billion total additional costs (relative to the Reference scenario) over the course of 30 years (Figure 3, Supplementary Figure 2).

The Zero Carbon scenario keeps 47 GW of nuclear capacity in 2050, which generates about 5% of 2050 total generation, and it deploys 56 GW of natural gas combined cycle with carbon capture and storage (Gas-CC-CCS) during 2040 to 2048 (Figure 2). In comparison, the 100% Renewable scenario retires nuclear capacity by 2040, and it also excludes the use of Gas-CC-

CCS in the interim of decarbonization process, so it requires 226 GW additional renewable (mostly solar PV and land-based wind) and 65 GW battery storage capacities (relative to the Zero Carbon scenario) to meet the 100% renewable goal in 2050, causing $160 billion additional investment mostly for renewable, battery, and transmission capacities (Figure 2, Figure 3, Supplementary Figure 2).

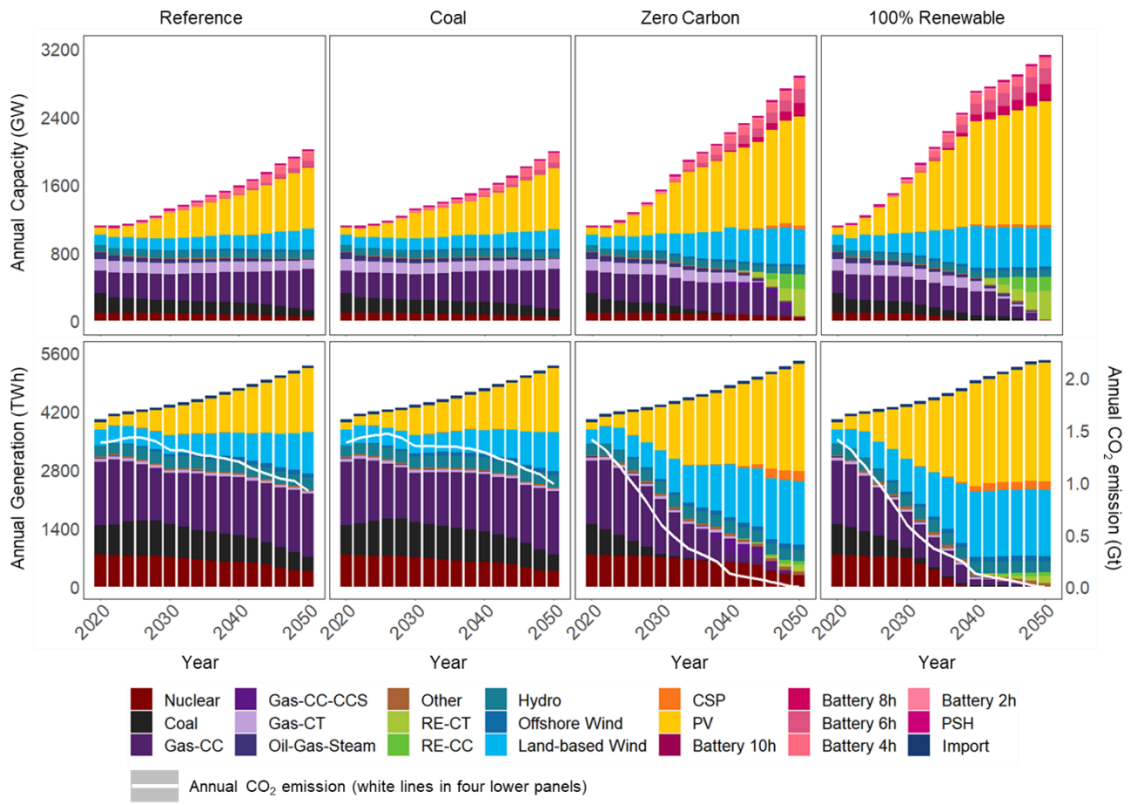


**Figure 2. The capacity, generation, and $CO_2$ emission of the U.S. electricity system from 2020 to 2050.** The upper four panels represent the capacity of generation and storage technologies under the four scenarios. The lower four panels represent the annual generation (broken down by technologies, corresponding to y-axis on the left) and $CO_2$ emission (as annual total amount shown by the white lines, corresponding to y-axis on the right) under the four scenarios. Electricity generation and storage technologies abbreviations include: CSP: Concentrated solar power; Gas-CC: Natural gas combined cycle; Gas-CC-CCS: Natural gas combined cycle with carbon capture and storage; Gas-CT: Natural gas combustion turbine, PSH: Pumped-storage hydropower; PV: Photovoltaic; RE-CC: Commercial combined cycle gas power plant fired with renewable fuels; RE-CT: Commercial gas combustion turbine fired with renewable fuels; Other includes biopower, landfill gas, and geothermal.

Coal and Reference scenarios follow very similar projections in total capacity (reaching 1,996 GW and 2,020 GW by 2050, respectively) over time, and their annual generations both increase from 4,009 TWh in 2020 to 5,297 TWh in 2050 (Figure 2). The relative similar results between Coal and Reference scenarios are mainly due to the small difference between the low (used for Coal scenario) and reference (used for Reference scenario) coal price projections. Coal electricity has slightly higher share (1% to 2% higher) in the annual generation of Coal scenario compared to that in Reference scenario over the 30 years (Figure 2), causing $17 billion additional costs from coal electricity, but this additional cost could be negated by the cost savings from building less renewable, battery, and transmission capacities (-$22 billion) and generating less electricity from Gas-CC (-$11 billion), resulting in $16 billion net cost reduction in Coal scenario (Figure. 3).

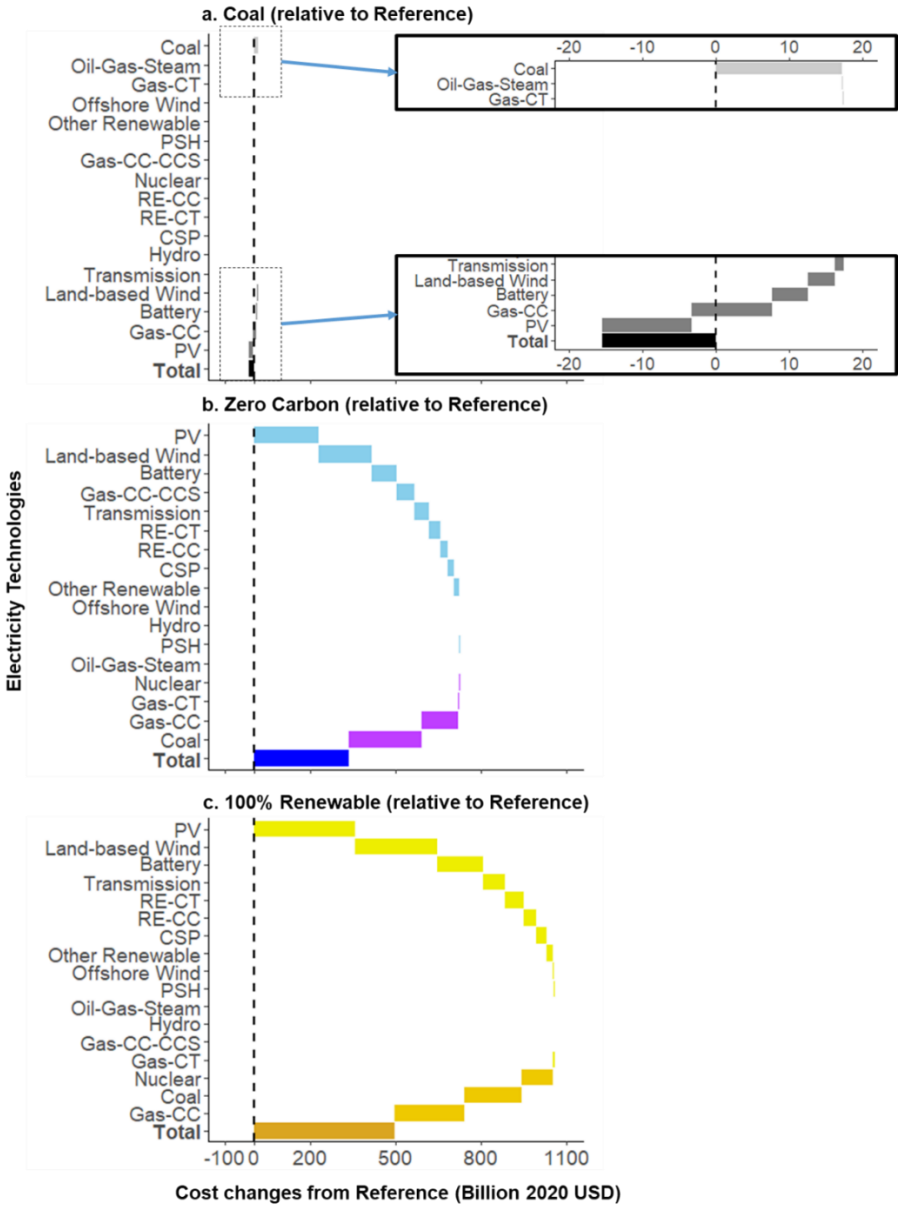


**Figure 3. The contribution of various electricity technologies to the net cost changes of the Coal (a), Zero Carbon (b), and 100% Renewable (c) scenarios from the Reference scenario.** In each panel, the horizontal bars (on the upper part of each panel) that accumulate from left to right correspond to technologies that lead to additional costs for each of the three scenarios relative to the reference scenario. The horizontal bars (on the lower part of each panel) that show reductions from right to left correspond to technologies that lead to cost savings for each of the three scenarios relative to the reference scenario. The horizontal bar at the bottom of each panel represents the total net cost change of each of the three scenarios relative to the reference scenario. The contribution to the net cost changes by both cost type and technology type can be found in Supplementary Figure 2.

2. Regional variability of electricity cost

The unit costs of electricity generation are calculated by dividing the present value of total cost by the present value of total generation from 2020–2050, and they show regional variability across 12 NERC regions in the contiguous U.S. Regional costs are a unique presentation in this work; however, it is important to caveat that these quantities do not account for the cost and revenue of power transfers between regions (i.e., imports and exports). As a result, values do not reflect how these costs might be allocated across regions to consumers or other entities in practice. For example, unit costs might increase in central plains regions as more wind capacity and transmission are installed there, but much of this power would likely be exported, reducing unit costs in importing regions and the national on average. Regional unit costs adopted here are purely a metric to understand how average investment and operation costs vary across the country.

Under the 100% Renewable scenario, the national unit cost of electricity generation (dashed lines in Figure 4c) is 3.8 cent/kWh, with a variation between 2.5 cent/kWh in Northwest (NW) to 4.7 cent/kWh in New England (NE). In general, the eastern regions, including NE (4.7 cent/kWh), New York (NY, 3.9 cent/kWh), Pennsylvania-New Jersey-Maryland (PJM, 3.9 cent/kWh), South-eastern Electric Reliability Council (SERC, 4.2 cent/kWh), Florida Reliability Coordinating Council (FRCC, 4.1 cent/kWh), and Midcontinent Independent System Operator (MISO, 4.0 cent/kWh) have higher unit costs than other regions in the central and western U.S. This is mainly because eastern regions and MISO have a higher reliance on fossil fuel (such as Gas-CC and coal) and nuclear sources, which incur higher O&M and fuel costs from these sources, causing higher overall unit costs in these regions. Higher unit costs in NE and NY regions are also driven by the investment in offshore wind capacity, which accounts for 14% and

19% of the unit costs in the two regions, respectively (Figure 4a, 4c, Supplementary Figure 9). The Zero Carbon scenario has a lower national unit cost being 3.6 cent/kWh, with a variation between 2.4 cent/kWh in NW to 4.3 cent/kWh in NE (Supplementary Figure 7).

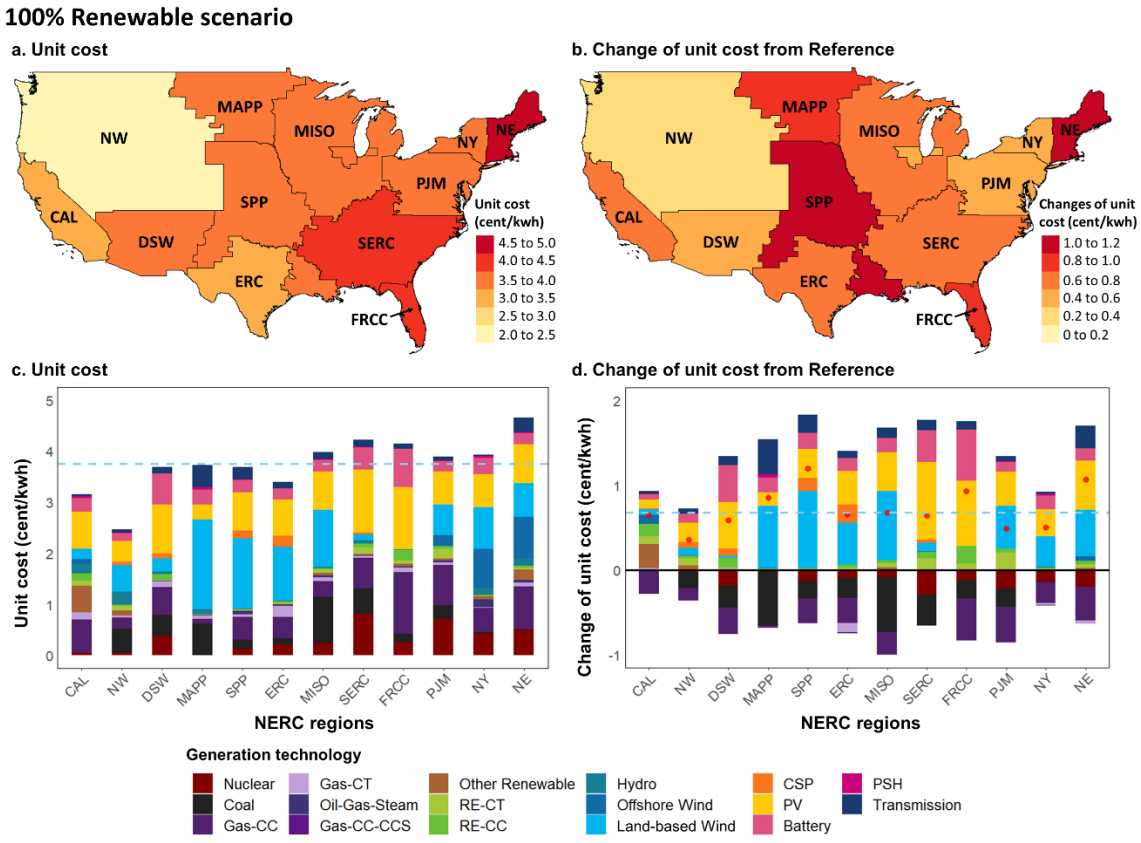


**Figure 4. The unit costs of electricity generation (a, c) under the 100% Renewable scenario and their changes relative to the Reference scenario (b, d) at 12 NERC regions across the U.S.** The map plots (a, b) show the costs at different regions, and the bar plots (c, d) show the contribution of different technologies to the costs. The dashed lines in the bar plots show the average values at the national level. The red dot in plot d shows the net additional unit cost at different NERC regions. NERC region: NE = New England; NY = New York; PJM = Pennsylvania-New Jersey-Maryland (covers Mid-Atlantic region); SERC = South-eastern Electric Reliability Council; FRCC = Florida Reliability Coordinating Council; MISO = Midcontinent Independent System Operator; MAPP = Mid-Continent Area Power Pool; SPP = Southwest Power Pool; ERC (ERCOT) = Electric Reliability Council of Texas; DSW = Southwest; NW = Northwest; CAL = California. The cost only includes the capital, O&M, and fuel cost of the electricity system, but it does not consider the electricity import and export among different NERC regions; therefore, the revenue and payment associated with electricity import and export are not included in the cost presented here. The results of the Reference, Zero Carbon, and Coal scenarios are presented in Supplementary Figure 3 – Supplementary Figure 8.

Compared to Reference scenario, higher capital investments in renewable, battery, transmission capacities exceed the savings mostly from fuel cost, leading to net additional unit costs in all regions (0.4 cent/kWh in NW to 1.2 cent/kWh in Southwest Power Pool (SPP)) under the 100% Renewable scenario. We also observed regional variability of the additional investment in different technologies across the NERC regions. For example, the additional unit costs in south-eastern regions (SERC and FRCC) and the Southwest (DSW) are primarily driven by PV and battery storage, which can be attributed to the relative abundant solar resources in these regions. For central (SPP, MISO, Mid-Continent Area Power Pool (MAPP), and Electric Reliability Council of Texas (ERC)) and north-eastern (PJM, NY, and NE) regions, the investment in wind electricity has significant contribution to the additional unit costs, which also corresponds to the high-quality wind resources in those regions (Figure 4b, 4d, Supplementary Figure 9).

3. $CO_2$ abatement cost of low-carbon electricity pathways

Compared to the Reference scenario, the Zero Carbon and 100% Renewable scenarios will incur higher total costs but reduce $CO_2$ emissions over the course of 30 years, so we calculated the average $CO_2$ abatement cost for 2020–2050 under four discount rates (2%, 3%, 5% and 7%) to represent the average cost of reducing 1 metric ton (t) $CO_2$ by pursuing these decarbonization pathways. This calculation differs from Cole et al., 2021[42], which included costs through 2069 to capture the economic life of investments made in 2050. This change generally results in lower abatement costs than observed in this previous study[42]; we use a 2020–2050 time frame to align with U.S. EPA social cost of carbon (SC-$CO_2$) estimations and restrict the calculations to a nearer-term period.

The average $CO_2$ abatement costs, depending on the discount rates, range from \$29–\$41/t $CO_2$ for the Zero Carbon scenario (higher discount rate leads to the lower abatement cost, and lower discount rate leads to higher abatement cost, same for the 100% Renewable scenario) and \$44–\$59/t $CO_2$ for the 100% Renewable scenario (Figure 5a). According to the SC-$CO_2$ estimated by U.S. EPA, the average SC-$CO_2$ ranges from \$15 to \$33/t $CO_2$ under 5% discount rate from 2020 to 2050 (these average SC-$CO_2$ is a marginal measure with the lower- and upper-bound representing the value in 2020 and 2050 respectively, same for the numbers at other discount rates), and this range increases to \$79 to \$121/t $CO_2$ with 2.5% discount rate[139]. In comparison, the average $CO_2$ abatement costs under the Zero Carbon and 100% Renewable scenarios are generally lower than the SC-$CO_2$ ranges when smaller discount rates are chosen (e.g., 2% to 3%). However, at a discount rate of 5% or higher, the average $CO_2$ abatement costs of the two scenarios will be above the upper bound of the SC-$CO_2$ range. The SC-$CO_2$ were also reported in several other studies. For example, one study that relied on a survey of experts showed that SC-$CO_2$ being around \$80 to \$100/t $CO_2$ at 2066 (3% discount rate)[140]. Another recent study that incorporated mortality costs reported an even higher SC-$CO_2$ of \$258 in 2020 (3% discount rate)[141]. These numbers are generally higher than the SC-$CO_2$ from the U.S. EPA at the same discount rate, which further support our finding that the average $CO_2$ abatement cost of decarbonizing the U.S. electricity system is smaller than the potential economic damage caused by additional $CO_2$ mission at discount rate equal to smaller than 3%.

The incremental $CO_2$ abatement costs (5% discount rate) increase non-linearly as the carbon abatement approaches to 100% (Figure 5b). Under the 100% Renewable scenario, the incremental $CO_2$ abatement cost increases monotonously to \$16/t $CO_2$ until 87% $CO_2$ reduction relative to 2005 levels. After that, the incremental $CO_2$ abatement cost curve starts to become

steeper. An additional 7% $CO_2$ reduction raises the cost by \$50/t $CO_2$, reaching \$66/t $CO_2$ at 94% reduction relative to 2005 level. Mitigating the remaining 6% $CO_2$ further increases the incremental abatement cost to \$122/t $CO_2$. A similar trend is also observed for the Zero Carbon scenario, with its incremental $CO_2$ abatement cost increasing to \$10/t $CO_2$ until 87% $CO_2$ reduction, while mitigating the last 10% of $CO_2$ raises the incremental $CO_2$ abatement cost by about \$70/t $CO_2$, reaching \$91/t $CO_2$ at 100% $CO_2$ reduction.

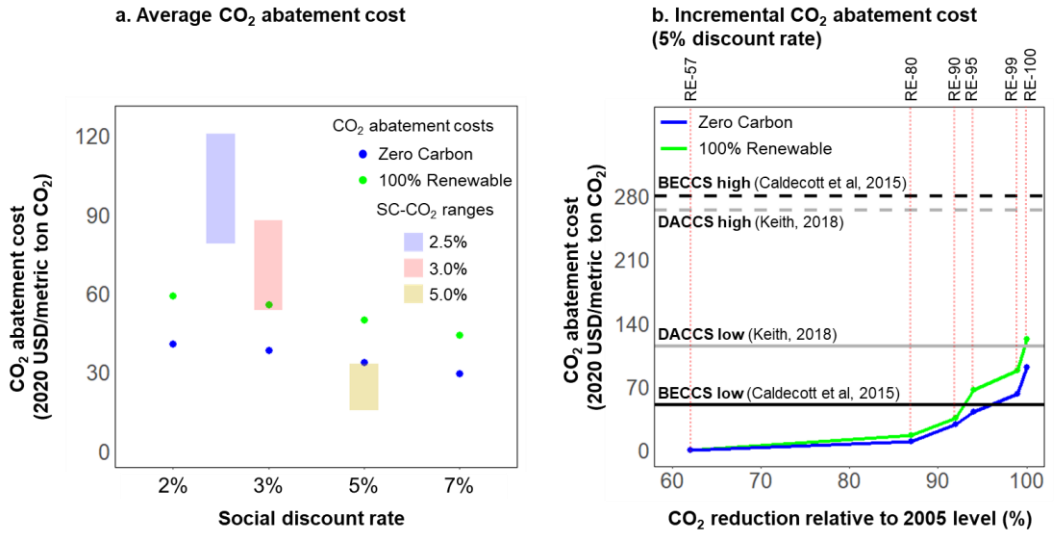


**Figure 5 | The average (a) and incremental (b) $CO_2$ abatement cost under the Zero Carbon and 100% Renewable scenarios.** In Fig. 5a, the dots represent the average $CO_2$ abatement costs of the Zero Carbon (blue) and 100% Renewable (green) scenarios under different discount rates (2.0%, 3.0%, 5.0%, and 7.0%). The three horizontal bands represent the average SC-$CO_2$ estimated by U.S. EPA under different discount rates (2.5%, 3.0% and 5.0%). The lower bound of each band represents the average SC-$CO_2$ in 2020, and upper bound represents the average SC-$CO_2$ in 2050. The SC-$CO_2$ was originally estimated based on 2007 US\$, and we converted them to 2020 US\$. In Fig. 5b, the lines represent the incremental $CO_2$ abatement costs (5% discount rate) under the Zero Carbon (blue) and 100% Renewable (green) scenarios at different $CO_2$ reduction targets (compared to 2005 level). The corresponding renewable shares of the 100% Renewable scenario are also indicated by texts on the upper right side (the numbers in the texts represent renewable share in 2050, for example, RE-100 stands for 100% renewable share in 2050). The horizontal lines represent costs of BECCS[142] and DACCS[143] for capturing and storing 1 metric ton of $CO_2$ which were collected from literature (Supplementary Table 5).

We further compare the incremental $CO_2$ abatement costs with the costs of capturing and sequestering carbon (collected from existing literature) using bioenergy with carbon capture and storage (BECCS) and direct air carbon capture and storage (DACCS). We find that the incremental $CO_2$ abatement costs exceed the lower bound of BECCS cost (\$52/t $CO_2$) at about 93% (corresponding to about 92% renewable share) and 96% $CO_2$ reduction levels for the 100% Renewable and Zero Carbon scenarios, respectively, indicating the possible economic advantage of BECCS as a carbon mitigation strategy beyond those $CO_2$ reduction levels. The cost of DACCS has higher lower bound (\$114/t $CO_2$), so DACCS may become an option for mitigating the last 0.4% $CO_2$ emission only under the 100% Renewable scenario (Figure 5b). However, $CO_2$ abatement costs never exceed the more conservative high cost estimates for BECCS and DACCS, indicating that substantial cost reductions are necessary for these technologies to be competitive.

### *D. Discussion*

In this study, we have shown that achieving a 100% $CO_2$ reduction in the U.S. electricity system by 2050 incurs \$335–\$494 billion additional costs over a 30-year period under two scenarios that transition towards different sources of low-carbon electricity. The additional costs are mainly driven by the capital investment in renewable generation technologies, battery storage, and transmission. Our conclusion aligns with the findings from many previous studies [10,42,132,144,145], albeit with lower abatement costs compared to the study of Cole et al., 2021 due to the nearer-term focus[42]. This work, on the other hand, also contradicts with the studies that show economic benefits of 100% renewable electricity system compared to the business-as-usual counterpart[125,43,146,147]. The difference can be attributed to several reasons, including that: 1. These studies performed single-year simulations for the target year and applied the LCOE-based

cost metric without actually modelling the progressive capacity expansion over time; 2. These studies considered the demand response and demand-side electrification, which create flexible load and increase energy use efficiency, thus helping avoid significant electricity curtailment and over-building capacity, while our study does not incorporate those factors; 3. These studies also included external social costs (climate and health costs due to carbon emission and other air pollutions) which could be significantly reduced under the low-carbon transition of electricity system, leading to lower aggregated cost (including both energy and social costs) of the 100% renewable case.

Pursuing a 100% $CO_2$ reduction for the U.S. electric power sector can lead to additional system cost compared to the reference case, but the additional cost varies depending on the technologies being used. We find that the Zero Carbon scenario, which allows the use of nuclear and Gas-CC-CCS, can achieve the same $CO_2$ reduction target while reducing about 6% total system cost compared to the 100% Renewable scenario, and this cost reduction effect become significant when the decarbonization target reaches above 90% $CO_2$ reduction. This finding highlights a consistent conclusion in the literature that having more clean generation options available generally allows cost-savings and more reliable electricity supply than relying on a more limited technology suite [10,148,149,145,150].

Furthermore, the NETs, such as BECCS and DACCS, may have an economic advantage in mitigating the last few percent of $CO_2$ emission. Our results show that the incremental $CO_2$ abatement cost of the 100% Renewable scenario increases more rapidly for eliminating approximately the last 10% $CO_2$ emissions of the U.S. electricity system, and the incremental $CO_2$ abatement costs also exceed the minimum cost estimates of BECCS beyond the 93% $CO_2$ reduction level (99.6% $CO_2$ reduction level for DACCS), suggesting that the NETs could be

more cost-effective decarbonization options for the U.S. electricity system than renewable and storage technologies beyond these $CO_2$ reduction levels. A previous study that included NETs in power system modelling also confirmed that adding NETs to a mix of low-carbon generation technologies could lower the costs of deep decarbonization[133]. On the other hand, given the fact that both BECCS and DACCS are still emerging technologies, and their future deployments remain largely uncertain, the electricity system needs to pursue its sectoral effects in decarbonization through the deployment of renewable and energy storage technologies, instead of relying on NETs as a main option for carbon reduction. To better quantify the capacity and operation pattern of NETs required by the electricity system and how they interact with the rest of the electric power sector, future studies may continue to integrate NETs into the electricity system modelling with region-specific resource availability and more up-to-date cost and operation data of NETs as these technologies improve over time.

Last, our results show that that the unit cost of electricity generation varies across different regions in the contiguous U.S. Under the Zero Carbon and 100% Renewable scenarios, the eastern regions in general have higher reliance on the fossil fuel sources, leading to higher unit cost of electricity production compared to other regions. Regions also vary in their additional expenditures (additional unit cost relative to Reference) in different electricity technologies. For example, under the 100% Renewable scenario, the additional unit costs in south-eastern and south-western regions are dominantly by PV and battery storage, while the investment in wind electricity has much higher contribution to the additional costs in the central and north-eastern regions. Such regional heterogeneity of electricity cost provides valuable guidance for implementing regional specific policies to support the low-carbon electricity with the consideration of regional resource and technology availabilities. Note that this regional analysis

focuses only on the cost of electricity generation within each region, which provides information about the investment and cost in different generation and storage technologies within each region. However, the analysis does not consider electricity import and export across different regions and the subsequent cost and revenue, so regional unit costs do not necessarily reflect wholesale or retail electricity costs for consumers in that region.

In conclusion, this study evaluates selected pathways of reaching a zero-carbon electricity system in the contiguous U.S. and quantifies their costs. Pursuing such a target would incur additional cost to the U.S. electric power sector compared to a reference scenario, but we show that keeping the nuclear and allowing the use of natural gas with CCS during the decarbonization could reduce additional cost (as compared to a 100% renewable target), especially when decarbonization is above 90% $CO_2$ reduction. We also observed the possible economic advantage of NETs in mitigating the last few percent of $CO_2$ emission from the U.S. electricity system, and future studies may continue to integrate NETs into electricity system modelling to evaluate their role in a net-zero carbon electricity system.

## *E. Appendix*

### Supplementary Note 1 – The total cost of U.S. electricity system from 2020 to 2050

In this study, we calculated the total cost of U.S. electricity system incurred during 2020 and 2050, and we did not include the capital cost of all capacity being built before 2020. Therefore, the initial (base) year $t_0$ was assumed to be 2020, and the final year $t_f$ is 2050. The discount rates $d$ was assumed to be 5%. The economic lifetime $n$, which defines the number of years that the capital investment will be paid off, was assumed to be 20 years.

The model output of capital cost $C_{Cap,t,s}$ represents the total cost for building the new capacity at year *t* under scenario *s*. Firstly, we calculated the amortized capital cost $C_{Amotized\ Cap,t,s}$ by multiplying $C_{Cap,t,s}$ to capital recovery factor ($CRF$):

$$C_{Amotized\ Cap,t,s} = C_{Cap,t,s} \times CRF \quad (7)$$

$$CRF(d,n) = \frac{d}{1 - \frac{1}{(1+d)^n})} \quad (8)$$

Then, we calculated the annual capital cost by summing up all the amortized capital costs that would be paid off in the same year. Here, we divided the 30-year timeframe into two periods:

From 2020 to 2039:

$$C_{Annual\ Cap,t,s} = \sum_{t_0}^{t} C_{Amotized\ Cap,t,s} \quad (9)$$

From 2040 to 2050:

$$C_{Annual\ Cap,t,s} = \sum_{t-19}^{t} C_{Amotized\ Cap,t,s} \quad (10)$$

The other cost components, such as O&M and fuel costs, were assumed to be paid off in the year when they are incurred, so they were all considered as operational cost here. ReEDS simulates the results for the even years of the studied period, and we calculated the operational cost of the odd years by taking the average between the two closest even years. The annual

operational cost is represented as $C_{Op,t,s}$. Then, the annual total cost can be calculated by summing the annual capital cost and operational cost shown as follow:

$$C_{Total\ cost,t,s} = C_{Annual\ Cap,t,s} + C_{Op,t,s} \quad (11)$$

The annual total cost $C_{Total\ cost,t,s}$ here does not consider the time value of the investment, so we calculated the present value of annual total cost with the base year of 2020 and summed them up from 2020 to 2050 to get the total cost (present value) of the U.S. electricity system from 2020 to 2050 under scenario s $PV_{Total\ cost,s}$:

$$PV_{Total\ cost,s} = \sum_{t_0}^{t_f}(C_{Total\ cost,t,s} \times \frac{1}{(1+d)^{t-t_0}}) \quad (12)$$

**Supplementary Table 1. Delivered prices of coal for electric power sector under the reference and high oil and gas supply scenarios from Annual Energy Outlook 2020**[137]**.** In the ReEDS model, the reference coal price is calculated each of the nine U.S. Energy Information Administration (EIA) census divisions, while the low coal price is not provided. In this study, we first divide the annual coal price under high oil and gas supply scenario by the annual coal price under reference scenario (data showing in this table) to get the annual ratios between the coal price under the two scenarios. Then we multiply the ratios to the reference coal price (for nine EIA census divisions) used in the ReEDS model to get the low coal price projections (also for nine EIA census division), which is further used to develop the Coal scenario in this study.

| Year | Reference (2019 USD/MMBtu) | High oil and gas supply (2019 USD/MMBtu) |
|---|---|---|
| **2010** | 2.05 | 2.05 |
| **2011** | 2.05 | 2.05 |
| **2012** | 2.05 | 2.05 |
| **2013** | 2.05 | 2.05 |
| **2014** | 2.05 | 2.05 |
| **2015** | 2.05 | 2.05 |
| **2016** | 2.05 | 2.05 |
| **2017** | 2.05 | 2.05 |
| **2018** | 2.05 | 2.05 |
| **2019** | 2.05 | 2.05 |
| **2020** | 2.06 | 2.05 |
| **2021** | 2.03 | 2.01 |
| **2022** | 2.00 | 1.95 |
| **2023** | 1.98 | 1.92 |
| **2024** | 1.97 | 1.90 |
| **2025** | 1.95 | 1.86 |
| **2026** | 1.96 | 1.85 |
| **2027** | 1.97 | 1.86 |
| **2028** | 1.96 | 1.85 |
| **2029** | 1.96 | 1.85 |
| **2030** | 1.96 | 1.84 |
| **2031** | 1.95 | 1.83 |
| **2032** | 1.95 | 1.83 |
| **2033** | 1.96 | 1.83 |
| **2034** | 1.96 | 1.83 |
| **2035** | 1.95 | 1.82 |
| **2036** | 1.95 | 1.82 |
| **2037** | 1.96 | 1.83 |
| **2038** | 1.96 | 1.82 |
| **2039** | 1.95 | 1.82 |
| **2040** | 1.95 | 1.82 |
| **2041** | 1.95 | 1.81 |
| **2042** | 1.95 | 1.81 |

| | | |
|---|---|---|
| **2043** | 1.95 | 1.81 |
| **2044** | 1.95 | 1.80 |
| **2045** | 1.95 | 1.79 |
| **2046** | 1.95 | 1.79 |
| **2047** | 1.95 | 1.79 |
| **2048** | 1.95 | 1.78 |
| **2049** | 1.95 | 1.78 |
| **2050** | 1.95 | 1.77 |

**Supplementary Table 2. Annual renewable penetration (%) assumptions of U.S. electricity system.** The 100% penetration case is used to develop the 100% Renewable scenario, while the other penetration cases are used to develop a group of other renewable scenarios for calculating the marginal $CO_2$ abatement cost of 100% Renewable scenario.

| Year | 80% renewable penetration by 2050 | 90% renewable penetration by 2050 | 95% renewable penetration by 2050 | 99% renewable penetration by 2050 | 100% renewable penetration by 2050 |
|---|---|---|---|---|---|
| **2020** | 20.0% | 20.0% | 20.0% | 20.0% | 20.0% |
| **2021** | 22.0% | 22.3% | 22.5% | 23.0% | 23.8% |
| **2022** | 24.0% | 24.7% | 25.0% | 27.0% | 27.5% |
| **2023** | 26.0% | 27.0% | 27.5% | 30.0% | 31.3% |
| **2024** | 28.0% | 29.3% | 30.0% | 34.0% | 35.0% |
| **2025** | 30.0% | 31.7% | 32.5% | 37.0% | 38.8% |
| **2026** | 32.0% | 34.0% | 35.0% | 40.0% | 42.5% |
| **2027** | 34.0% | 36.3% | 37.5% | 44.0% | 46.3% |
| **2028** | 36.0% | 38.7% | 40.0% | 47.0% | 50.0% |
| **2029** | 38.0% | 41.0% | 42.5% | 51.0% | 53.8% |
| **2030** | 40.0% | 43.3% | 45.0% | 54.0% | 57.5% |
| **2031** | 42.0% | 45.7% | 47.5% | 58.0% | 61.3% |
| **2032** | 44.0% | 48.0% | 50.0% | 61.0% | 65.0% |
| **2033** | 46.0% | 50.3% | 52.5% | 64.0% | 68.8% |
| **2034** | 48.0% | 52.7% | 55.0% | 68.0% | 72.5% |
| **2035** | 50.0% | 55.0% | 57.5% | 71.0% | 76.3% |
| **2036** | 52.0% | 57.3% | 60.0% | 75.0% | 80.0% |
| **2037** | 54.0% | 59.7% | 62.5% | 78.0% | 83.8% |
| **2038** | 56.0% | 62.0% | 65.0% | 81.0% | 87.5% |
| **2039** | 58.0% | 64.3% | 67.5% | 85.0% | 91.3% |
| **2040** | 60.0% | 66.7% | 70.0% | 88.0% | 95.0% |
| **2041** | 62.0% | 69.0% | 72.5% | 92.0% | 95.5% |
| **2042** | 64.0% | 71.3% | 75.0% | 95.0% | 96.0% |
| **2043** | 66.0% | 73.7% | 77.5% | 95.5% | 96.5% |
| **2044** | 68.0% | 76.0% | 80.0% | 96.0% | 97.0% |
| **2045** | 70.0% | 78.3% | 82.5% | 96.5% | 97.5% |
| **2046** | 72.0% | 80.7% | 85.0% | 97.0% | 98.0% |
| **2047** | 74.0% | 83.0% | 87.5% | 97.5% | 98.5% |
| **2048** | 76.0% | 85.3% | 90.0% | 98.0% | 99.0% |
| **2049** | 78.0% | 87.7% | 92.5% | 98.5% | 99.5% |
| **2050** | 80.0% | 90.0% | 95.0% | 99.0% | 100.0% |

**Supplementary Table 3. Annual $CO_2$ emission constraints (Gt) of U.S. electricity system.** 87%, 92%, 94%, 99%, and 100% represent the reduction target of $CO_2$ emission by 2050 relative to 2005 level. These $CO_2$ emission constraints are the projected $CO_2$ emission output of the renewable scenarios (matches 80%, 90%, 95%, 99%, and 100% renewable penetration assumptions, respectively) based on renewable penetration assumptions described in Supplementary Table 1. The 100% $CO_2$ reduction case is used to develop the Zero Carbon scenario, while the other $CO_2$ reduction cases are used to develop a group of $CO_2$ reduction scenarios for calculating the marginal $CO_2$ abatement cost of Zero Carbon scenario.

| Year | 87% $CO_2$ reduction target | 92% $CO_2$ reduction target | 94% $CO_2$ reduction target | 99% $CO_2$ reduction target | 100% $CO_2$ reduction target |
|---|---|---|---|---|---|
| **2010** | 2459.7 | 2459.7 | 2459.7 | 2459.7 | 2459.7 |
| **2011** | 2181.5 | 2182.5 | 2183.9 | 2183.9 | 2183.9 |
| **2012** | 1903.2 | 1905.2 | 1908.0 | 1908.0 | 1908.0 |
| **2013** | 2091.3 | 2092.6 | 2094.6 | 2094.6 | 2094.6 |
| **2014** | 2279.4 | 2280.1 | 2281.2 | 2281.2 | 2281.2 |
| **2015** | 1982.4 | 1985.5 | 1989.0 | 1989.0 | 1989.0 |
| **2016** | 1685.4 | 1690.9 | 1696.9 | 1696.9 | 1696.9 |
| **2017** | 1712.1 | 1716.6 | 1721.4 | 1721.4 | 1721.4 |
| **2018** | 1738.9 | 1742.2 | 1745.9 | 1745.9 | 1745.9 |
| **2019** | 1568.3 | 1574.6 | 1580.5 | 1580.5 | 1580.5 |
| **2020** | 1397.8 | 1406.9 | 1415.1 | 1415.1 | 1415.1 |
| **2021** | 1403.9 | 1396.0 | 1400.0 | 1373.9 | 1363.0 |
| **2022** | 1410.0 | 1385.1 | 1384.8 | 1332.7 | 1310.8 |
| **2023** | 1395.3 | 1368.4 | 1352.9 | 1264.0 | 1232.5 |
| **2024** | 1380.6 | 1351.7 | 1321.0 | 1195.4 | 1154.1 |
| **2025** | 1357.4 | 1314.3 | 1280.5 | 1123.0 | 1071.5 |
| **2026** | 1334.1 | 1276.9 | 1240.0 | 1050.5 | 988.9 |
| **2027** | 1304.0 | 1222.3 | 1187.8 | 967.4 | 898.6 |
| **2028** | 1273.9 | 1167.7 | 1135.6 | 884.2 | 808.3 |
| **2029** | 1225.3 | 1119.8 | 1070.5 | 798.8 | 704.7 |
| **2030** | 1176.7 | 1071.8 | 1005.3 | 713.3 | 601.1 |
| **2031** | 1119.5 | 999.1 | 939.4 | 622.0 | 538.2 |
| **2032** | 1062.3 | 926.4 | 873.5 | 530.8 | 475.3 |
| **2033** | 1007.8 | 862.7 | 803.5 | 479.1 | 421.7 |
| **2034** | 953.3 | 799.0 | 733.4 | 427.4 | 368.1 |
| **2035** | 913.9 | 758.9 | 683.6 | 396.6 | 340.8 |
| **2036** | 874.4 | 718.7 | 633.7 | 365.9 | 313.6 |
| **2037** | 829.6 | 654.5 | 574.7 | 338.6 | 280.2 |
| **2038** | 784.9 | 590.4 | 515.7 | 311.4 | 246.9 |
| **2039** | 731.1 | 540.4 | 485.7 | 277.2 | 187.0 |
| **2040** | 677.3 | 490.4 | 455.7 | 243.1 | 127.2 |
| **2041** | 628.6 | 463.8 | 426.1 | 188.4 | 112.6 |
| **2042** | 580.0 | 437.1 | 396.5 | 133.7 | 98.0 |
| **2043** | 542.8 | 396.8 | 359.3 | 118.7 | 88.1 |

| | | | | | |
|---|---|---|---|---|---|
| **2044** | 505.5 | 356.5 | 322.1 | 103.6 | 78.2 |
| **2045** | 471.8 | 319.8 | 283.9 | 92.9 | 64.8 |
| **2046** | 438.1 | 283.1 | 245.7 | 82.2 | 51.4 |
| **2047** | 409.6 | 258.3 | 214.5 | 67.2 | 35.9 |
| **2048** | 381.0 | 233.4 | 183.3 | 52.2 | 20.3 |
| **2049** | 352.6 | 208.9 | 162.6 | 36.5 | 10.2 |
| **2050** | 324.1 | 184.5 | 141.9 | 20.9 | 0.0 |

a. Annual renewable penetration (%) assumptions of U.S. electricity system.

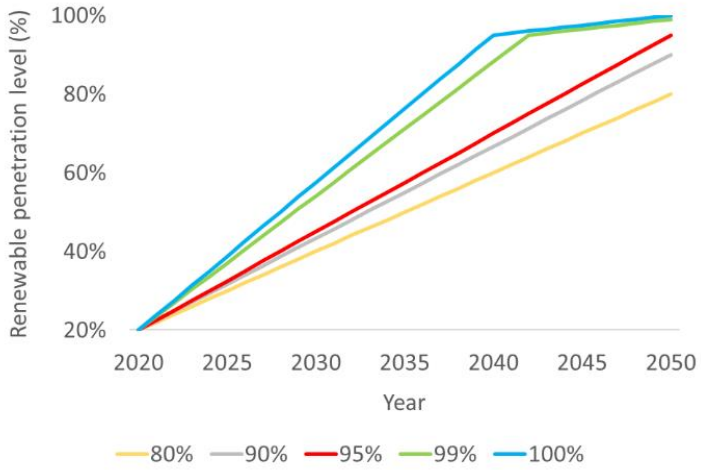


b. Annual $CO_2$ emission constraints (Gt) of U.S. electricity system.

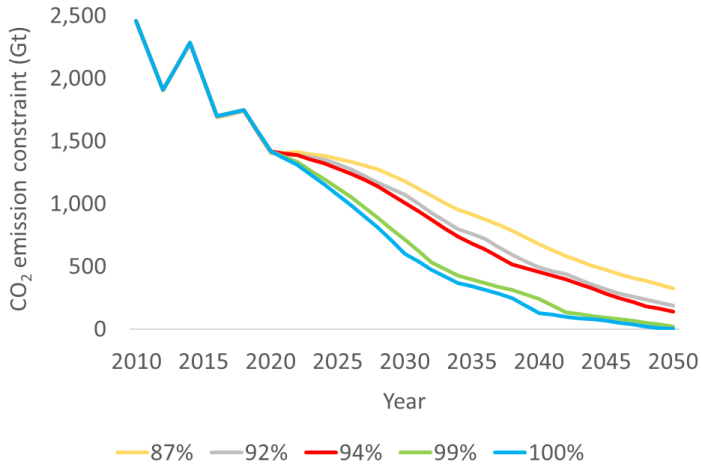


**Supplementary Figure 1. Annual renewable penetration assumptions (a) and annual $CO_2$ emission constraints (b) of U.S. electricity system showing in figures.**

**Supplementary Table 4. Electricity generation and storage technologies considered in this study.**

| **Main categories** | **Technologies** |
|---|---|
| Fossil fuel sources | Coal,<br>Natural gas combustion turbine (Gas-CT),<br>Nature gas combined cycle (Gas-CC),<br>Natural gas combined cycle with carbon capture and storage (Gas-CC-CCS),<br>Oil-Gas-Steam |
| Renewable sources | Biopower,<br>Geothermal,<br>Hydropower,<br>Landfill gas,<br>Commercial combined cycle gas power plant fired with renewable fuels (RE-CC)<br>Commercial gas combustion turbine fired with renewable fuels (RE-CT)<br>Concentrated solar power (CSP),<br>Offshore wind,<br>Land-based wind,<br>Photovoltaic (PV), |
| Nuclear source | Nuclear |
| Storage | Battery storage with 2-, 4-, 6-, 8- and 10-hour duration.<br>Pumped-storage hydropower (PSH) |

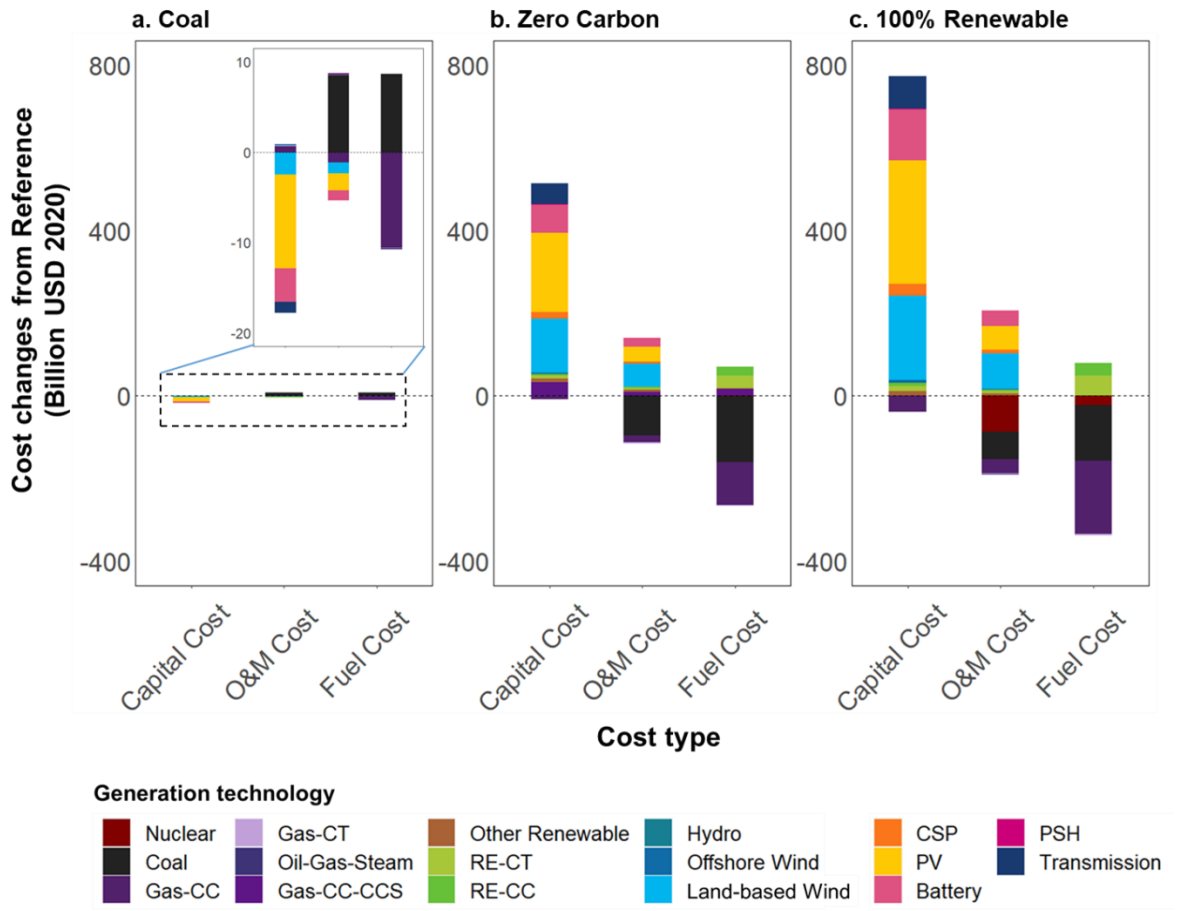


**Supplementary Figure 2. The changes of total costs of the Coal (a), Zero Carbon (b), and 100% Renewable (c) scenarios from the Reference scenario (breakdown by cost and technology types).** Three bars in each panel represent the changes of capital cost, O&M cost, and fuel cost at each scenario from 2020 to 2050, and each cost type is broken down by technologies in different colours. The costs are present value (2020 US$) based on 5% discount rate.

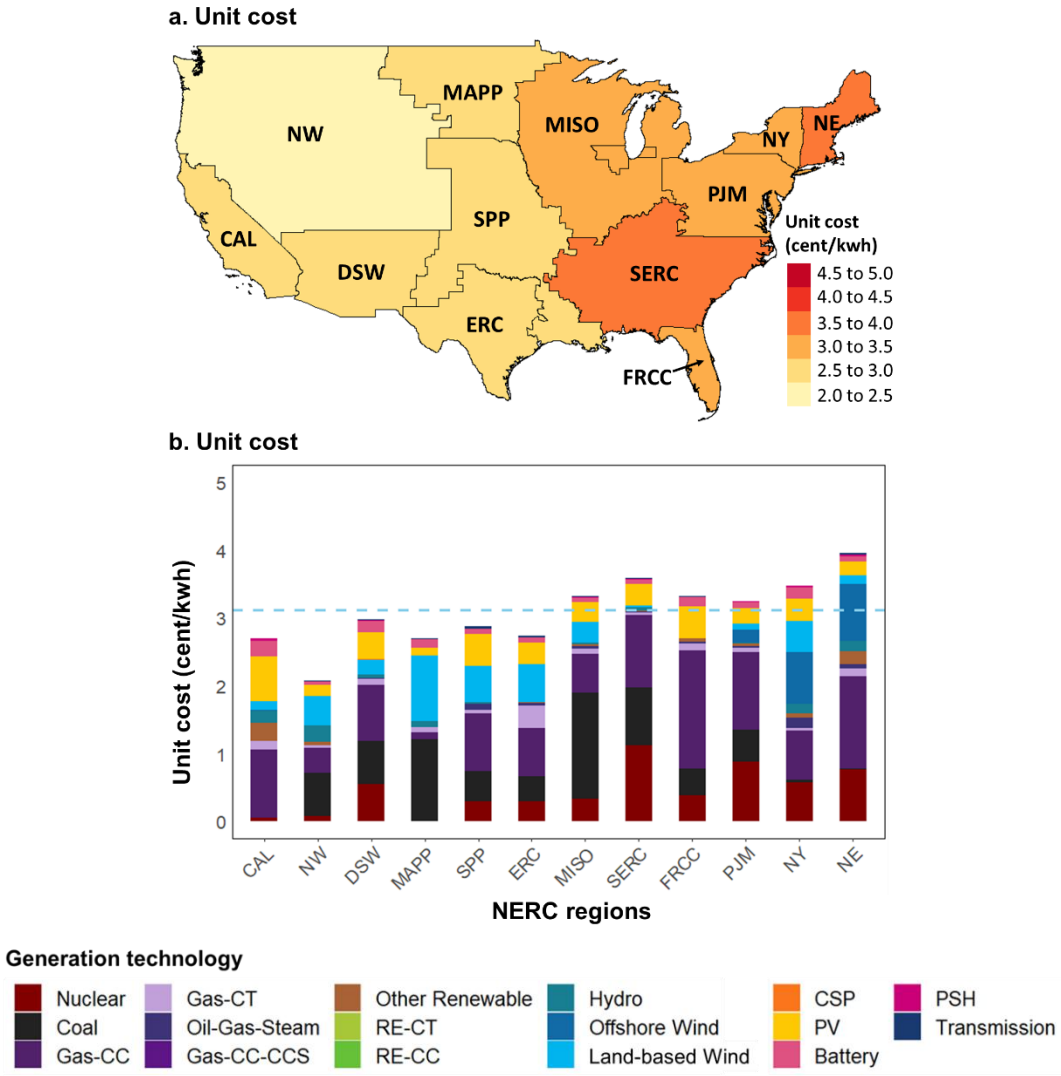


**Supplementary Figure 3. The unit costs of electricity under the Reference scenario at 12 North American Electric Reliability Corporation (NERC) regions across the U.S.** The map plot (a) shows the costs at different regions, and the bar plot (b) shows the contribution of different technologies to the costs. The dash lines in the bar plot shows the average unit costs at the national level. The cost only includes the capital cost, O&M cost, and fuel cost of the electricity system, but it does not consider the electricity import and export among different NERC regions, therefore the revenue and payment associated with electricity import and export are not included in the cost presented here. The costs are present value (2020 US$) based on 5% discount rate.

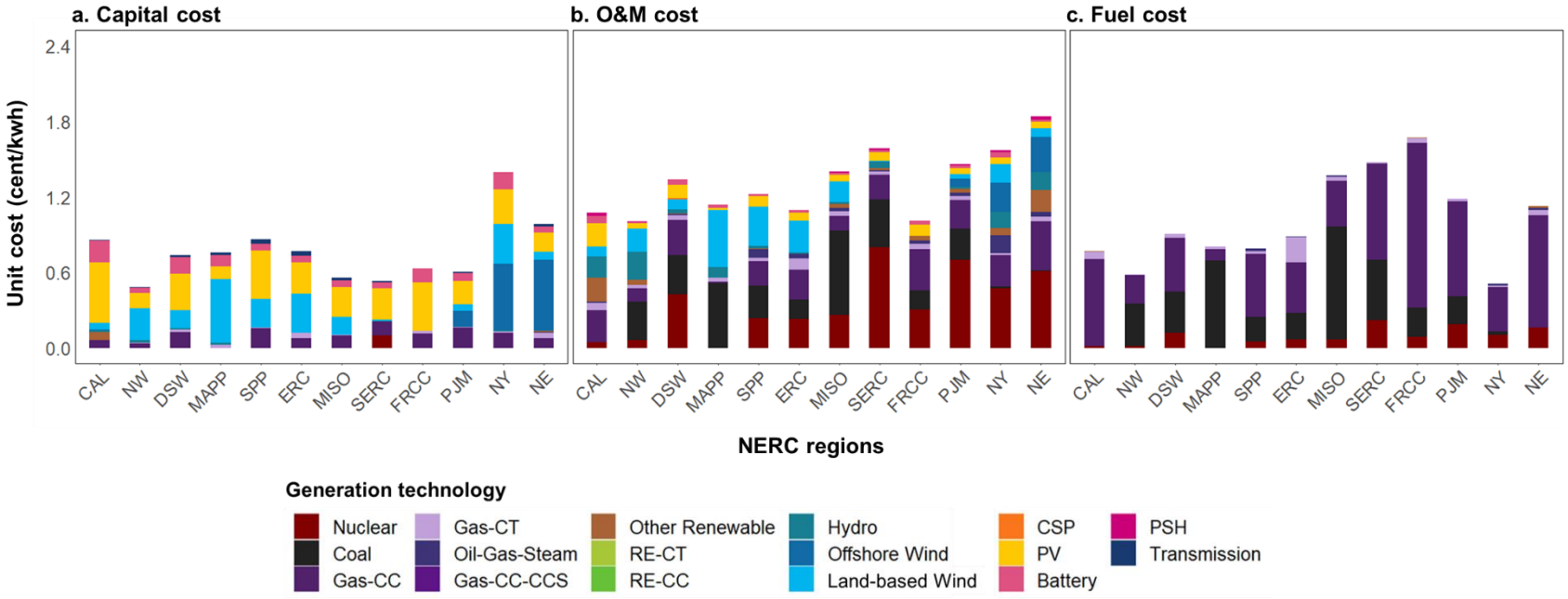


**Supplementary Figure 4. The unit capital cost (a), O&M cost (b), and fuel cost (c) under the Reference scenarios at 12 NERC regions across the U.S.** The unit costs are present value (2020 US$) based on 5% discount rate.

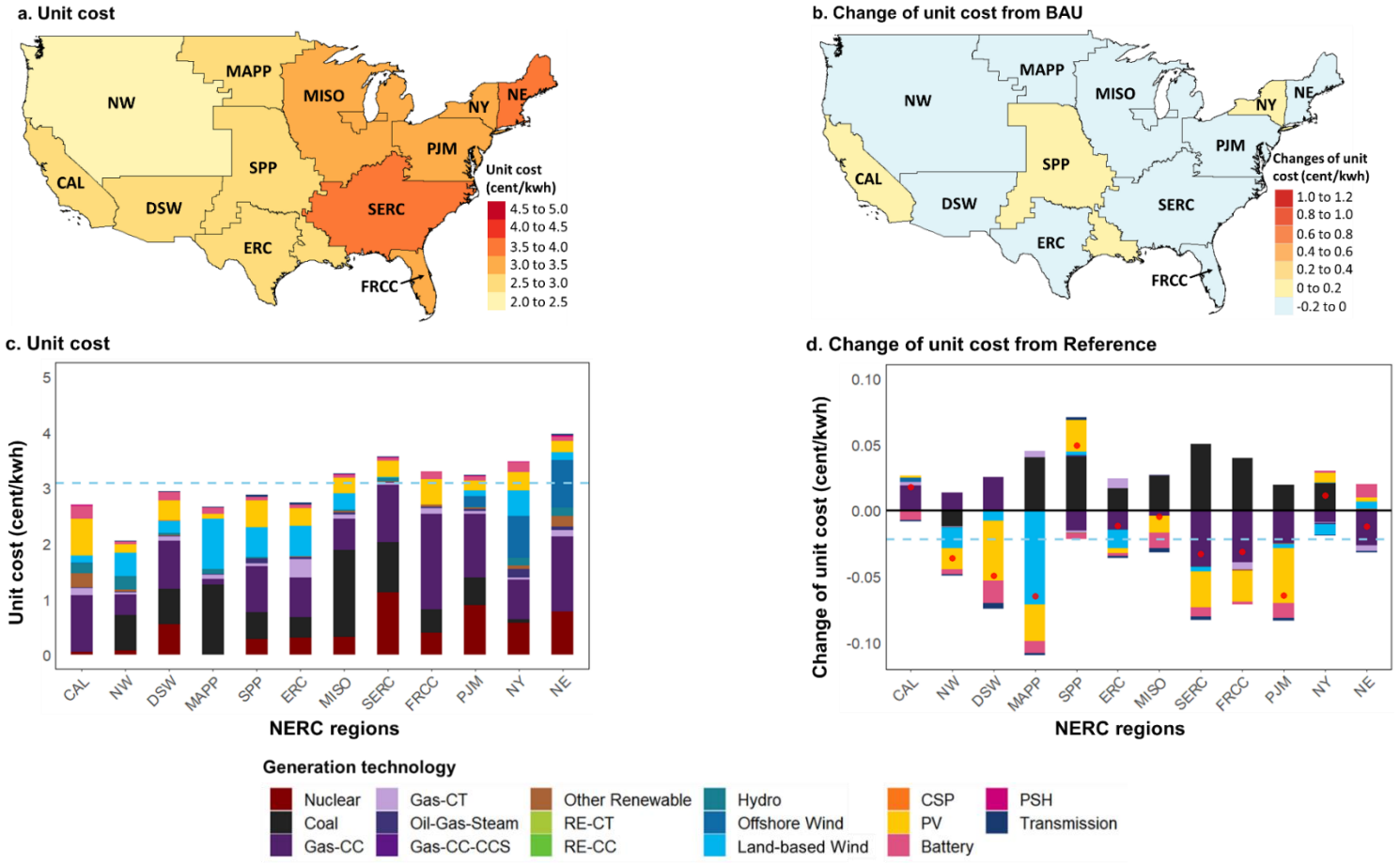


**Supplementary Figure 5. The unit costs of electricity generation (a, c) under the Coal scenario and their changes relative to the Reference scenario (b, d) at 12 NERC regions across the U.S.** The map plots (a, b) show the costs at different regions, and the bar plots (c, d) show the contribution of different technologies to the costs. The dash lines in the bar plots show the average costs at the national level. The red dot in plot (d) shows the net additional unit cost at different NERC regions. The cost only includes the capital cost, O&M cost, and fuel cost of the electricity system, but it does not consider the electricity import and export among different NERC regions, therefore the revenue and payment associated with electricity import and export are not included in the cost presented here. The costs are present value (2020 US$) based on 5% discount rate.

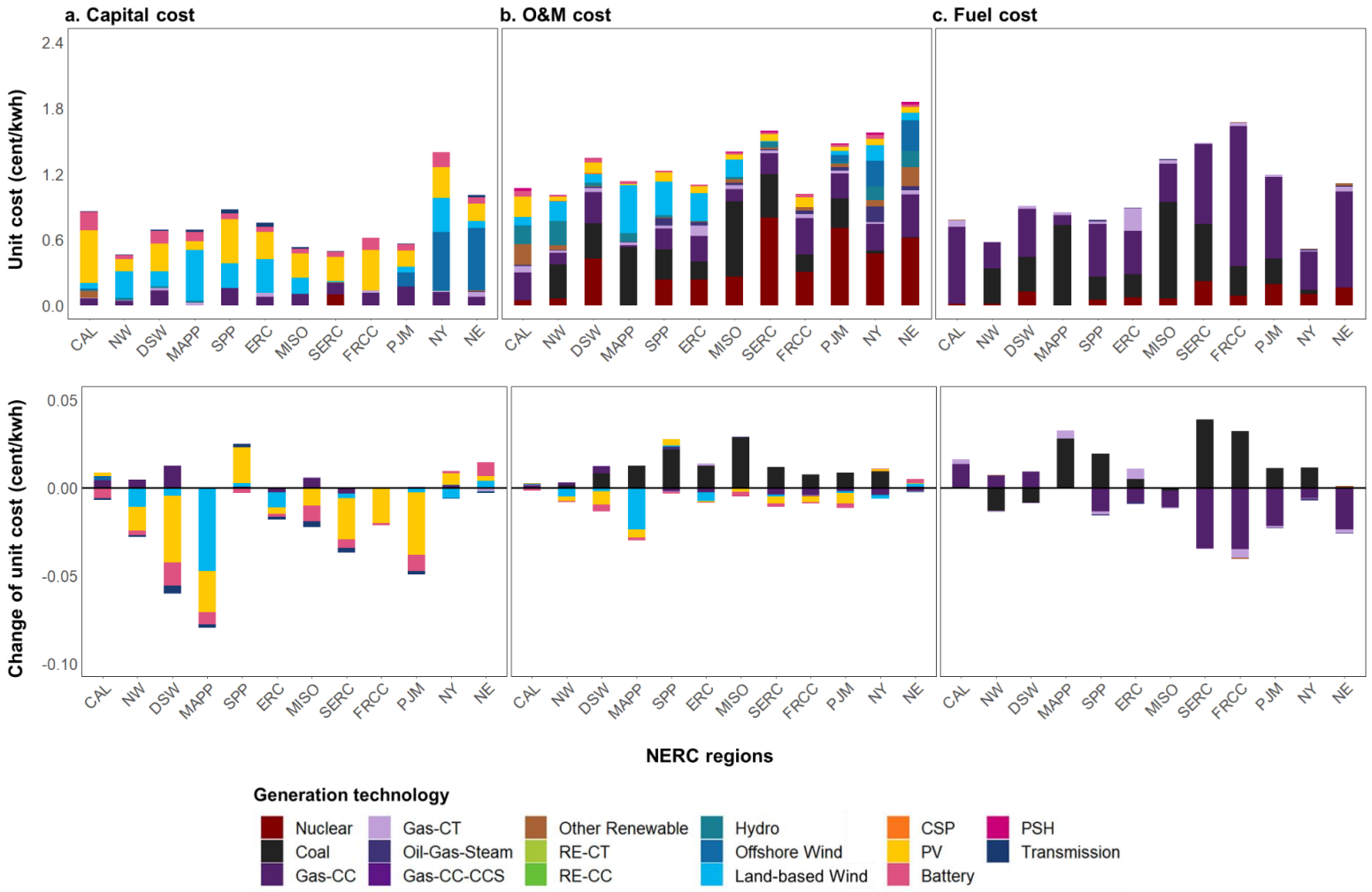


**Supplementary Figure 6. The unit cost and their changes relative to the Refernece scenario under the COAL scenario at 12 NERC regions across the U.S.** The upper three plots represent the unit cost broken down into capital cost (a), O&M cost (b), and fuel cost (c), while the lower three plots represent the change of unit cost broken down into capital cost (a), O&M cost (b), and fuel cost (c). These costs are present value (2020 US$) based on 5% discount rate.

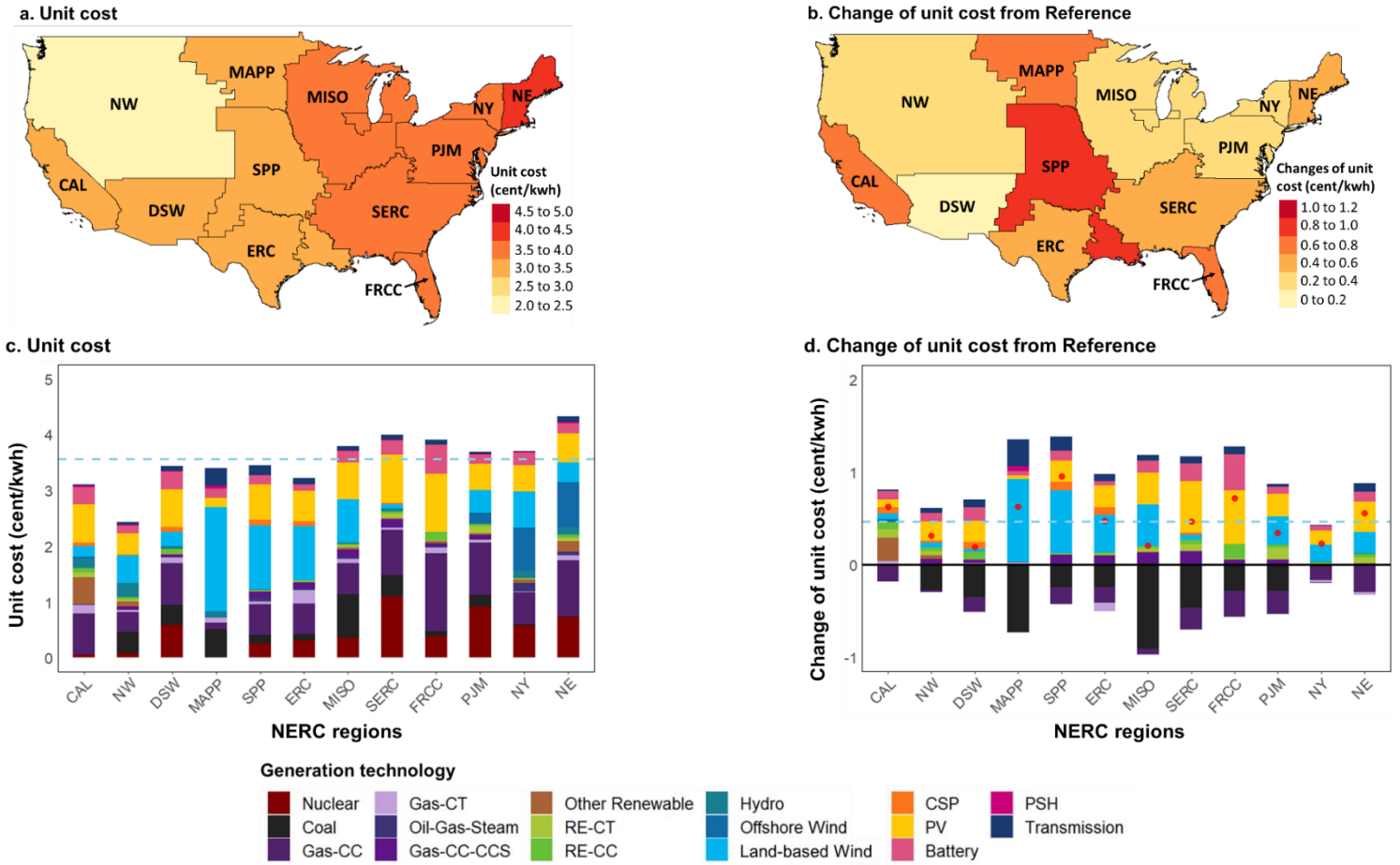


**Supplementary Figure 7. The unit costs of electricity generation (a, c) under the Zero Carbon scenario and their changes relative to the Reference scenario (b, d) at 12 NERC regions across the U.S.** The map plots (a, b) show the costs at different regions, and the bar plots (c, d) show the contribution of different technologies to the costs. The dash lines in the bar plots show the average costs at the national level. The red dot in plot (d) shows the net additional unit cost at different NERC regions. The cost only includes the capital cost, O&M cost, and fuel cost of the electricity system, but it does not consider the electricity import and export among different NERC regions, therefore the revenue and payment associated with electricity import and export are not included in the cost presented here. The costs are present value (2020 US$) based on 5% discount rate.

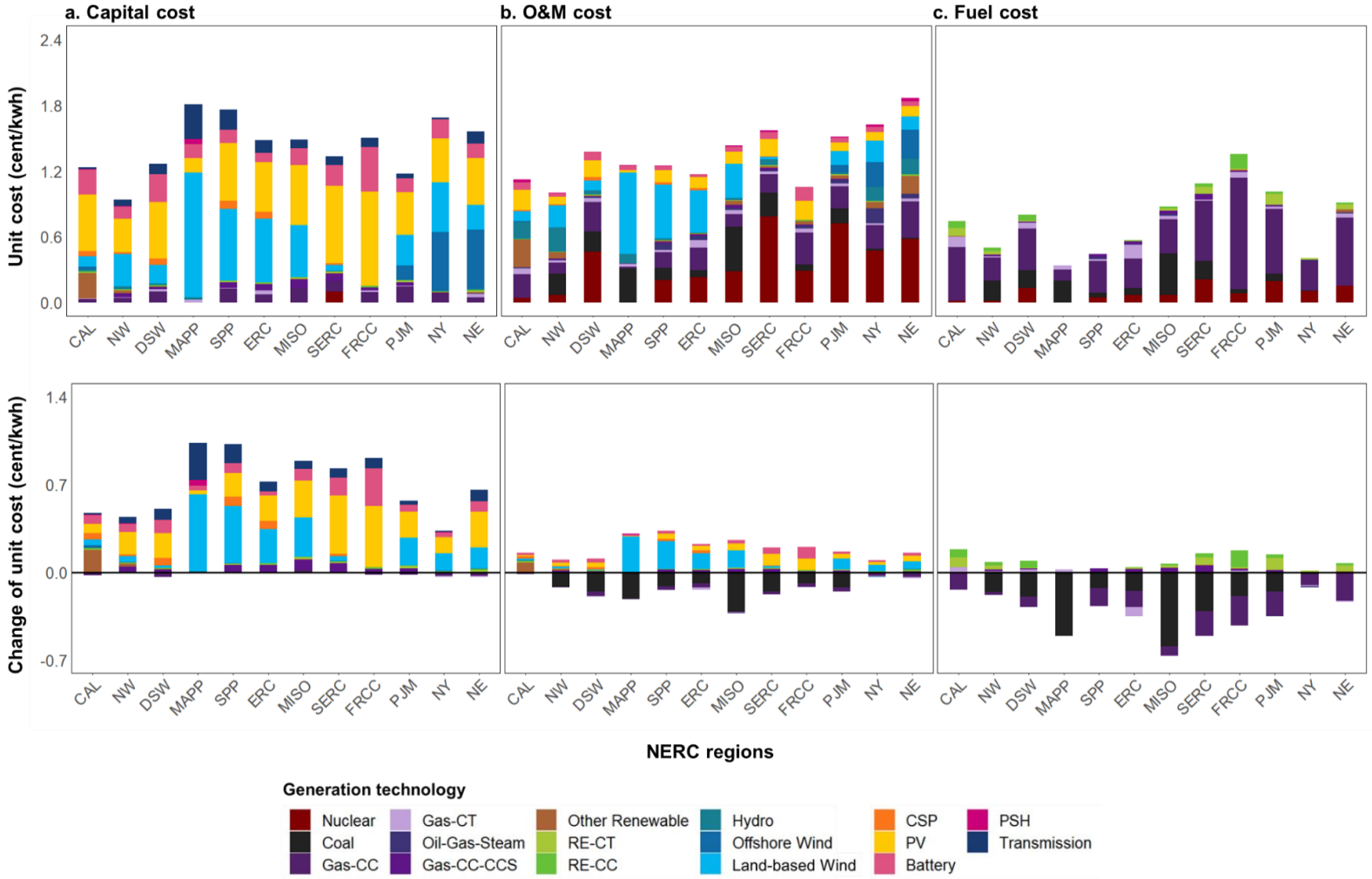


**Supplementary Figure 8. The unit cost and their changes relative to the Reference scenario under the Zero Carbon scenario at 12 NERC regions across the U.S.** The upper three plots represent the unit cost broken down into capital cost (a), O&M cost (b), and fuel cost (c), while the lower three plots represent the change of unit cost broken down into capital cost (a), O&M cost (b), and fuel cost (c). These costs are present value (2020 US$) based on 5% discount rate.

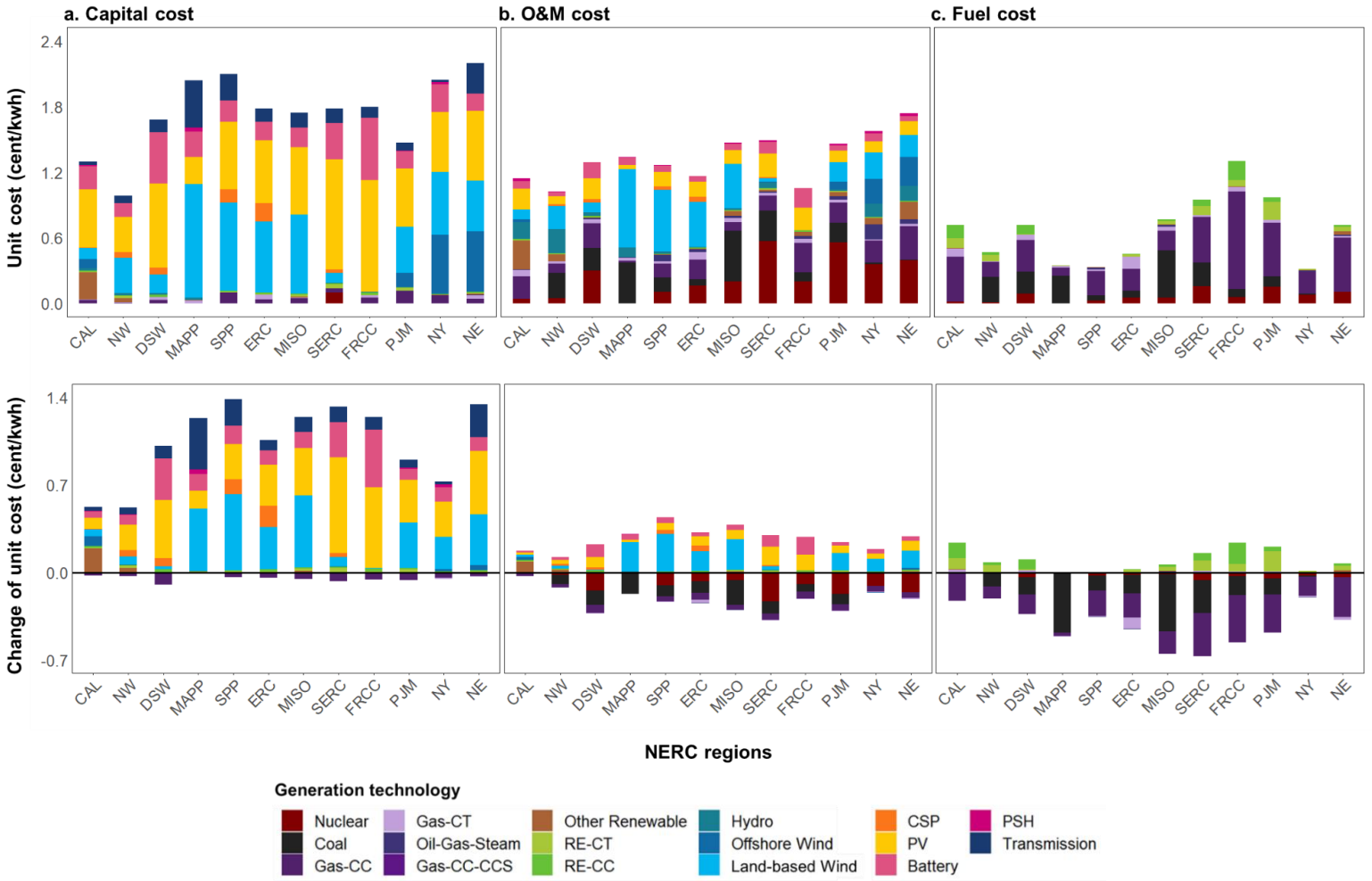


**Supplementary Figure 9. The unit cost and their changes relative to the Reference scenario under the 100% Renewable scenario at 12 NERC regions across the U.S.** The upper three plots represent the unit cost broken down into capital cost (a), O&M cost (b), and fuel cost (c), while the lower three plots represent the change of unit cost broken down into capital cost (a), O&M cost (b), and fuel cost (c). These costs are present value (2020 US$) based on 5% discount rate.

**Supplementary Table 5. Cost of capturing and storing 1 metric ton of $CO_2$ using bioenergy with carbon capture and storage (BECCS) and direct air carbon capture and storage (DACCS) technologies.**

| **Technologies** | | **Cost** |
|---|---|---|
| BECCS | | \$45–\$250/t $CO_2$ (2012 USD*)[142] |
| DACCS** | Direct air capture | \$94–\$232/t $CO_2$ (2016 USD)[143] |
| | Storage | \$11/t $CO_2$ (2018 USD)[151] |

* The cost data of BECCS provided in Caldecott et al, 2015[142] was collected from another study[152] published in 2012. Because the study did not indicate the year of the monetary value, so we assume it to be 2012, which is the year when the study is published.
** The cost of DACCS was calculated by the summing the cost of capturing and storing 1 metric ton of $CO_2$.

# IV. Environmental trade-offs of direct air capture in climate change mitigation toward 2100

Material from:

Qiu, Y., Lamers, P., Daioglou, V., McQueen, N., de Boer, H. S., Harmsen, M., ... & Suh, S. (2022). Environmental trade-offs of direct air capture technologies in climate change mitigation toward 2100. Nature Communications, 13(1), 1-13.

https://doi.org/10.1038/s41467-022-31146-1



**Abstract.** Direct air carbon capture and storage (DACCS) is critical for achieving stringent climate targets, yet the environmental implications of its large-scale deployment have not been evaluated in this context. Performing a prospective life cycle assessment for two promising technologies in a series of climate change mitigation scenarios, we find that electricity sector decarbonization and DACCS technology improvements are both indispensable to avoid environmental problem-shifting. Decarbonizing the electricity sector improves the sequestration efficiency, but also increases the terrestrial ecotoxicity and metal depletion levels per tonne of $CO_2$ sequestered via DACCS. These increases can be reduced by improvements in DAC material and energy use efficiencies. DACCS exhibits regional environmental impact variations, highlighting the importance of smart siting related to energy system planning and integration. DACCS deployment aids the achievement of long-term climate targets, its environmental and climate performance however depend on sectoral mitigation actions, and thus should not suggest a relaxation of sectoral decarbonization targets.

### *A. Introduction*

Climate change mitigation scenarios used by the Intergovernmental Panel on Climate Change (IPCC)[3] suggest that a rapid decarbonization in energy and material related services is likely to be insufficient to keep global mean temperature increase well below 2°C by the end of the 21st century. The remaining global carbon budget of 420-1,170 gigatonnes (Gt) $CO_2$ is expected to be depleted in 10-30 years under present annual emission rates and projected Nationally Determined Contributions (NDCs)[153]. Most IPCC emission scenarios overshoot the carbon budget at first and then remove excess carbon via Carbon Dioxide Removal (CDR) technologies, i.e., intentional efforts to remove $CO_2$ from the atmosphere and store it on land or in the oceans on the order of 200-1,200 Gt $CO_2$ toward the year 2100[153].

CDR strategies include the enhancement of natural above- and belowground carbon sinks in plants, rock formations, and soils as well as scalable engineering solutions designed to sequester, store, or utilize concentrated atmospheric $CO_2$. Direct Air Capture (DAC), despite being at an early stage of development, is gaining increasing attention and recognized as a promising climate change mitigation strategy[3]. Given the homogeneous atmospheric $CO_2$ concentration levels around the world, DAC facilities can be deployed in locations that provide abundant cheap and carbon-free energy and/or that are close to pipeline infrastructure, underground storage, or utilization facilities for reducing the $CO_2$ transportation cost[154]. Also, compared to bioenergy with carbon capture and storage (BECCS), an alternate CDR technology facilitating stringent mitigation targets[155], DAC is expected to have much lower footprints in water and land uses[156], reducing concerns around food security and biodiversity loss[157].

Direct Air Carbon Capture and Storage (DACCS) uses chemical or physical processes to separate $CO_2$ from ambient air and sequesters it permanently in geological storage sites. Due to

the highly dilute nature of atmospheric $CO_2$ (currently around 415 parts per million), DACCS technologies require substantial energy and material inputs, so their future deployment and role in climate change mitigation will depend heavily on process-design and resulting technoeconomic and environmental performances[154]. Two types of technologies are presently considered promising from a technoeconomic perspective: solvent-based DACCS, typically relying on aqueous hydroxide solutions (potassium hydroxide, sodium hydroxide) for capturing $CO_2$[158–161], and sorbent-based DACCS, mostly using amine materials bonded to a wide range of porous solid supports[162–165]. Solvent-based DACCS requires dedicated high-temperature (900°C) heat for $CO_2$ regeneration[161]. Thus, from a thermodynamic perspective, heat supply options are largely limited to combusting energy dense fuels such as (renewable) natural gas or (renewable) hydrogen, while electric resistance heating and electrochemical regeneration approaches are in development. Sorbent-based DACCS can function with low temperature (80-120°C) heat for $CO_2$ regeneration[166], offering a larger variety of thermal energy supply options (e.g., heat pump, geothermal, and industrial waste heat).

A growing number of studies have included DACCS in integrated assessment modelling (IAM) scenarios. They highlight the critical role of DACCS in meeting stringent climate targets, but they also reveal the trade-offs of deploying DACCS, which, on the one hand, could reduce mitigation cost and relax the competition for land-use. On the other hand, large scale DACCS deployment and operation could also require large amounts of additional energy[15,20,167,168]. Depending on the modeling approach and scenario, these studies project that the DACCS deployment levels for meeting a 2°C or stricter climate target by 2100 can reach up to 40 Gt of annual $CO_2$ sequestration[167,20,15,169]. At this scale, DACCS (assuming a solvent-based process) could consume up to 12% and 60% global electric and non-electric energy by 2100[20,19]. Evidently, for DACCS

facilities connected to electric power grids, their environmental performance will depend on the electricity system context in which they will operate. Previous studies have shown that DACCS can achieve negative emissions, but capture efficiencies are sensitive to the operational efficiency and the energy source[18,170–172]. A recent life cycle assessment (LCA) of DACCS technologies also identified potential environmental trade-offs in increased land transformation if DACCS is operated by solar electricity (as compared to using grid electricity)[173]. These studies, however, assume DACCS is powered either by a specific generation technology or static electricity systems. Thus, they neither reveal how environmental impacts of DACCS might change with energy system transitions following stringent mitigation scenarios[3], nor do they quantify the potential broader environmental trade-offs of power system transitions with and without DACCS deployment in such scenarios toward 2100. Also, these studies do not fully account for long-term potential technological improvements of DACCS, which are expected to affect the environmental impacts of technologies by changing their physical material and energy inputs[33,31,94].

Here, we calculate a prospective LCA of DACCS under climate change mitigation scenarios developed by the IMAGE 3.2 Integrated Assessment Model[174,175] which are consistent with the climate targets of the Paris Agreement. IMAGE 3.2 has been used to project future energy supply, conversion, and demand toward 2100 across 26 global regions based on the demographic, economic, technological and behavioral narratives of the Shared Socioeconomic Pathways (SSPs)[176,177]. This study uses the 'Middle of the Road' pathway (SSP2), which assumes future developments in-line with historical patterns. This is then linked with climate targets defined by the Representative Concentration Pathways (RCPs)[178] to determine required carbon prices which lead to changes in the energy system consistent with the achievement of specific climate targets. We use three distinct scenarios: An SSP2 baseline without any climate

policies and measures to limit radiative forcing or to enhance adaptive capacity (*SSP2-baseline*). An SSP2 baseline linked with a strict climate change mitigation effort to limit global warming to less than 1.5°C, i.e., a radiative forcing level of 1.9 W/m$^2$ (RCP1.9), by 2100, allowing DACCS as a CDR option (*SSP2-RCP1.9 w/ DACCS*). Finally, a counterfactual that follows the same socioeconomic and climate change mitigation target but does not feature DACCS as a CDR option (*SSP2-RCP1.9 w/o DACCS*).

In an LCA study, the technological changes in both background and foreground systems can affect the environmental impacts of the studied object. The foreground system consists of processes directly related to the object, while the background system includes the upstream or downstream processes in the supply chain that are indirectly related to the object[179,180]. Here, we adapt a novel and open-source LCA framework[35,181] to modify electricity-related data in the background LCI database using regionally and temporally explicit IMAGE projections (on electricity mix, generation efficiency, and electricity-associated emissions) from 2020 to 2100 under the three scenarios. The regional impacts are differentiated for the United States (US) and compared to China, Russia, Western Europe, and a global average. Changes in the foreground material and energy inputs of the two technologies (solvent- and sorbent-based DACCS) over the same period are estimated based on the IMAGE projection of global DACCS deployment using a one-factor learning curve approach. We thus assume a commercial-scale operation and technology improvements via learning-by-doing. To capture the uncertainty related to the specific future learning rates, we apply different rates as part of a sensitivity analysis. Two types of heat supply options are also considered for solvent- (natural gas or biomethane) and sorbent-based DACCS (biomethane or heat pump) to understand how heat sources affect their environmental profiles. Furthermore, we also quantify the effect of DACCS deployment on the

changes in power system loads, grid mixes, and related shifts in environmental impacts by comparing the strict mitigation scenario (*SSP2-RCP1.9*) with and without DACCS as a CDR option.

The following sections outline the mutual dependence between the electricity system and DACCS technologies. First, we compare and evaluate the effects of the electricity system evolution (background dynamics) vs. DACCS technology learning (foreground dynamics) on the environmental impact per tonne of $CO_2$ sequestered. Second, we quantify the effects of DACCS deployment on electricity demand, grid mix, and the environmental impacts per kWh of electricity generated. These results are illustrated in a US context. Following, we present the environmental impacts of DACCS in a global context by comparing results across four world regions before the paper closes with a discussion on implications and policy recommendations.

### *B. Methods and Data*

In this study, we adapt a cradle-to-grave LCA framework that evaluates temporal- and regional-explicit environmental impacts of direct air carbon capture and storage (DACCS) in future electricity systems projected by climate mitigation contexts[35]. The dynamic framework aligns the temporal dimensions of the foreground technology learning and the background electricity system contexts. The life cycle impacts for the respective DACCS technologies are calculated using Python-coded LCA framework Brightway2[182] based on foreground life cycle inventory (LCI) of DACCS systems and background LCI data from the ecoinvent database3.6[183]. The (background) electricity system context is provided by TIMER, the energy module of the IMAGE3.2 Integrated Assessment Model (IAM)[175]. TIMER develops regionally and temporally explicit projections on electricity mix, generation efficiency, and electricity-associated emissions, and these outputs are incorporated into another python-coded framework (Wurst)[35] to

update the electricity-related LCI in the ecoinvent database, which is then reflected in the Brightway2 calculated impacts per DACCS technology and time-step. The calculations are performed for 10-year timesteps from 2020 to 2100.

1. Models

*IMAGE 3.2* is an IAM framework developed to describe the relationships between humans and natural systems and the impacts of these relationships on the provision of ecosystem services to sustain human development[175]. The energy module of IMAGE 3.2, TIMER, is a recursive dynamic (i.e. no-foresight) energy system model representing the global energy system, disaggregated across 26 global regions, with projections till 2100[175]. It includes fossil and renewable primary energy carriers (coal, heavy/light oil, natural gas, modern/traditional biomass, nuclear, concentrated/photovoltaic solar, onshore/offshore wind, hydropower, and geothermal). Primary energy carriers can be converted to secondary and final energy carriers (solids, liquids, electricity, hydrogen, heat) to provide energy services for different end-use sectors (heavy industry, transport, residential, services, chemicals and other). The model projects future (useful) energy demand for each end-use sector (industry, transport, residential, commercial, other) based on relationships between energy services and activity, the latter of which is related to economic growth. For each demand sector, secondary energy carriers (including solid and liquid biofuels) compete based on relative costs with each other to meet the useful energy demand. The energy system representation of the IMAGE model does include demand elasticity with carbon prices. This is represented via two distinct mechanisms: (i) Investment in energy efficiency, and (ii) reduced demand in energy services (i.e., reducing consumption and foregoing activities and amenities which demand energy/emissions). The former is represented via technological options (i.e., invest in insulation, more efficient technologies, etc.) and the latter is represented based on

econometric data. Energy prices are based on supply curves of energy carriers[184,185]. For non-renewable sources, these are formulated in terms of cumulative extraction; while for renewable sources, these are formulated in terms of annual production [186–188].

*Brightway2* is an open source framework for Life Cycle Assessment (LCA) calculations in Python[182]. It consists of several modules that handles data import, managing and accessing data, calculating, and analyzing LCA results. The combination of a modular structure, the interactivity of Python, and tunable calculation pathways allows for flexibility and user-defined functionalities in conducting LCA studies and offers new possibilities compared to existing LCA tools.

*Wurst* is also a Python-based software that enables the systematic modification of life cycle inventory (LCI) databases with external scenario data[35]. Wurst supports several generic modification types, including changing material efficiency, emissions, relative shares of markets inputs, and separating a global dataset into multiple regions. The current version of Wurst focuses on modifying the ecoinvent LCI database using IMAGE scenario data. More detailed information regarding modification steps of Wurst are discussed in the "LCI database modifications with climate scenario data" section.

2. Scenario description

*Baseline scenario (SSP2)* projections assume no climate policy whatsoever, thus acting as a counterfactual to which policy efforts can be compared. The *RCP1.9 scenarios* project the required effort needed to meet a climate target, defined as an emission budget consistent with a 1.5˚C global mean temperature increase. These scenarios also include current climate policy, per region, as defined by the NDCs[189]. For the *RCP1.9 scenarios,* the IMAGE model determines the additional effort needed to meet the 1.5˚C target, represented by emission price projection across all GHG

emission sources (fossil fuels, industry, and land use), applied globally, resulting in a cost-effective mitigation pathway. The emission price can reduce emissions via two mechanisms: (i) the increase in aggregate energy costs promotes investments in energy efficiency, (ii) by attaching this price to the carbon content of primary energy carriers, and it affects their competitiveness at meeting final energy demand services, thus promoting cleaner energy carriers. The application of an emission price makes DACCS competitive as it is assumed that sequestered carbon is renumerated, thus overcoming capital and variable costs (which in turn are affected by the projected cost of energy supply and technological learning). We present two RCP1.9 variations (*SSP2-RCP1.9 w/ DACCS* and *SSP2-RCP1.9 w/o DACCS*) to determine the impact of DACCS availability on climate change mitigation strategies. Regional cost-effectiveness in DACCS depends on capital and O&M costs (including endogenous learning-by doing reductions), electricity price, and $CO_2$ transport and storage costs linked to storage potential limitations[190]. A single DACCS technology (with technology parameters and cost data based on plant capacity of 1 Mt $CO_2$/year) is included in IMAGE, represented by aggregate of different solvent-based technologies summarized in previous studies[159,191,192], but we assume that the DACCS deployment result estimated by IMAGE will represents the total deployment of a wide range of DACCS technologies (including both solvent- and sorbent-based DACCS). In IMAGE, it is assumed that DACCS is not available before 2030, and its global growth rate is limited to 1 $GtCO_2$/year. This growth rate limit is a binding constraint in the projection once DACCS becomes cost effective, while in the long-term storage potential limitation may limit its further expansion. DACCS becomes cost effective when emission prices exceed approximately \$300/$tCO_2$. This emission price is surpassed in 2050 for both *SSP2-RCP1.9 w/ DACCS* and *SSP2-RCP1.9 w/o DACCS.* In the long-term, the application of DACCS limits the growth of the emission price, projected to be \$423/$tCO_2$ and \$885/$tCO_2$ 2100 for *SSP2-RCP1.9 w/*

*DACCS* and *SSP2-RCP1.9 w/o DACCS* respectively. By calculating the differences of electricity generation and the associated environmental impacts between the two RCP1.9 variations, we can also evaluate the effect of DACCS deployment on the electricity and energy demand systems.

3. Technology assumptions and details of DACCS systems

We focus on two types of DACCS technologies: a solvent-based and a sorbent-based DACCS, which rely on different capture and release mechanisms to remove $CO_2$ from the atmosphere.

*Solvent-based DACCS* applies aqueous hydroxide solutions (potassium hydroxide, sodium hydroxide) to capture atmospheric $CO_2$ via a chemical reaction[158–161]. Here, we assume the solvent-based DACCS uses potassium hydroxide solution for $CO_2$ capture. In an air contactor, the potassium hydroxide solution reacts with $CO_2$ and forms potassium carbonate, which then, in a separate reactor, reacts with calcium hydroxide and generates calcium carbonate. The calcium carbonate precipitates, and potassium hydroxide solution can be regenerated and recycled back to the air contactor. The precipitated calcium carbonate is collected, dried, and then calcined under high temperature (about 900 °C) heat, which is typically provided by natural gas combustion in pure oxygen, to release the $CO_2$. The $CO_2$ released from calcium carbonate and the $CO_2$ generated by natural gas combustion are mixed and collected for further storage[161]. The high temperature heat requirements limit the heat supply options for solvent-based DACCS. In this study, we consider natural and renewable gas (biomethane) as the two heat options for the solvent-based DACCS (Supplementary Figure 1). Other proposed methods include electric resistance heating and electrochemical regeneration, which were not studied here.

Sorbent-based DACCS typically uses amine materials bonded to a wide range of porous solid supports for $CO_2$ capture[162–165]. Here, we considered the use of amine-based silica as the solid

sorbent[18]. The process consists of two main steps that operate cyclically: adsorption and desorption. In the adsorption step, a fan blows air through the air contactor, and the $CO_2$ in the air reacts with the sorbent and binds to it. When the solid sorbent has been saturated with $CO_2$, the desorption step will start in the air collector. Before heat is supplied, a vacuum is pulled to remove residual air from the contactor and decrease the temperature required for regeneration. Then, heat at about 100°C will be supplied into the air contactor to desorb the $CO_2$. The collected $CO_2$ will then go through a cooling unit, where extra moisture can be removed through condensation and $CO_2$ will be brought to ambient temperature. In the desorption step, the temperature of heat is about 80 – 120°C, so a wide variety of thermal energy sources (natural gas, heat pump, geothermal heat, and waste heat) can be used as the heat supply. Here, we model heat pump (with coefficient of performance of 2.5[18]) and renewable gas (biomethane) as the two main options (Supplementary Figure 1).

*$CO_2$ transport and storage*. Once the $CO_2$ is released from either process, we assume the $CO_2$ flow will be compressed through a compressor to 11 MPa and then transported through a pipeline to the storage site. The length of the transport pipeline is assumed to be 50 km. At the storage site, the $CO_2$ will be further compressed to 15 MPa and injected into a geological reservoir through wells with the depth of 3 km each. Here, the $CO_2$ will be permanently stored as supercritical phase[193](Supplementary Figure 1).

4. Life cycle impact assessment

The system boundary starts at the inlet air with a $CO_2$ concentration being 415 ppm, and is followed by $CO_2$ capture, regeneration, compression, transport, and ends with geological storage. Our analysis also accounts for upstream emissions due to indirect energy demands for the construction of energy conversion technologies, fuel production and handling. The functional unit

is capturing and sequestering one metric tonne (1t) of atmospheric $CO_2$ by DACCS technologies. The LCI data of the two studied DACCS technologies and subsequent compression and storage were collected from literature or estimated through bottoms-up materials requirements analysis (with the assumed plant capacities of 1 Mt $CO_2$ and 0.1 Mt $CO_2$ per year for solvent- and sorbent-based DACCS respectively), which are discussed in detail in *Supplementary Note 2*. The LCI data are assumed to represent the status quo material and energy consumptions over the life cycle of the two selected DACCS technologies. ReCiPe 2016 v1.1 hierarchist perspective is used as the characterization method to convert emissions and natural resource extractions to environmental impact categories at mid-point level[194].

In this study, when we compare the environmental impacts of DACCS under different electricity decarbonization pathways (*SSP2-baseline* vs *SSP-RCP1.9 w/ DACCS*), the results are calculated based on static LCI data of DACCS that represent their current material and energy uses without considering technology learning. Then, we also calculated another set of LCA results for DACCS under *SSP-RCP1.9 w/ DACCS* scenario based on dynamic LCI data that are estimated using learning curve approach, so it captures the effects of both background electricity decarbonization and foreground technology learning. By comparing the LCA results of DACCS calculated using static and dynamic LCI data under *SSP-RCP1.9 w/ DACCS* scenario, we can evaluate and compare the effects of background electricity decarbonization and foreground technology learning on the environmental impacts of DACCS.

5. Technology learning of DACCS systems

The learning curve approach has been used as an empirical method to study the unit cost reduction over time with cumulative production increases for a wide range of manufacturing[195] and energy technologies[196]. The learning effect can be characterized by various mechanisms,

including technology advancement, increased labor productivity, economies-of-scale, and improved material and energy efficiency. The learning curve approach has also been acknowledged as one critical means to explore the future expected life cycle impacts of present-day emerging technologies[197,198]. Here, we apply the one-factor learning curve approach to inform our prospective LCA. While the two technologies under investigation are presently operating in pilot- or demonstration scale, we assume a commercial-scale operation for both and apply constant learning rates, affecting the future life cycle material and energy consumption. Yet, for both technologies assessed herein, these learning effect on material and energy consumption are missing in the published literature. Thus, we assumed changes of material and energy consumption proportional to the changes of unit cost for the DACCS technologies.

It has been shown that the capital costs of solvent- and sorbent-based DACCS are likely to follow different learning rates given their different design characteristics. The solvent-based DACCS is site-built and large-scale, benefitting from economy of scale, but it is also less likely to incorporate rapid design or manufacturing improvement, while sorbent-based DACCS is based on standardized and modular units, and these units can be mass-produced and deployed, which enables fast iteration and learning[199]. Therefore, we assumed the average learning rates of 10% and 15% for the material and energy consumption that are related to capital investment for solvent- and sorbent-based DACCS, respectively. Then, as for the material and energy consumption related to operational costs, we assumed average learning rates of 2.5% for both solvent- and sorbent-based DACCS, respectively. We also consider variation ranges for the learning rates to reflect their uncertainty (Supplementary Table 10), these variation ranges are used to develop a sensitivity analysis to understand how speed of learning affect the environmental impacts of DACCS. Furthermore, to avoid unrealistic reduction of material and

energy consumption under technology learning, we also set up minimum material and energy use factors of both DACCS technologies based on experts' estimation. As for the solvent-based DACCS, the lower bound of material and energy uses related to capital and operational costs cannot be lower than 44% and 50% of their original amounts, respectively, and the sorbent-based DACCS, the lower bound of material and energy uses related to capital and operational costs cannot be lower than 18% and 50% of their original amounts in 2020, respectively. To incorporate the minimum material and energy use factors into the learning curve formula, we adjusted the learning curve formula into the following Eq. 1:

$$D_{i,t} = (D_{i,0} - D_{i,min}) \times (1 - LR_i)^{log_2(X_t/X_0)} + D_{i,min} \quad (1)$$

In equation (1), $X_0$ represents the initial DAC deployment capacity at year 0; $X_t$ represents the cumulative DAC deployment capacity at year $t$. For a specific material or energy item $i$, $LR_i$ represents the learning rate of the item $i$; $D_{i,0}$ typically represents the unit consumption of the material or energy item $i$ at year 0 (corresponding to the initial $CO_2$ capture $X_0$). Here our goal is to calculate the material and energy use factors (instead of actual unit consumption) under technology learning, so we normalize the $D_{i,0}$ to be 1; $D_{i,t}$ is also a normalized material and energy use factors of item $i$ at year $t$ (corresponding to the cumulative $CO_2$ capture $X_t$); $D_{i,min}$ represents the minimum material and energy use factors of item $i$.

Finally, we assume that solvent- and sorbent-based DACCS each account for half of the global cumulative capacity of DACCS (IMAGE model outputs), respectively. Then, we estimated material and energy use factors for both solvent- and sorbent-based DACCS from 2020 to 2100 based on their cumulative capacity, and the results are presented in Supplementary Table 11. By multiplying the material and energy use factors at a specific year to the actual unit material and energy consumption at the initial year, we can get the actual unit material and

energy consumption in that specific year. Assumptions on technology learning rates and minimum material and energy use factors of solvent- and sorbent-based DACCS are discussed in detail in *Supplementary Note 3*.

6. LCI database modifications with climate scenario data

The ecoinvent database[23] is the most widely used LCI database which offers fully interlinked unit process supply chains for products presented in the database. It covers all relevant environmental flows, material and energy inputs, and products of around 18,000 activities, where researchers can collect data about the supply chain to form a comprehensive background system in an LCA study. However, since the data in ecoinvent are usually collected in a specific year, the database describes the material and energy flows among processes based on an existing supply chain system. Therefore, the ecoinvent database is limited in conducting prospective LCA studies, which assess the environmental impacts associated to future technologies or emerging technologies that evolve over time.

Here, to evaluate the environmental impacts of DACCS technologies in a context of a changing background electricity system, we adapt a novel approach (Wurst)[35] that systematically integrates the IMAGE projections on electricity mix, generation efficiency, and electricity-associated emissions with the ecoinvent database, and change the parameters in electricity-related activity data in the ecoinvent database. Due to the differences of generation technologies between IMAGE and ecoinvent database, we develop a matching list to map the available technologies for both data sources (*Supplementary Note 4*). More detailed information regarding parameter modification for ecoinvent database using Wurst can be found in a previous study[35]. After the parameter modification, we developed 27 versions of ecoinvent databases, which

correspond to 9 different years from 2020 to 2100 under the *SSP2-baseline, SSP2-RCP1.9 w/ DACCS,* and *SSP2-RCP1.9 w/o DACCS* scenarios.

### *C. Results*

1. Prospective life-cycle environmental impacts of DACCS in the US

DACCS achieves net negative greenhouse gas (GHG) emissions across all technologies and heat sources investigated per metric tonne (1t) of atmospheric $CO_2$ captured and geologically sequestered in a US context by 2020. The net sequestration efficiency varies by DACCS technology and heat source (Figure 1a) with life cycle climate change impacts ranging from -0.36 to -0.94t $CO_2$-eq for a baseline grid-mix in 2020 (Figure 1a). Net GHG negative implies that the DACCS technologies release less GHG emissions than they capture and geologically sequester over the plants' life cycle (cradle-to-grave approach). The influence of different background electricity system contexts can be seen by comparing results for the *SSP2-baseline* vs. the *SSP2-RCP1.9 w/ DACCS* scenarios. In the *SSP2-baseline*, the US electricity system reduces the share of coal generation from 31% in 2020 to 7% in 2100, while its combined share of nuclear and renewable generation increases from 35% to 61% over the same period (Figure 2a). As a result, the climate change impact of DACCS is further reduced to -0.72 to -1.12t $CO_2$-eq by 2100. The highest sequestration efficiency is achieved by solvent-based DACCS using biomethane as a heat source (SV+BM). Since the process collects and sequesters $CO_2$ released during the heat generation process step, using biomethane, a non-fossil, burden-free $CO_2$ fuel, creates a negative $CO_2$ emission profile beyond the 1t of atmospheric $CO_2$ sequestered.

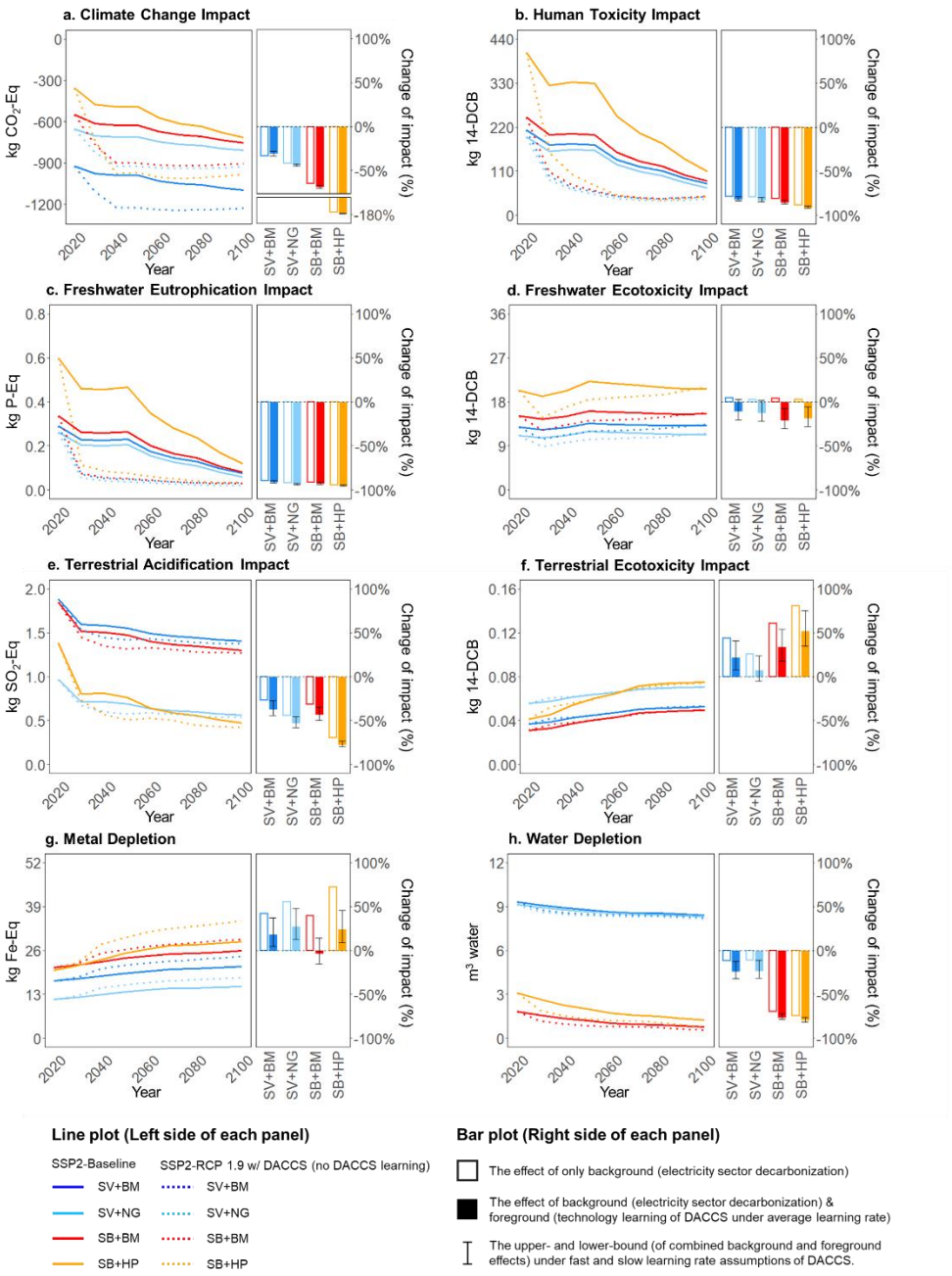


**Figure 1. Prospective LCA results of DACCS technologies (per 1 t atmospheric $CO_2$ captured and sequestered) from 2020 to 2100 considering background electricity sector decarbonization (US grid mix) and foreground technology learning of DACCS.** Solvent-based DACCS (SV) can use either biomethane (*SV+BM*) or natural gas (*SV+NG*) as a heat source. Sorbent-based DACCS (SB) can use either biomethane (*SB+BM*) or heat pump (*SB+HP*) as a heat source. In each panel, the line plot (left side of each panel) shows the trajectory of environmental impacts due to the electricity sector decarbonization (*SSP2-baseline* and *SSP2-RCP1.9 w/ DACCS*) excluding technological learning of DACCS. The bar plot (right side of each panel) includes technological learning of DACCS and thus compares the effects of the background and foreground systems (all under *SSP2-RCP1.9 w/ DACCS* scenario) on the environmental impacts of the four DACCS systems. The bars without color

filling (only with boarder color) mark the percentage changes of impacts in 2100 relative to the 2020 level only due to the background electricity sector decarbonization, while the bars with color filling mark the percentage changes of impacts in 2100 relative to the 2020 level due to both background electricity sector decarbonization and foreground technology learning (based on reference learning rates) of DACCS. The error bars (associated to the bars with color filling) represent the results under slow and fast learning rates (Supplementary Table 10).

In the *SSP2-RCP1.9 w/ DACCS* scenario, the US electricity sector achieves a full decarbonization by 2035 (Fig, 2d), which is in-line with current targets and an economy-wide decarbonization by 2050[200]. The scenario features an earlier phase-out of coal and natural gas (by 2050) and higher renewable energy penetration (81%) by 2100 (Figure 2c). In this scenario, the climate change impact of DACCS exhibits more rapid reductions before 2050 and reaches levels of -0.91 to -1.25 t $CO_2$-eq by 2100 (Figure 1a).

The life cycle human toxicity, freshwater eutrophication, terrestrial acidification, and water depletion of DACCS are sensitive to the shares of coal and natural gas generation in the electricity grid mix (Supplementary Figure 9). These impacts decrease from 2020 to 2100, showing environmental co-benefits with decarbonizing the power sector (Figure 1b, 1c, 1e, and 1h). Still, the US electricity system decarbonization creates environmental trade-offs for DACCS in other impact categories. We find increases for both terrestrial ecotoxicity (by 33%-80% across four DACCS-heat source combinations for both *SSP2-baseline* and *SSP2-RCP1.9 w/ DACCS scenarios*) and metal depletion levels (by 23%-42% and 40%-73% across four DACCS-heat source combinations for *SSP2-baseline* and *SSP2-RCP1.9 w/ DACCS scenario*, respectively) from 2020 to 2100 given the growing contributions from solar photovoltaic (PV) and wind energy generation in the background electricity system (Figure 2f, 2g, Supplementary Figure 9). The increased ecotoxicity impact in scenarios with high renewable energy generation is largely due to emissions from the production of silicon-based solar PV cells and copper processing (as copper is used for wiring in solar PV and wind turbines). The higher relative metal demand (per

kW installed) for the construction of solar PV and wind farms also increases mineral extraction. The electricity decarbonization barely affects the freshwater ecotoxicity of DACCS due to the counteracting effect of increased solar and wind penetrations (which raise the impact) and reduced coal generation (which decreases the impact) in the grid mix (Figure 2d, Supplementary Figure 9).

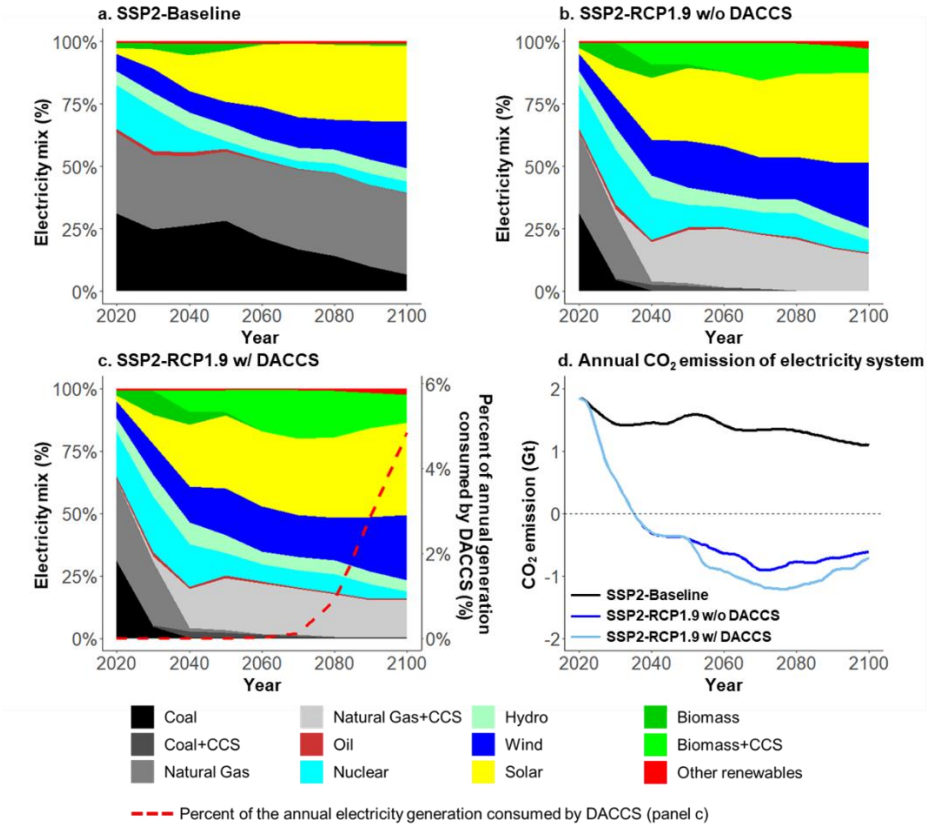


**Figure 2. The United States electricity mix under (a) SSP2-baseline, (b) SSP2-RCP1.9 w/o DACCS, (c) SSP2-RCP1.9 w/ DACCS scenarios and (d) the annual $CO_2$ emissions of the US electricity system under the three scenarios.** In the electricity mix panels (a, b, c), the stacked area represents the market shares of the grid mix. "Solar" includes both solar PV and concentrated solar power (CSP). "Oil" combines both oil with and without CCS as oil with CCS accounts for less than 1% of the grid mix. Other renewables include wave, tidal, and geothermal power. In panel c, the red dashed line shows the percent of the annual electricity generation consumed by DACCS, corresponding to the secondary y-axis.

The life cycle environmental impacts of DACCS are affected by the technology type and heat source. The sorbent-based DACCS + heat pump (*SB+HP*) system has the highest climate change

impact in 2020 because the heat is converted from fossil-dominated grid electricity, which has a higher carbon intensity than other heat supplies, but this impact is also more sensitive to electricity-sector decarbonization, so it shows a faster decrease over time. Under the *SSP2-RCP1.9 w/ DACCS* scenario, the climate change impact of the *SB+HP* system becomes the lowest compared to three other counterparts after 2040. For solvent-based DACCS, using biomethane as a heat source leads to a lower climate change impact than using natural gas due to the additional biogenic carbon sequestration. Hence, the *SV+BM* exhibits a lower life cycle climate change impact compared to the solvent-based DACCS system with natural gas (*SV+NG*) (Figure 2a).

As for other non-climate metrics, sorbent-based DACCS generally exhibits higher impacts in human toxicity, freshwater eutrophication and ecotoxicity, and metal depletion mainly due to its higher unit electricity consumption. In contrast, solvent-based DACCS shows a higher water depletion (per 1 t $CO_2$ captured, 3-12 times more than sorbent-based DACCS), because it captures $CO_2$ using aqueous hydroxide solution, which evaporates during the operation, while sorbent-based DACCS uses solid amine-based sorbents, which consumes much less water during the production and use phases. It has also been shown that, due to the affinity of amine sorbents for water, sorbent-based DACCS even co-produces water in humid environments, which can be used as fresh water or further purified into drinking water[166]. In terms of the heat source, solvent-based DACCS using natural gas heat has lower impacts for all studied categories compared to biomethane except for terrestrial ecotoxicity (higher impact due to the discarding of toxic drilling waste during natural gas production) and water depletion (which is more sensitive to the technology type than the heat source). Sorbent-based DACCS exhibits a lower environmental impact profile using biomethane for heat. The only increase compared to the heat pump derived

heat is terrestrial acidification, which is mostly driven by the anaerobic digestion of biowaste in biomethane production (Figure 2b-2h).

Our results show that continuous improvements via learning-by-doing can mitigate some environmental impacts. Under the *SSP2-RCP1.9 w/ DACCS* scenario, technology learning starts to reduce material and energy inputs after 2050 when DACCS is deployed on a large-scale worldwide (Supplementary Table 11). Still, the climate change, human toxicity, and freshwater eutrophication impacts are mainly attributable to the electricity consumption (Supplementary Figure 6) and the electricity sector decarbonization already decreases these impacts (of electricity generation) by more than 80% until 2050 (relative to 2020 levels) (Supplementary Figure 9). Therefore, DACCS technology learning contributes less than 10% of the total changes (over the 80 years) in these impacts (Figure 1a-c). While the electricity sector decarbonization increases freshwater ecotoxicity (slightly), terrestrial ecotoxicity, and metal depletion per tonne of $CO_2$ sequestered via DACCS from 2020 to 2100, improvements in material and energy efficiency, induced by learning effects, have the potential to offset the increases across these categories. A sensitivity analysis confirms the prominent effect of learning in these impacts. Varying the learning rates between lower- and upper-bounds (Supplementary Table 10) causes additional increases (13% to 23%) or decreases (-10% to -13%) to the total changes of these impacts, while varying the learning rates barely affects the total impact changes for climate change, human toxicity, and freshwater eutrophication. Water depletion of solvent-based DACCS shows higher sensitivity to the change of learning rates compared to that of sorbent-based DACCS (Figure 1h) as the solvent use accounts for more than 80% of the total water depletion for solvent-based DACCS (Supplementary Figure 6). So, reducing the water evaporation during the operation can be an important strategy to decrease the life cycle water depletion of solvent-based DACCS.

2. The impact of DACCS on the US electricity sector

The CDR capability provided by DACCS also affects the long-term development of the energy system. In our projections, carbon prices are used as a proxy to promote required changes in the energy system to limit emissions. Under the strict mitigation scenario with DACCS (*SSP2-RCP1.9 w/ DACCS*), DACCS deployment in the US starts around 2050, and its annual operational capacity reaches 0.85 $GtCO_2$/year by 2100 (Figure 3a), consuming about 5% (352 TWh) of annual US electricity generation (Figure 2c). The availability of DACCS essentially acts as a cap on the long-term carbon price, causing hard-to-abate sectors to offset their emissions using DACCS as opposed to investing in alternative technologies (e.g., electrification, energy efficiency improvement), and this leads to an increase in overall energy demand which is partially met by additional consumption of fossil fuel (natural gas, oil, and coal) (Supplementary Figure 7a). Consequently, these hard-to-abate sectors promote additional CDR deployment, which is first met by additional $CO_2$ sequestration from BECCS, which starts to increase after 2050, leading to an average 15% higher BECCS use as compared to the w/o DACCS scenario by 2080 (Supplementary Figure 8a). Subsequently, as DACCS capacity increases more rapidly after 2080 and gradually meets the additional CDR demand, the annual $CO_2$ sequestration from BECCS stabilizes around 1.3 $GtCO_2$/year by 2100, like the levels in the strict mitigation scenario without DACCS. It is important to note, that on a global scale, the requirement of BECCS is lower in the *SSP2-RCP1.9 w/ DACCS* scenario than in the *SSP2-RCP1.9 w/o DACCS* case (Supplementary Figure 8a).

The expansion of BECCS after 2050, peaking at 420 TWh/year by 2080, and reaching 113 TWh/year by 2100 is noticeable in the US generation mix when mapping out the differences between the two mitigation scenarios (Figure 3a). With DACCS, we also see that less electricity

is generated from natural gas with carbon capture and storage (CCS) and nuclear during the same period, and the annual US electricity generation drops consistently during the BECCS expansion phase until 2080 (at -160 TWh/year or -2.3% compared to the without DACCS case). Thereafter, the rapid increase of DACCS operational capacity and the respective increase in electricity demand narrows the demand gap between the two scenarios. By 2100, 35 TWh/year of additional electricity are required under a mitigation scenario with DACCS.

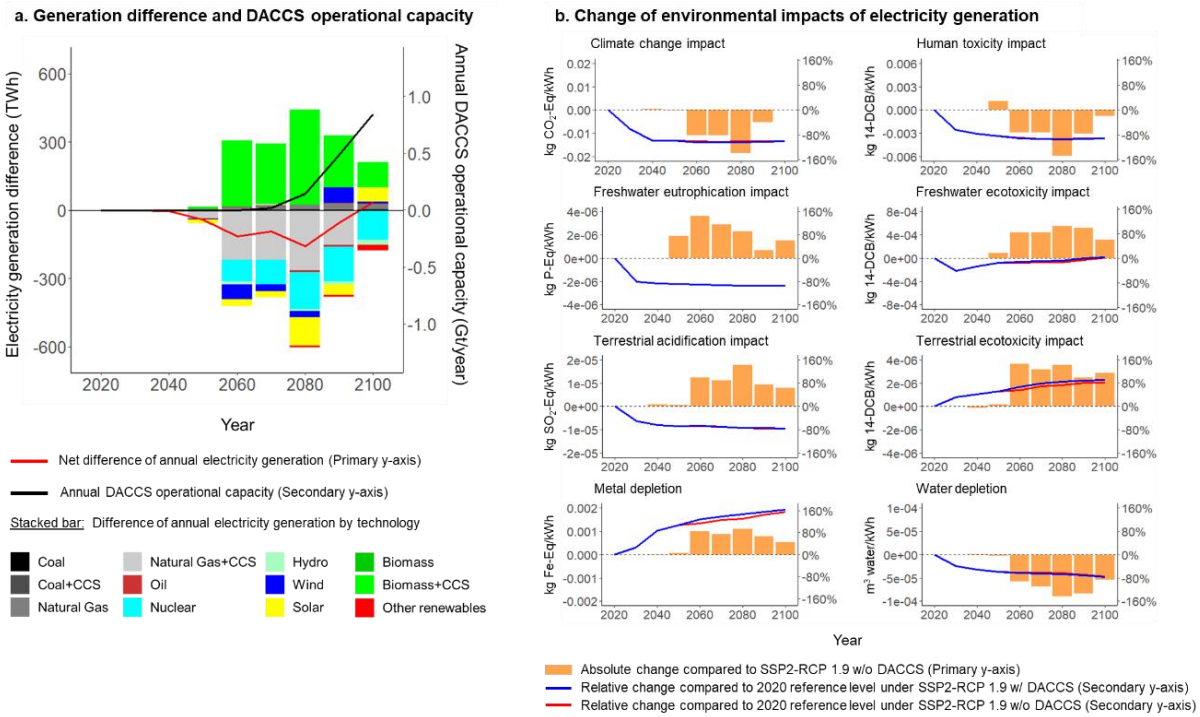


**Figure 3. (a) The change in US power generation with DACCS deployment and (b) the change in life cycle impacts per unit (1 kWh) of US based power generation with DACCS deployment.** In panel a, stacked bars show the change of annual generation by technologies when DACCS is a CDR option in the same mitigation scenario. The red line represents the net difference in annual power generation subtracting the *SSP2-RCP1.9 w/o DACCS* from the *w/ DACCS* scenario (primary y-axis). The black line represents the annual DACCS operational capacity (secondary y-axis). In panel b, the bar in each subplot represents the absolute change (per 1 kWh generation) of each impact subtracting the *SSP2-RCP1.9 w/o DACCS* from the *w/ DACCS* scenario from 2020 to 2100 (primary y-axis). The lines in each subplot represent the relative change (percentage) of impact compared to the 2020 reference level (secondary y-axis) under an *RCP1.9 w/* (red) and *w/o DACCS* scenario (blue).

The availability of DACCS barely changes the annual decarbonization rate of the US electricity system (about 6% across both scenarios based on the annual life cycle climate change

impact). In both strict mitigation scenarios, the US power system reaches carbon neutrality by 2035 (Figure 1d), which is in-line with the present US administration's decarbonization target for the sector[200]. Beginning in 2050, the US grid mix starts to change with increasing DACCS deployment, leading to shifts in the long-term life cycle environmental impacts per kWh produced. We find a decrease in climate change impact up to -0.019 kg $CO_2$-eq/kWh, which is mainly attributable to additional power generation from BECCS. Reductions also occur in water depletion and human toxicity impacts per kWh. At the same time, impacts of US power generation increase for several other categories including freshwater eutrophication and ecotoxicity, terrestrial acidification and ecotoxicity, and metal depletion (bars in Figure 3b). This environmental problem-shifting is directly attributable to the power grid mix change caused by DACCS. Still, for most impact categories, the changes are indiscernible compared to those caused by the electricity system decarbonization overall (lines in Figure 3b). Exceptions are metal depletion and terrestrial ecotoxicity, whose levels increase by 123% and 77% respectively from 2020 to 2100 due to the decarbonization of the power sector. DACCS deployment contributes an additional 10% (on average) after 2050 to both impact categories (Figure 3b).

3. Environmental impacts of DACCS in other world regions

To put the US-specific results in a global context, we calculate the life cycle environmental impacts of DACCS using regionally explicit LCI data for electricity generation in China, Western Europe, and Russia as well as a global average under a *SSP2-RCP1.9 w/ DACCS* scenario (considering technology learning of DACCS). Since the solvent- and sorbent-based DACCS systems are commonly associated with thermal energy supply from natural gas (*SV+NG*) and heat pumps (*SB+HP*) respectively, these two configurations were considered representative processes for a global comparison. The results show that, in 2020, the climate

change impact of *SV+NG* systems deployed in Russia and China are 12% and 19% higher than the same system at world level, because the electricity grid mixes in these regions are dominated by coal and natural gas, respectively (Figure 4a, Supplementary Figure 2, Supplementary Figure 3). A higher climate change impact is also observed for *SB+HP* systems deployed in these two regions (14% and 23% for Russia and China, respectively) (Figure 4b). Both DACCS systems exhibit lower climate change impacts than the 2020 world level if they are deployed in the US (9% and 10% less for *SV+NG* and *SB+HP* systems) and Western Europe (29% and 35% less for *SV+NG* and *SB+HP* systems) given the regions' lower carbon-intensive electricity (Figure 2, Supplementary Figure 4). With time, the climate change impacts of DACCS decrease across all regions, and so do the regional variations. By 2100, climate change impacts barely differ across regions and the global average level, with slightly higher numbers observed for DACCS in Russia whose electricity mix is largely dominated by natural gas with CCS (33% of annual generation) (Supplementary Figure 3). Similarly, decreasing trends of regional variations are observed for human toxicity, freshwater eutrophication, and terrestrial acidification impacts resulting from a worldwide decarbonization of the electricity sector under the mitigation scenario to limit global mean temperature change to below 1.5°C by 2100. The ranges of regional variations remain stable for freshwater and terrestrial ecotoxicity and increase for metal depletion over time due to different renewable penetration levels and grid mix profiles across the regions. The water depletion of *SB+HP* systems is more sensitive to the regional electricity system context compared to that of *SV+NG* systems. Thus, *SB+HP* systems can reduce their already lower water demand even further with increasingly cleaner electricity toward 2100 (Figure 4).

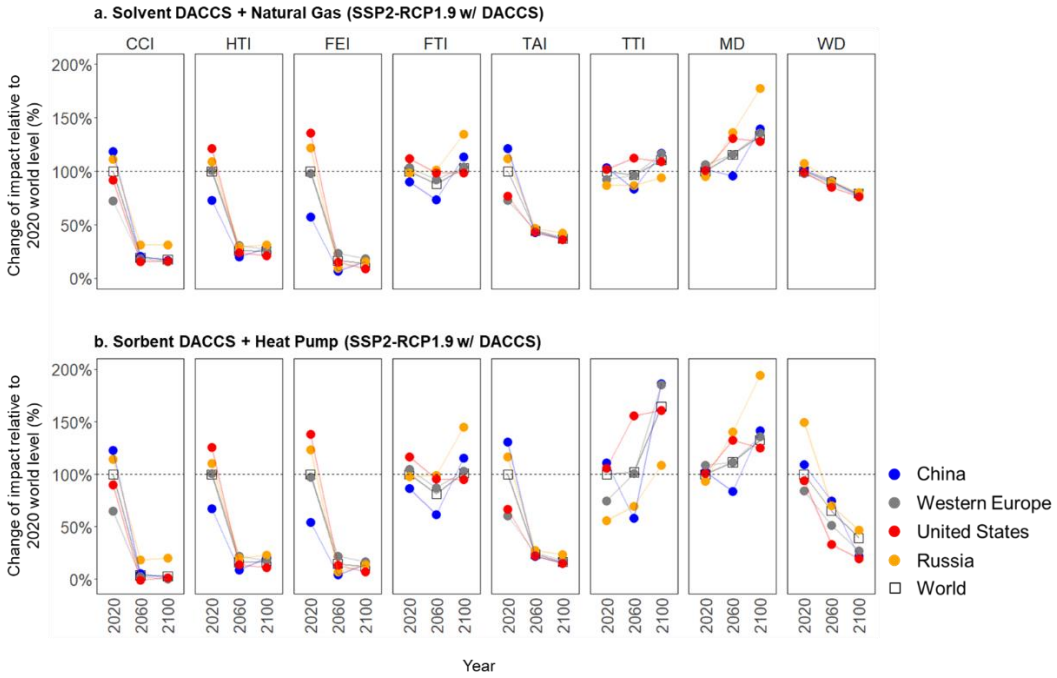


**Figure 4. The regional variation of life cycle environmental impacts of DACCS technologies.** Impacts of solvent-based DACCS using natural gas (*SV+NG*) and sorbent-based DACCS using heat pump generated heat (*SB+HP*) in four regions and the world under a *SSP2-RCP1.9 w/ DACCS* scenario (considering technology learning of DACCS with the reference learning rates). Per impact category, the reference (100% in 2020) is the World level. The results of other region-year combinations are shown as a relative change to the reference. These impact changes were calculated based on capturing and sequestering 1t atmospheric $CO_2$ by DACCS. Since the technologies' net negative life cycle Climate Change Impacts (CCI) (Figure 1) would create a positive increase in impacts relative to the 2020 world level, we do not account for the 1t $CO_2$ captured in the CCI in this figure. Other impact category abbreviations: HTI – Human Toxicity Impact, FEI – Freshwater Eutrophication Impact, FTI – Freshwater Ecotoxicity Impact, TAI – Terrestrial Acidification Impact, TTI – Terrestrial Ecotoxicity Impact, MD – Metal Depletion, WD – Water Depletion.

### *D. Discussion*

As more IAM scenarios start to include DACCS as a critical CDR technology for meeting stringent climate targets, the performance of DACCS should be evaluated in the context of those targets to better guide policy decision and deployment of DACCS in the future. As our LCA shows, a rapid decarbonization of the power and energy demand sectors that is consistent with the 1.5°C climate target can increase the net sequestration efficiency of DACCS and facilitate its

climate change mitigation potential, suggesting DACCS deployment and electricity system decarbonization should act synergistically in climate change mitigation efforts.

Several DACCS technologies can offset GHG emissions and aid with long-term climate change mitigation efforts, but their net sequestration efficiencies and holistic environmental performance are interdependent with the energy system in which they operate. Merely shifting to low-carbon energy sources for DACCS plant operation could lead to environmental trade-offs. These findings are in-line with other DACCS LCA studies[18,170,173]. We find that solvent-based DACCS generally has lower impacts than sorbent-based DACCS in five (climate change, human toxicity, freshwater eutrophication, freshwater ecotoxicity, and metal depletion) out of eight impact categories studied herein. This is contrary to the conclusions of another study, which states sorbent-based DACCS has lower environmental impacts for the impact categories considered therein (under the reference case)[201]. These differences appear to be linked to the study's optimistic electricity (180 kWh/t $CO_2$) and heat (2.6 GJ/t $CO_2$) consumption assumptions for sorbent-based DACCS (under the reference case). These are less than half of those reported by several other studies[18,151,173] and also used herein (470–700 kWh/t $CO_2$ for electricity and 5.4-5.8 GJ/t $CO_2$ for heat). Also, the study assumed that DACCS is powered by grid electricity in British Columbia, Canada, which is dominated by hydroelectricity (accounting for 72% of grid mix[183]) with low emissions for most impact categories. Thus, the environmental impacts (e.g., climate change, fossil depletion) of solvent-based DACCS were mainly driven by other factors such as a higher heat consumption. Furthermore, the study ignored the typical process-configuration for solvent-based DACCS in which the $CO_2$ released during thermal energy generation[161] is also captured and sequestered, thus artificially increasing the climate change impact of that technology and underestimating its potential sequestration efficiency. Neglecting

this purposefully integrated process step not only alters the technology evaluation, it also leads to an underestimation of the storage capacity requirements and related inputs to regional planning and integration efforts. Solvent-based DACCS requires about 30% additional storage capacity (based on the 0.05 kg $CO_2$/MJ[202], which is the $CO_2$ emission factor of natural gas combustion) per tonne of $CO_2$ sequestered compared to sorbent-based DACCS.

Electricity consumption is a major contributor to the terrestrial ecotoxicity and metal depletion levels of DACCS, which are mainly driven by the solar and wind penetration levels in the background electricity system in our scenarios. Therefore, as the decarbonization of the electricity system progresses with expanding renewable energy generation and storage capacities, additional efforts are needed to facilitate sustainable mining, manufacturing, and expanding the circular economy of energy materials used in those technologies, which will reduce these impact levels.

Carbon management policies should consider research and development efforts to improve process and material efficiencies of DACCS and low-carbon energy generation technologies. DACCS technologies have already acquired very high reuse rates of solvent and sorbent[18,161], but our results show that technology learning prominently reduces levels of ecotoxicity, metal depletion, and water depletion (solvent-based DACCS only), highlighting its important role in avoiding potential environmental problem-shifting of DACCS deployment under a climate change mitigation pathway. Whereas large-scale DACCS deployment will affect the supply and demand dynamics of the overall energy system, this effect is negligible compared to the effects of decarbonizing the power sector. Thus, the deployment of DACCS is complementary to the expansion of other net-zero emission technologies as well as BECCS in stringent climate change mitigation scenarios.

Decarbonizing the electricity system substantially reduces regional differences of impacts, such as climate change, human toxicity, freshwater eutrophication, and terrestrial acidification, which are mostly driven by fossil-based energy generation. Still, varying environmental profiles across ecotoxicity and metal depletion persist toward 2100 under different renewable energy deployment strategies. This stresses the need for smart siting of DACCS, incorporating a wide range of environmental and socioeconomic metrics in the future to assess regional trade-offs. Given its load profile, DACCS deployment should also be integrated into regional energy system planning, including grid-connected and off-grid location assessments. DACCS could for instance be intentionally sited in locations with high renewable energy potential and where grid interconnections would be expensive.

The prospective LCA framework presented herein can inform policy discussions around research and development prioritization for emerging technologies that support energy sector decarbonization and long-term climate change mitigation targets. By incorporating regionally and temporally explicit electricity sector scenarios and technology projections for grid-connected DACCS, it captures the complex non-linear relationships between a CDR technology and its environmental impacts, caused by either changes in the broader energy system[203–205] or its specific technology context[94,36]. Future study needs to enhance the capability of this framework to model material circularity and capture the technological changes in broader energy and industrial sectors.

## *E. Appendix*

1. Supplementary Note 1: Process flow diagrams of two direct air carbon capture and storage (DACCS) technologies with subsequent compression and storage system.

### a. Solvent-based DACCS system

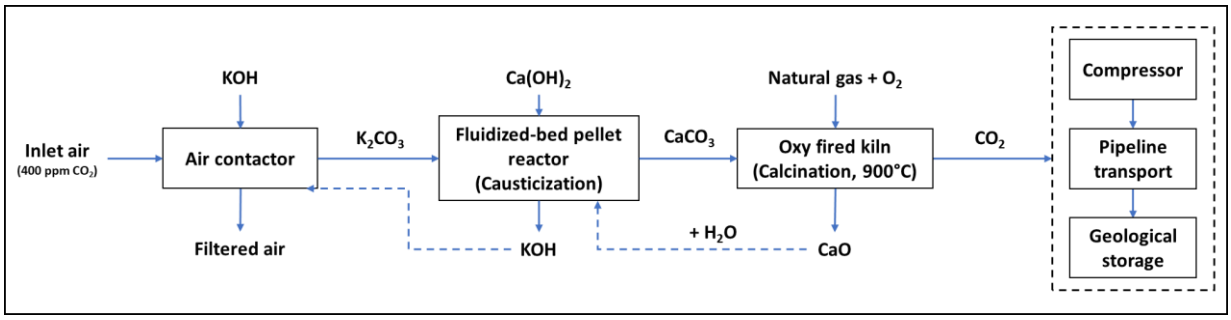


### b. Sorbent-based DACCS system

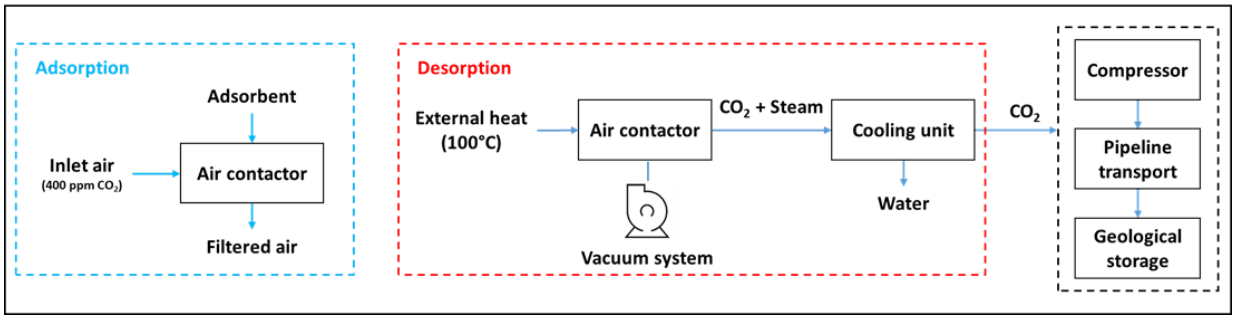


**Supplementary Figure 1. The process flow diagrams of solvent-based DACCS system (a) and sorbent-based DACCS system (b) with subsequent compression and storage system.**

2. Supplementary Note 2: Life cycle inventory

In this section, we provide the life cycle inventory (LCI) data of both solvent- and sorbent-based direct air capture (DAC) systems and subsequent compression and storage system. In the literature, some life cycle inventory (LCI) data of construction and operation of solvent-based DAC systems are missing, so we estimate some of the missing data based on engineering analysis of the material flow, equipment heuristics.

In this study, solvent-based DAC uses aqueous potassium hydroxide (KOH) solutions to capture atmospheric $CO_2$. The plant has an annual capacity of capturing 1 million metric tonnes (Mt) $CO_2$, with a lifetime of 20 years. The plant has four major components (contactor, pallet reactor, calciner, and slaker) and some auxiliary equipment. The material requirement data for constructing the air contactor of a solvent-based DAC plant are provided de Jong et al.[206], so these data are directly used as LCI of air contactor in this study. As for other components, the LCI data are missing in the literature, so their material requirements data were determined by sizing the equipment in accordance with the material flows in Keith et al (2018)[207] , engineering equipment heuristics, sizing approximations based on existing images and industry standards, and existing patents held by Carbon Engineering, which are described below.

*Material requirements: Pellet reactor*

The pellet reactor used by Carbon Engineering (CE) is a customized version of a wastewater treatment reactor designed by Royal HaskoningDHV, called the Crystalactor®[207]. From the renderings provided in Keith et al (2018), it was estimated that a 1 $MtCO_2$/year plant requires 48 pellet reactors. Each reactor shell is a stainless-steel cylinder with a height of 12 m and a diameter of 1.2 m. The actual shell may be more complex, but specific data could not be found. The wall thickness is assumed to be 0.022 m. This thickness comes from a safety factor of 3.5

given for a vertical vessel under pressure and with a diameter about 1 m, which account for potential corrosion risks[208]. The reactor shell has a 60-degree conical base with a diameter of 1.2 m. From this, the sidewall height of the base was calculated to be 3.6 m. The base thickness was assumed to be, again, 0.022 m due to the given conditions. The reactor lid was assumed to be a flat cap with a diameter of 1.2 m and a thickness of 0.022 m. Extra material required for a more complex lid was considered negligible. For the 48 vessel shells, bases, and lids, this results in a total stainless-steel requirement of 454 t/plant. Additional material required for automatic addition of seeds, washing and drying of seeds, and processing of fines were included in the Material requirements: Other equipment.

*Material requirements: Calciner*

The process proposed in Keith et al (2018). employs an oxy-fired fluidized bed calciner to produce calcium oxide (CaO) from calcium carbonate ($CaCO_3$). The calcination step can be broken up into three steps: preheat, calcination and cooling:

The preheat step includes two cyclone heat exchangers (preheat 1 and preheat 2), that heat up solid stream (mostly $CaCO_3$) up to about 650°C. Since the material flow to the calciner is greater than 2,500 t/day, we assume that these cyclones are built as twin systems for a total of four cyclone preheaters. The diameters of the preheat 1 and preheat 2 are estimated at 8.1 m and 7.6 m, respectively (scaled based on the increased diameter and throughput presented in a previous study[209]). Further, the material requirements were determined based on the circumference of the preheat cyclone and materials information from literature[210]. The preheat system also requires additional ducts leading from cyclone to cyclone, a draft fan for each set of cyclone preheaters, or a dip tube to increase material separation efficiency. These material requirements are included in Material requirements: Other equipment.

The calcination step in the Keith et al (2018) is based on fluidized bed calciner reactor, but we estimate the calciner material requirements using a rotary kiln, which is more widely deployed in industries such as cement making and pulp and paper production. While the two calciner configurations are different, the differences are assumed to have negligible effects on the material requirements for the calciner. Most of the material requirements for the calciner are from the metal body (in this case, steel) and the refractory (in this case, red brick refractory or alumina brick refractory). The material requirements for the calciner can be estimated using a cylindrical reactor with single refractory brick lining. The two primary material requirements are steel for the kiln shell and alumina bricks for the working refractory. Assuming the inside of the rotary kiln capable of processing 1,600 t raw material per day is 5.5 m, the working refractory layer is 0.254 m (or 10 inches) and the steel kiln shell is 0.04 m thick, this adds 1,000 t of steel and 2,050 t of red refractory brick for 1 Mt $CO_2$/year facility. These material requirements are then scaled linearly to achieve a throughput 3,960 t/day. Since the rotary kiln configuration is different than the fluidized bed, we then adjust the material requirements linearly using the projected cost. The cost of an oxy-fired rotary calciner is assumed to be $120 million[211]., where the projected cost for the oxy-fired fluidized bed calciner is $44 million from Keith et al (2018). Scaling these values yields material requirements of 910 t steel/plant and 1,856 t refractory/plant.

The cooling is a step after the calcination where the produced CaO is sent to an additional cyclone heat exchanger that preheats the incoming oxygen stream. Similar to the preheat, we assume that there are two, identical cyclones necessary on account of the high flow rate. The material requirements for the cyclone are estimated to be identical to cyclone preheat 2 with a radius of 7.6 m.

The complete material requirements for the calciner, broken down into the three sections, is shown in Supplementary Table 1**Error! Reference source not found.**.

**Supplementary Table 1: Material requirements for the calciner unit of 1 Mt $CO_2$/year solvent-based DAC plant**

| Material Type | Material requirements (t/plant) | | | |
|---|---|---|---|---|
| | Preheat | Single-Lined Calciner | Cooling | Total |
| Steel | 135 | 910 | 110 | 1155 |
| Refractory Bricks | 346 | 1856 | 168 | 2370 |
| Concrete | 195 | 0 | 95 | 290 |

*Material Requirements: Steam Slaker*

Two processes occur simultaneously inside of the slaker at 300°C: an exothermic reaction between CaO and water to produce $Ca(OH)_2$ and the heat transfer to solid $CaCO_3$ as a preheat to the calciner system[212]. The reaction vessel processes the solid CaO stream leaving the oxygen preheat (170 t/hr, 97% CaO, 3% $K_2CO_3$), water condensed from the steam turbine (70.2 t/hr), solids from the upstream $CaCO_3$ filter (306 t/hr, 98.2% $CaCO_3$, 1.8% $K_2CO_3$) and a recycle steam stream[207]. We assume this vessel is primarily steel (used to form the shell of the reactor) and refractory brick (used as insulation).

The solvent process presented in Keith et al[207] and detailed in Heidel and Rossi[212] uses a novel slaker configuration, mixing both the $CaCO_3$ streams and CaO streams to dry the $CaCO_3$ stream and recycle uncalcined material to the calciner, as well as create $Ca(OH)_2$. On account of the lower temperature requirement (300°C), we assume a refractory thickness of 6 inches (0.1524 m) total[213,214]. We assume that for the two calciners, there will be two slaking units, processing a total of 476 t/hr of solid material and roughly 70.2 t/hr of liquid/gaseous materials with equal distribution[207].

The outer shell of the slaker is assumed to be 40 mm, consistent with the metal shell thickness used for the calciner. The fluidization velocity is 1 m/s [207]. Assuming that the

fluidizing medium is primarily steam, the specific volume of the superheated steam stream can be determined at 300°C and 1 bar (2.6 $m^3$/kg) to give a gas volumetric flowrate of 0.46 $m^3$/s. Therefore, we assume each slaker is a 0.4 m diameter cylindrical reaction vessel with an attached chamber for a recycle stream that is estimated using a factor 1.5 for the additional steel and refractory requirements based on the relative sizing of the cylindrical vessel to the recycle chamber. Assuming that the solid particle size entering the slacker experiences little to no particle size reduction occurring in the calciner, all particles will be roughly 0.85 mm in diameter when entering the slaker[207].

For most industrial fluidized beds, the length to diameter ratio lies between 3 and 16[215] and the typical reactor length is between 1 and 10 m[216]. For this analysis, we assume a bed length of 7.6 m (or a L/D ratio of 10). For the refractory thickness of 0.1524 m, the red silica brick requirement per vessel is roughly 9 t/ reactor. For the steel thickness of 40 mm, the steel requirements are roughly 8 t/reactor. The total requirements for capturing 1 $MtCO_2$/year from air is shown in Supplementary Table 2.

**Supplementary Table 2: Material requirements for the steam slaker of 1 Mt $CO_2$/year solvent-based DAC plant**

| Material type | Material requirements (t/plant) |
|---|---|
| Refractory Brick Required | 18.0 |
| Steel Required | 15.8 |

The steam slaker requires additional equipment, such as a cyclone that separates the outlet gas stream, a baghouse unit, fines filter (separating $CaCO_3$ and $Ca(OH)_2$ post-slaker), heat exchangers and coolers. The material requirements for these smaller unit operations are included in Material requirements: Other equipment.

*Material requirements: Other equipment*

The material requirements for additional process equipment are assumed to be primarily concrete and steel. These additional units include the fines filter, quicklime mix tank, heat exchanger, and pumps, as well as any additional auxiliary equipment. To estimate the requirement for concrete, we assume 34% of the material costs from Keith et al. (2018) is distributed to concrete which is based on the American Institute of Steel Construction (AISC) construction material cost ratio to estimate the concrete requirements[217]. This is also similar to the methodology used in the Rhodium Group report Capturing New Jobs[218]. We assume a cost of concrete is \$61/t[219], consistent with the commodity price as of 2018. The resulting concrete requirements for the facility are calculated and outlined in Supplementary Table 3.

**Supplementary Table 3: Concrete requirements of a 1 Mt $CO_2$/year solvent-based DAC plant**

| Module | Material cost[207] (Million \$) | Total cost for cement (Million \$) | Concrete requirements (t/plant) |
|---|---|---|---|
| Pellet Reactor | 28.4 | 9.7 | 157,230 |
| Calciner-Slaker | 18.1 | 6.2 | 100,207 |
| Others | 31.8 | 10.8 | 176,054 |

The material requirements associated with piping and instrumentation are primarily steel and aluminum, and we estimate that separately based on a refinery configuration. The material requirements of any subsets (pipe, tubing, valves, fittings, and flanges) of the refinery (at three capacity levels: 10,000, 75,000, and 150,000 barrels/stream day) are provided in the Critical Materials Requirements for Petroleum Refining[220], then we calculated the steel requirements of the refinery with total capital cost of \$6.06 billion (2018\$) and a capacity of 50,000 barrel/stream day[221] using the scaling factor shown in Eq. 1 below.

$$\text{Scale Factor} = \frac{\log\left(\frac{\text{Capacity B}}{\text{Capacity A}}\right)}{\log\left(\frac{\text{Material Requirements B}}{\text{Material Requirements A}}\right)} \quad (2)$$

Then, we calculate the material requirements associated with piping and instrumentation of the solvent-based DAC as proportionate to that of the refinery plant (50,000 barrel/stream day) based on their capital costs (total capital cost are $6.06 billion for the refinery, total capital cost is $1.13 billion for solvent-based DAC[207], both on 2018$). The material requirements associated with piping and instrumentation are given in Supplementary Table 4.

**Supplementary Table 4: Material requirements for piping and instrumentation of a 1 Mt $CO_2$/year solvent-based DAC plant**

| | Carbon Steel (t/plant) | Alloy Steel (t/plant) | Stainless Steel (t/plant) | Aluminum (t/plant) |
|---|---|---|---|---|
| Material requirements of piping and instrumentation | 5,481 | 951 | 651 | 50 |

*Chemical Requirements: Calcium Carbonate (CaCO3)*

The initial requirements of $CaCO_3$ are required to start up the system. This is calculated using Figure 2 from Keith et al.[207]. The inlet $CaCO_3$ includes the three streams of $CaCO_3$ entering the pellet reactor: (1) $CaCO_3$ Seed (4.5 t/h), (2) $CaCO_3$ Makeup (3.4 t/h) and (3) $CaCO_3$ Seed from Calciner (6.0 t/h). The total startup $CaCO_3$ is 13.9 t/h for the duration of the startup period. The startup period discussed here is for the calcium loop (or calcining loop) and it primarily depends upon the calciner. Here, we assume a startup time of 24 hours to account for transit time through the calciner and associated equipment, which results in an initial $CaCO_3$ requirements to be 330 t. After the initial startup period, the annual make-up $CaCO_3$ is 3500 t/year[222]. Therefore, the annualized $CaCO_3$ consumption is 3,517 t (= 330t/20 + 3,500t).

*Chemical Requirements: Potassium Hydroxide (KOH)*

The initial KOH requirements are also directly dependent on the startup time of the system. Keith et al. [207] uses a 2 mol/L KOH solution that flows to both the contactor and post-combustion absorber at a flow rate of 35,000 t/hr. This is equivalent to roughly 3,000 t of KOH per hour for

the duration of the startup period. We assume the same startup time of 24 hours to startup, including circulation from the contactors to the regeneration facility and the fluid residence time in the pellet reactors. In other words, the startup time accounts for the complete circulation of the fluid through the caustic recovery loop. So, the initial KOH requirement is 72,000 t. Although KOH is recycled through the system, but drift losses leads to an annual make-up KOH of 400 t/year[222]. Therefore, the annualized KOH consumption is 4,000 t (= 72,000t/20 + 400t).

*Chemical Requirements: Water*

The initial water requirements can also be estimated using the 35,000 t/h solvent flow to the contactor[207], which implies a water usage of roughly 31,000 t/h for the startup period of the contacting loop. With a startup time of 24 hours, the initial water usage is 744,000t. The temperature and relative humidity are used to estimate the water losses using the correlation given in Keith et al.[207]. We assumed a 60% relative humidity and 20°C, which resembles the temperature and humidity near Midland Texas November to March[223]. At these conditions, the evaporative losses are 3.8 t water/t $CO_2$ (430 t water/hour). By assuming a 90% operation capacity of DAC facility (7,884 hour/year), the annual make-up water is 3.4 Mt water/year. Therefore, the annualized water consumption is 3.44 Mt/year (= 0.74 Mt/20 + 3.4 Mt).

The overall material requirements for the construction of a 1 Mt$CO_2$/year solvent-based DAC (except for air contactor) and its annualized chemical and water consumption of are summarized in Supplementary Table 5.

**Supplementary Table 5: The overall material requirements for the construction of a 1 Mt $CO_2$/year solvent-based DAC plant (except for air contactor) and its annualized chemical and water consumption.**

| Material requirements for the construction (t/plant) | | | | | | |
|---|---|---|---|---|---|---|
| Module | Concrete | Stainless-steel | Alloy steel[a] | Carbon steel | Aluminum | Refractory bricks |
| Pellet Reactors | 157,230 | 454 | 0 | 0 | 0 | 0 |
| Calciners-Slakers | 100,497 | 0 | 1,171 | 0 | 0 | 2,388 |
| Other Equipment | 176,054 | 651 | 951 | 5,481 | 50 | 0 |
| The annualized chemical and water consumption (t/plant·year) | | | | | | |
| | KOH | | $CaCO_3$ | | | Water |
| Chemical Requirements | 4,000 | | 3,517 | | | 3,440,000 |

Note:

[a] Alloy steel combines both alloy steel and any other unspecified steel

*Life cycle inventory of sorbent-based DAC*

The material and energy requirement data are converted to LCI data for solvent-based DAC systems and the subsequent compression and storage system based on 1 functional unit (capturing 1 t $CO_2$), which are summarized in Supplementary Table 6.

**Supplementary Table 6. Life cycle inventory of the solvent-based DAC system (based on a sorbent-based DAC facility with annual capture capacity of 1 Mt $CO_2$ and lifetime of 20 years).**

| Input | | Inventory Dataset[a] | Amount | Unit (per t $CO_2$ captured) |
|---|---|---|---|---|
| Construction | | | | |
| Air contact | Concrete | RoW: market for concrete, normal | 0.0067[b] | $m^3$ |
| | Low-alloyed steel | GLO: market for steel, low-alloyed | 0.27[b] | kg |
| | Stainless steel | RoW: steel production, chromium steel 18/8, hot rolled | 0.0017[b] | kg |
| | Polyurethane | RoW: market for polyurethane, flexible foam | 0.0005[b] | kg |
| | Glass fiber | GLO: market for glass fibre | 0.0038[b] | kg |
| | Polypropylene | GLO: market for polypropylene, granulate | 0.0008[b] | kg |
| | Polyvinyl Chloride | GLO: market for polyvinylchloride, bulk polymerised | 0.76[b] | kg |
| Pellet reactor | Concrete | RoW: market for concrete, normal | 0.0033[c] | $m^3$ |
| | Stainless steel | RoW: steel production, chromium steel 18/8, hot rolled | 0.023[c] | kg |
| Calciner slaker | Concrete | RoW: market for concrete, normal | 0.0021[c] | $m^3$ |
| | Low-alloyed steel | GLO: market for steel, low-alloyed | 0.059[c] | kg |
| | Refractory brick | GLO: market for refractory, basic, packed | 0.12[c] | kg |
| Other equipment | Concrete | RoW: market for concrete, normal | 0.0037[c] | $m^3$ |
| | Aluminium | GLO: market for aluminium, wrought alloy | 0.0025[c] | kg |

| | | | | |
|---|---|---|---|---|
| | Low-alloyed steel | GLO: market for steel, low-alloyed | 0.048[c] | kg |
| | Stainless steel | RoW: steel production, chromium steel 18/8, hot rolled | 0.033[c] | kg |
| | Carbon steel | GLO: market for steel, unalloyed | 0.27[c] | kg |
| Operation | | | | |
| Potassium hydroxide | | GLO: market for potassium hydroxide | 4.0[c] | kg |
| Calcium carbonate | | RoW: market for limestone, crushed, for mill | 3.5[c] | kg |
| Water | | RoW: market for tap water | 3,437[c] | kg |
| Electricity[d] | | US: market group for electricity, medium voltage<br>CN: market group for electricity, medium voltage<br>ENTSO-E: market group for electricity, medium voltage<br>RU: market group for electricity, medium voltage<br>GLO: market group for electricity, medium voltage | 345[b] | kWh |
| Heat[d] | Natural gas | RoW: heat production, natural gas, at industrial furnace >100kW | 6,280[b] | MJ |
| | Biomethane | RoW: heat production, biomethane, at boiler condensing modulating <100kW[e] | | |
| End-of-life[f] | | | | |
| Concrete | | RoW: treatment of waste concrete, inert material landfill | 38[g] | kg |
| Steel | | RoW: treatment of waste reinforcement steel, recycling | 0.6 | kg |
| Glass fiber | | RoW: treatment of waste plastic, mixture, municipal incineration | 0.0038 | kg |
| Polyvinyl Chloride | | RoW: treatment of waste polyvinylchloride, municipal incineration | 0.76 | kg |
| Polypropylene | | RoW: treatment of waste polypropylene, municipal incineration | 0.0008 | kg |
| Polyurethane | | RoW: treatment of waste polyurethane, municipal incineration | 0.0005 | kg |

| | | | |
|---|---|---|---|
| Refractory brick | RoW: treatment of waste brick, collection for final disposal | 0.12 | kg |
| Aluminium | RoW: treatment of aluminium scrap, post-consumer, prepared for recycling, at remelter | 0.0023 | kg |
| Potassium hydroxide | RoW: treatment of spent solvent mixture, hazardous waste incineration | 4.0 | kg |
| Calcium carbonate | RoW: treatment of limestone residue, inert material landfill | 3.5 | kg |

Notes:

[a] The upstream and downstream inventory datasets are collected from ecoinvent 3.6.

[b] de Jong et al., 2019[206].

[c] Data collected based on the bottoms-up materials requirements analysis described in *Supplementary Note 2*.

[d] Here, we consider DAC system can be deployed in five regions, and the inventory data of electricity production are provided for these five regions: the United States (US), China (CN), Western Europe (ENTSO-E), Russia (RU) and World (GLO). Two heat supply options (natural gas and biomethane) are considered for solvent-based DAC system, and the inventory data of the heat supply are provided.

[e] ecoinvent 3.6 database does not include LCI data of the "RoW: heat production, biomethane, at boiler condensing modulating <100kW" process, but the LCI data of this process is included in the newest version (ecoinvent 3.7). Therefore, we collected the LCI datasets related this process from ecoinvent 3.7 and added them to ecoinvent 3.6 to create an extended ecoinvent 3.6. The data is also summarized in "4_LCI_biomethane_heat.xlsx" excel file in "LCI_data" folder.

[f] End-of-life (EoL) phase includes the treatment of materials used in construction and operation of DAC facility. We assume 85% steel (including low-alloyed and stainless steel, and steel pipe) used in the construction phase is recycled during end-of-life phase, and 90% aluminium used in the construction phase is recycled during end-of-life phase. All other materials (100%) are either incinerated or landfilled.

[g] Unit conversion of concrete from volume to mass by assuming the density of concrete as 2400 $kg/m^3$.

*Life cycle inventory of sorbent-based DAC*

For the sorbent system, the LCI data are collected from the work of Deutz and Bardow based on the Climeworks system[18]. We used the LCI data of the plant with an annual capacity of 100 kt $CO_2$/year and a lifetime of 20 years. The LCI data are summarized in Supplementary Table 7.

**Supplementary Table 7. Life cycle inventory of the sorbent-based DAC system (based on a sorbent-based DAC module with annual capture capacity of 100 kt $CO_2$ and lifetime of 20 years).**

| Input | | Inventory Dataset | Amount | Unit (per t $CO_2$ captured) |
|---|---|---|---|---|
| Construction | | | | |
| Civil Engineering | Concrete for fundamentals | RoW: market for concrete, normal | 0.004 | $m^3$ |
| | Steel for fundamentals | GLO: market for reinforcing steel | 0.471 | kg |
| Hall | Concrete for fundamentals | RoW: market for concrete, normal | 0.003 | $m^3$ |
| | Steel for fundamentals | GLO: market for reinforcing steel | 0.274 | kg |
| | Steel structure | GLO: market for steel, low-alloyed | 0.06 | kg |
| | Insulation | GLO: market for stone wool | 0.008 | kg |
| Collector containers (without sorbent) | Carbon steel | GLO: market for steel, unalloyed | 0.138 | kg |
| | Stainless steel | RoW: steel production, chromium steel 18/8, hot rolled | 0.112 | kg |
| | Insulation | GLO: market for stone wool | 0.005 | kg |
| | Plastics (TPE) | RoW: market for polyurethane, rigid foam | 0.006 | kg |
| | Copper | GLO: market for copper | 0.005 | kg |
| | Aluminium | GLO: market for aluminium, wrought alloy | 0.08 | kg |
| | Paints, coating | RoW: market for alkyd paint, white, without solvent, in 60% solution state | 0.005 | kg |
| Process unit | Stainless steel | RoW: steel production, chromium steel 18/8, hot rolled | 0.169 | kg |
| | Low-alloyed steel | GLO: market for steel, low-alloyed | 0.014 | kg |
| | Insulation | GLO: market for polystyrene foam slab for perimeter insulation | 0.047 | kg |

| | | | | |
|---|---|---|---|---|
| | Plastics (TPE) | RoW: market for polyurethane, rigid foam | 0.005 | kg |
| | Copper | GLO: market for copper | 0.005 | kg |
| Spare parts (5 % exchange rate) | Stainless steel | RoW: steel production, chromium steel 18/8, hot rolled | 0.011 | kg |
| | Low-alloyed steel | GLO: market for steel, low-alloyed | 0.006 | kg |
| Operation | | | | |
| Amine-based sorbent (amine on silica) | | Inventory data of amine-based sorbent is collected from literature and summarized in SI-Tab.8 | 3.0 | kg |
| Electricity | | US: market group for electricity, medium voltage<br>CN: market group for electricity, medium voltage<br>ENTSO-E: market group for electricity, medium voltage<br>RU: market group for electricity, medium voltage<br>GLO: market group for electricity, medium voltage | 500 | kWh |
| Heat[a] | Heat pump | US: market group for electricity, medium voltage<br>CN: market group for electricity, medium voltage<br>ENTSO-E: market group for electricity, medium voltage<br>RU: market group for electricity, medium voltage<br>GLO: market group for electricity, medium voltage | 5,400 | MJ |
| | Biomethane | RoW: heat production, biomethane, at boiler condensing modulating <100kW[g] | | |
| End-of-life | | | | |
| Concrete | | RoW: treatment of waste concrete, inert material landfill | 14.7 | kg |
| Steel | | RoW: treatment of waste reinforcement steel, recycling | 1.07 | kg |
| Aluminium | | RoW: treatment of aluminium scrap, post-consumer, prepared for recycling, at remelter | 0.072 | kg |

| | | | |
|---|---|---|---|
| Plastics (TPE) | RoW: treatment of waste plastic, mixture, municipal incineration | 0.058 | kg |
| Copper | RoW: treatment of scrap copper, municipal incineration | 0.01 | kg |
| Stone wool | RoW: treatment of waste mineral wool, inert material landfill | 0.013 | kg |
| Amine-based sorbent (amine on silica) | RoW: treatment of spent anion exchange resin from potable water production, municipal incineration | 3 | kg |

Notes:

[a] Two heat supply options (heat pump and biomethane) are considered for sorbent-based DAC system, and the inventory data of the heat supply are provided. The heat pump considered in this study has a coefficient of performance (COP) of 2.5, and it converts electricity into heat, so we use inventory of electricity production to represent the inventory of heat generation from heat pump. Heat requirement of sorbent-based DAC is 5,400 MJ/t $CO_2$ captured. If heat pump with COP of 2.5 is used to provide heat, the electricity consumption is 2,160 MJ/t $CO_2$ captured (600 kWh/t $CO_2$ captured).

*Life cycle inventory of amine-based silica*

The specific solid sorbent we choose for the sorbent-based DAC is amine-based silica, which can be synthesized by impregnate amines polyethylenimine (PEI) on solid silica gel. The LCI of amine-based silica is collected from literature (taking average between the best- and worst-case)[18] and summarized in Supplementary Table 8 based on the *composition* that 1 kg amine-based silica requires of 0.64kg silica gel and 0.36 kg PEI[224] (The data is also summarized in "3_LCI_amine_based_sorbent.xlsx" excel file in "LCI_data" folder).

**Supplementary Table 8. Life cycle inventory of 1 kg amine-based silica.**

| Input | Dataset | Amount | Unit (per 1 kg amine-based silica) |
|---|---|---|---|
| Silica gel (64% in mass composition of 1 kg amine-based silica)[a] | | | |
| Sodium silicate | RoW: market for sodium silicate, solid | 0.13 | kg |
| Sulfuric acid | RoW: market for sulfuric acid | 0.02 | kg |
| Thermal energy | RoW: market for heat, central or small-scale, natural gas | 0.63 | MJ |
| Water | RoW: market for water, deionised | 1.29 | kg |
| Wastewater treatment | RoW: treatment of wastewater, average, capacity 1E9l/year | 1.12 | $m^3$ |
| Particulates (<2.5 um) | Emission to air | 0.000042 | kg |
| PEI (36% in mass composition of 1 kg amine-based silica) | | | |
| Ethanolamine | GLO: market for monoethanolamine | 0.71 | kg |
| Sulfuric acid | RoW: market for sulfuric acid | 1.14 | kg |
| Sodium hydroxide | GLO: market for sodium hydroxide, without water, in 50% solution state | 1.00 | kg |
| Hydrochloric acid | RoW: market for hydrochloric acid, without water, in 30% solution state | 0.07 | kg |
| Ethanol | GLO: market for ethanol, without water, in 99.7% solution state, from fermentation | 1.24 | kg |
| Diethyl ether | RoW: market for diethyl ether, without water, in 99.95% solution state | 14.84 | kg |
| Water | RoW: market for water, deionised | 5.24 | kg |
| Electricity | GLO: market group for electricity, low voltage | 0.12 | kWh |
| Thermal energy | RoW: market for heat, central or small-scale, natural gas | 2.69 | MJ |

| | | | |
|---|---|---|---|
| Sodium sulfate (co-product as output) | RoW: market for sodium sulfate, anhydrite | 1.65 | kg |
| Unreacted raw materials and solvents | RoW: treatment of spent solvent mixture, hazardous waste incineration | 0.54 | kg |
| End-of-Life | | | |
| amine-based silica | RoW: treatment of spent anion exchange resin from potable water production, municipal incineration | 0.36[b] | kg |

Notes:

[a] Silica gel is assumed to be recycled with a rate of 95 %[18], so the material and energy flows in this table (for silica gel) have factored in the recycling rate, meaning the amounts are 5% of the original required amount.

[b] This process only applies for the PEI, because 95% of silica are recycled.

*Life cycle inventory of pipeline transport and storage system*

Once the captured $CO_2$ is release from the DAC system, we assume the $CO_2$ flow will be compressed through a compressor to 11 MPa and then transported through a pipeline to the storage site. The length of the transport pipeline is assumed to be 50 km. At the storage site, the $CO_2$ will be further compressed to 15 MPa and injected into a geological reservoir through wells with the depth of 3 km each. The LCI data of transport and storage system are collected from a previous study[193] and summarized in Supplementary Table 9.

**Supplementary Table 9. Life cycle inventory of compression, pipeline transport and storage system.**

| Input | | Dataset | Amount | Unit (per t $CO_2$ compressed and stored) |
|---|---|---|---|---|
| Construction | | | | |
| Compression facility | Concrete | RoW: market for concrete, normal | 0.000001 | $m^3$ |
| | Copper | GLO: market for copper | 0.0001 | kg |
| | Low alloyed steel | GLO: market for steel, low-alloyed | 0.001 | kg |
| | Polyethylene | GLO: market for polyethylene, low density, granulate | 0.0003 | Kg |
| | Diesel | RoW: market for diesel | 0.032 | MJ |
| | Electricity | US: market group for electricity, medium voltage<br>CN: market group for electricity, medium voltage<br>ENTSO-E: market group for electricity, medium voltage<br>RU: market group for electricity, medium voltage<br>GLO: market group for electricity, medium voltage | 0.001 | kWh |
| Pipeline transport | Sand | RoW: market for sand | 1.04 | $m^3$ |
| | Reinforcing steel | GLO: market for reinforcing steel | 0.13 | kg |
| | Steel pipes | GLO: market for drawing of pipe, steel | 0.13 | kg |
| | Bitumen | GLO: market for bitumen seal | 0.0012 | Kg |

| | | | | |
|---|---|---|---|---|
| | Polyethylene | GLO: market for polyethylene, low density, granulate | 0.0025 | kg |
| | Diesel | RoW: market for diesel | 1.8 | MJ |
| | Transport | RoW: market for transport, freight, lorry, unspecified | 0.12 | t*km |
| Geological storage | Well construction | GLO: market for onshore well, oil/gas | 8.2E-08 | km |
| | Sand | RoW: market for sand | 3.3 | kg |
| | Un-alloyed steel | GLO: market for steel, unalloyed | 0.017 | kg |
| | Low alloyed steel | GLO: market for steel, low-alloyed | 0.037 | kg |
| | Concrete | RoW: market for concrete, normal | 0.000048 | $m^3$ |
| | Copper | GLO: market for copper | 0.0019 | kg |
| | Transport | RoW: market for transport, freight, lorry, unspecified | 0.34 | t*km |
| Operation | | | | |
| Electricity | | US: market group for electricity, medium voltage<br>CN: market group for electricity, medium voltage<br>ENTSO-E: market group for electricity, medium voltage<br>RU: market group for electricity, medium voltage<br>GLO: market group for electricity, medium voltage | 118 | kWh |
| End-of-life | | | | |
| Concrete and sand | | RoW: treatment of waste concrete, inert material landfill | 4.4 | kg |
| Steel | | RoW: treatment of waste reinforcement steel, recycling | 0.26 | kg |
| Copper | | RoW: treatment of scrap copper, municipal incineration | 0.002 | kg |
| Polyethylene | | RoW: treatment of waste polyethylene, municipal incineration | 0.0028 | kg |
| Bitumen | | RoW: treatment of waste bitumen, sanitary landfill | 0.0012 | kg |

3. Supplementary Note 3: Technology learning assumption of solvent- and sorbent-based DAC

Solvent-based DAC approach uses a liquid solvent and high surface area packing material to capture ambient $CO_2$. Current applications require strong bases, such as NaOH and KOH, with uptake of 3.1E-5 mol $CO_2/cm^2$·second (0.52 mol $CO_2$/minute·$m^3$)[225]. If innovative approaches can increase the uptake rate to 7.0E-5 mol $CO_2/cm^2$·second (1.18 mol $CO_2$/minute·$m^3$), this would result in a 2.3 times increase in the uptake rate. This could result from an improved packing material that increases the solvent's exposed surface area, or by the development of novel liquid solvents with higher uptake capacities. The increase in uptake translates to a roughly proportional decrease in the bed depth of the contactor and a roughly 56% decrease in the cost of the contactor unit. The decreased bed depth additionally causes a reduction in the system fan power by the same percentage. Then, we also assumed that increased deployment improves the system thermal efficiency, which results in a reduction of system thermal energy demand by 2.4 GJ/t$CO_2$ for a total energy requirement of 6 GJ/t$CO_2$[226]. As described in the 2019 National Academies of Sciences Engineering and Medicine (NASEM) report on negative emissions technologies, the inlet surface area dimensions of contactor are assumed to be 20 m by 200 m in both uptake scenarios[227]. Instead, the bed depth is varied. The cost reduction for the contactor is proportional to the size change of contact unit.

For initial cost of solvent-based DAC, we used the upper bound cost data from the NASEM report, which is \$264/t$CO_2$ (capital cost = \$151/t $CO_2$, operating cost = \$113/t $CO_2$, with a capacity of 1 Mt $CO_2$/year)[227]. To estimate the how these costs will come down, we applied the 56% decrease to the capital cost of contactor, and we assumed that innovation in other unit operations will result in achievement of the lower bound capital costs as described in the

NASEM report. So, we developed the theoretical minimum capital cost at \$67/t $CO_2$ (44% of today's capital cost). (A capital recovery factor of 12.4% was used annualize the capital costs of the system). Then, we adopted a learning rate range (1% to 15%)[228] from various existing emerging technologies to project the reduction of capital cost. Under 10% learning rate, the capital cost approximates to the minimum \$67/t $CO_2$ when the learning effect is saturated, so the 10% is chosen as the reference learning rate for capital costs of solvent-based DAC. Furthermore, we adopted a range of learning rate (5%–15%) for the capital cost of solvent-based DAC from the literature to reflect uncertainty in the actual learning rate[199]. Similarly, to adjust the operating cost, the fan energy was reduced by 56% and a reduction of 2.4 GJ/t$CO_2$ is applied to the thermal energy demand, which give the minimum operating costs at \$56/t$CO_2$ (50% of today's operating cost). As for the learning rate, a few previous studies adopted a conservative assumption by considering a fixed operating cost (no learning) over time[199,228], so here we assumed an reference learning rate of 2.5% for the operating cost, with a range varying from 0% (no learning) to 5%.

Sorbent-based DAC uses solid sorbents to uptake $CO_2$ in a batch-wise process. The first area for innovation lies within the sorbent itself. Sorbents designed with higher uptake rate and longer lifetimes can reduce the amount of sorbent necessary in the DAC contactors. Since the sorbent makes up roughly 80% of the system's capital cost[151], this has a huge impact on the process economics. The current uptake observed in commercial sorbents is 2.5 mol $CO_2$/kg over 3,000 s (3.53 mol $CO_2$/minute·$m^3$)[225,227]. Higher capacity sorbents are described to reach an uptake of 3.4 mol $CO_2$/kg over 12 hours in an aminopolymer-impregnated silica sorbent [229]. If future innovation can lead to similar uptakes in 3,000 s, this increases the specific uptake to 4.76 mol $CO_2$/minute·$m^3$. Additionally, we assume that the average lifetime will lengthen from 0.5 years

to 2 years [227], which reduces the amount of makeup sorbent by four times the original value. The joint impact of increased uptake and longer sorbent lifetime results in a sorbent cost decrease of roughly 82%, resulting in a 74% decrease in the overall capital costs compared to the middle case NASEM report. The cost per unit sorbent is assumed to remain consistent at $50/kg.

The cost data from scenario 4 – High in the same NASEM represent the cost of sorbent-based DAC with the plant capacity 1 Mt $CO_2$/year too. After adjusting the capital cost to represent an economic lifetime of 10 years and a 11.6% discount rate, the total cost is \$386/t$CO_2$ (capital cost = \$364/t $CO_2$, operating cost = \$22/t $CO_2$). In this study, life cycle inventory data we used for sorbent-DAC is based on plant capacity of 0.1 Mt CO2/year, so we further estimated the initial cost of a sorbent-DAC with the capacity of 0.1 Mt CO2/year using the learning curve approach. We assumed the plant with the capacity of 4,000t $CO_2$/year to be \$900/t $CO_2$ (by averaging the costs of 4,000t $CO_2$/year sorbent-based plant from multiple sources[228,230]), and then the cost of a plant with the capacity of 1 Mt CO2/year was assumed to be \$386/t$CO_2$. We fitted these data into a regression of one factor learning curve equation, and then we estimated the cost of a sorbent-DAC with the capacity of 0.1 Mt $CO_2$/year to be \$550/t$CO_2$ (capital cost = \$518/t $CO_2$, operating cost = \$32/t $CO_2$), and we use this cost as the initial cost of sorbent-based DAC plant (with the capacity of 0.1 Mt $CO_2$/year).

The aforementioned changes to the sorbent capacity and lifetime coupled to the assumption that other process innovations will shift the capital cost from scenario 4 – High to scenario-2 Low described in the NASEM report result in a reduction of the system's levelized capital costs by 82% (\$101/t$CO_2$). For the operating cost, we also shift it from scenario 4 – High to scenario 2 – Low, resulting in a minimum operating cost of \$16/t$CO_2$ (50% of initial operating cost). Using similar method for developing the learning rate as described in the solvent-based DAC, we

adopted a learning rate range for sorbent-based DAC, which is from 5% to 20%. The higher range is chosen is because, compared to solvent-based DAC which is highly integrated and large-scale, sorbent-based DAC relies on standardized and modular units, which can be mass-produced and deployed, and therefore enables fast iteration and learning[199]. The learning rate chosen to best represent the capital costs of sorbent-based DAC is 15% (as the reference learning rate), and the uncertainty range was set to be 10%–20%[199]. For the operating cost, we used the same learning rate as the solvent-based DAC, with the reference rate being 2.5% and variation range being 0%–5%.

Here, we also assume that the subsequent $CO_2$ transport and storage facilities will follow the same learning rates as the corresponding solvent- and sorbent-based DAC systems. The selected learning rates and theoretical minimum costs of both solvent- and sorbent-based DACCS are summarized in the Supplementary Table 10. Because the effects of technology learning on material and energy use of DACCS are so far missing in the published literature, we assume the changes of material and energy consumption are proportional to the changes of the costs of DACCS technologies. Therefore, we used these learning rates and their theoretical minimum values to estimate the corresponding material and energy uses that are related to these cost metrics.

**Supplementary Table 10. Assumed reference learning rate (and their uncertainty ranges), theoretical minimum value of capital and operational costs (also representing the material and energy consumption associated to these cost metrics) of DACCS technologies.**

| Technology type | | Solvent-based DACCS | Sorbent-based DACCS |
|---|---|---|---|
| Learning rate[a] | Capital cost | 10% (5%–15%) | 15% (10%–20%) |
| | Operational cost | 2.5% (0%–5%) | 2.5% (0%–5%) |
| Theoretical minimum values (percentage of initial cost) | Capital cost | 44% | 18% |
| | Operational cost | 50% | 50% |

Note:
[a] Numbers in the parenthesis represent the uncertainty ranges

There is no concrete way to imply the learning rate between two points. This approximation has DACCS approaching a theoretical minimum cost at different rates. Future innovation is unpredictable and, therefore, the actual minimum cost may be different from the estimated values.

**Supplementary Table 11. Cumulative DACCS deployment and material and energy use factors of DACCS technologies from 2020 to 2100**

| Year | Cumulative DACCS deployment (Gt/yr)[a] | Solvent-based DACCS | | | | | | Sorbent-based DACCS | | | | | |
|---|---|---|---|---|---|---|---|---|---|---|---|---|---|
| | | Material and energy use factor (capital cost)[b] | | | Material and energy use factor (operational cost)[b] | | | Material and energy use factor (capital cost)[b] | | | Material and energy use factor (operational cost)[b] | | |
| | | Slow | Reference | Fast | Slow | Reference | Fast | Slow | Reference | Fast | Slow | Reference | Fast |
| 2020 | 0 | 1.00 | 1.00 | 1.00 | 1.00 | 1.00 | 1.00 | 1.00 | 1.00 | 1.00 | 1.00 | 1.00 | 1.00 |
| 2025 | 0 | 1.00 | 1.00 | 1.00 | 1.00 | 1.00 | 1.00 | 1.00 | 1.00 | 1.00 | 1.00 | 1.00 | 1.00 |
| 2030 | 0 | 1.00 | 1.00 | 1.00 | 1.00 | 1.00 | 1.00 | 1.00 | 1.00 | 1.00 | 1.00 | 1.00 | 1.00 |
| 2035 | 0 | 1.00 | 1.00 | 1.00 | 1.00 | 1.00 | 1.00 | 1.00 | 1.00 | 1.00 | 1.00 | 1.00 | 1.00 |
| 2040 | 0 | 1.00 | 1.00 | 1.00 | 1.00 | 1.00 | 1.00 | 1.00 | 1.00 | 1.00 | 1.00 | 1.00 | 1.00 |
| 2045 | 0 | 1.00 | 1.00 | 1.00 | 1.00 | 1.00 | 1.00 | 1.00 | 1.00 | 1.00 | 1.00 | 1.00 | 1.00 |
| 2050 | 0.003 | 1.00 | 1.00 | 1.00 | 1.00 | 1.00 | 1.00 | 1.00 | 1.00 | 1.00 | 1.00 | 1.00 | 1.00 |
| 2055 | 0.021 | 0.92 | 0.86 | 0.80 | 1.00 | 0.97 | 0.93 | 0.79 | 0.70 | 0.62 | 1.00 | 0.97 | 0.93 |
| 2060 | 0.069 | 0.88 | 0.79 | 0.71 | 1.00 | 0.95 | 0.89 | 0.69 | 0.57 | 0.48 | 1.00 | 0.95 | 0.90 |
| 2065 | 0.209 | 0.85 | 0.73 | 0.65 | 1.00 | 0.93 | 0.86 | 0.61 | 0.48 | 0.39 | 1.00 | 0.93 | 0.86 |
| 2070 | 0.680 | 0.82 | 0.69 | 0.60 | 1.00 | 0.91 | 0.83 | 0.54 | 0.41 | 0.32 | 1.00 | 0.91 | 0.83 |
| 2075 | 1.758 | 0.79 | 0.65 | 0.57 | 1.00 | 0.90 | 0.81 | 0.49 | 0.36 | 0.28 | 1.00 | 0.90 | 0.81 |
| 2080 | 3.284 | 0.77 | 0.63 | 0.55 | 1.00 | 0.89 | 0.80 | 0.46 | 0.34 | 0.27 | 1.00 | 0.89 | 0.80 |
| 2085 | 5.036 | 0.76 | 0.62 | 0.54 | 1.00 | 0.88 | 0.79 | 0.44 | 0.32 | 0.25 | 1.00 | 0.88 | 0.79 |
| 2090 | 6.906 | 0.76 | 0.61 | 0.53 | 1.00 | 0.88 | 0.78 | 0.43 | 0.31 | 0.25 | 1.00 | 0.88 | 0.78 |
| 2095 | 8.828 | 0.75 | 0.61 | 0.53 | 1.00 | 0.87 | 0.77 | 0.42 | 0.31 | 0.24 | 1.00 | 0.87 | 0.78 |
| 2100 | 10.671 | 0.75 | 0.60 | 0.53 | 1.00 | 0.87 | 0.77 | 0.42 | 0.30 | 0.24 | 1.00 | 0.87 | 0.77 |

Note:

[a] The cumulative DACCS deployment are calculated by dividing the global cumulative DACCS deployment results (IMAGE output under SSP2-RCP1.9 w/ DACCS scenario) by half, because we assume solvent- and sorbent-based DACCS contribute the same to the DACCS deployment globally.

[b] The material and energy use factors are developed based on cumulative DACCS deployment, learning rates, and theoretical minimum value of capital and operational costs (Supplementary Table 10). The material and energy use factors are 1 in the starting year (2020), and then factors of the following year are expressed as the ratios relative to those in 2020 as the technology learning starts. By multiplying these material and energy use factors to the actual amount of material and energy uses of DACCS systems in 2020, we can get the dynamic material and energy use data of DACCS, which can be used as LCI data to evaluate the prospective environmental impacts of DACCS with the consideration of technology learning. The results under the columns named by "Reference" were estimated based on the reference learning rates in Supplementary Table 10. The results under columns named by "Slow" and "Fast" were estimated based on the lower bound (slow) and upper bound (fast) learning rates, respectively, and that is why the results under "Slow" column (representing slow learning) have higher numeric values, while the results under "Fast" column (representing fast learning) have lower numeric values.

4. Supplementary Note 4: Technologies map between IMAGE 3.2 and ecoinvent v3.6

Given the differences of generation technologies between IMAGE and ecoinvent database, here we adopted the matching list from a previous study[35] to map the available technologies in both data sources (Supplementary Table 12). Most of the generation technologies in IMAGE can be linked to one or more processes in the ecoinvent 3.6, which provides their LCI data. But there are some electricity generation technologies that appears in IMAGE scenarios but are missing in ecoinvent databases, so we imported their LCI data from external data sources to extend our the ecoinvent database (indicated as foot notes in Supplementary Table 12).

**Supplementary Table 12. Technologies map between IMAGE 3.2 and ecoinvent v3.6**

| IMAGE technology | Ecoinvent processes |
|---|---|
| Solar PV power (central) | electricity production, photovoltaic, 570kWp open ground installation, multi-Si |
| Solar PV power (decentral/residential) | electricity production, photovoltaic, 3kWp facade installation, multi-Si, laminated, integrated,<br>electricity production, photovoltaic, 3kWp facade installation, multi-Si, panel, mounted,<br>electricity production, photovoltaic, 3kWp facade installation, single-Si, laminated, integrated,<br>electricity production, photovoltaic, 3kWp facade installation, single-Si, panel, mounted,<br>electricity production, photovoltaic, 3kWp flat-roof installation, multi-Si,<br>electricity production, photovoltaic, 3kWp flat-roof installation, single-Si,<br>electricity production, photovoltaic, 3kWp slanted-roof installation, a-Si, laminated, integrated,<br>electricity production, photovoltaic, 3kWp slanted-roof installation, a-Si, panel, mounted,<br>electricity production, photovoltaic, 3kWp slanted-roof installation, CdTe, laminated, integrated,<br>electricity production, photovoltaic, 3kWp slanted-roof installation, CIS, panel, mounted,<br>electricity production, photovoltaic, 3kWp slanted-roof installation, multi-Si, laminated, integrated,<br>electricity production, photovoltaic, 3kWp slanted-roof installation, multi-Si, panel, mounted,<br>electricity production, photovoltaic, 3kWp slanted-roof installation, ribbon-Si, laminated, integrated, |

| | |
|---|---|
| | electricity production, photovoltaic, 3kWp slanted-roof installation, ribbon-Si, panel, mounted,<br>electricity production, photovoltaic, 3kWp slanted-roof installation, single-Si, laminated, integrated |
| Concentrated solar power | electricity production, solar thermal parabolic trough, 50 MW,<br>electricity production, solar tower power plant, 20 MW |
| Onshore wind power | electricity production, wind, <1MW turbine, onshore,<br>electricity production, wind, 1-3MW turbine, onshore,<br>electricity production, wind, >3MW turbine, onshore |
| Offshore wind power | electricity production, wind, 1-3MW turbine, offshore |
| Wave power[a] | electricity production, wave |
| Hydro power | electricity production, hydro, reservoir, alpine region,<br>electricity production, hydro, reservoir, non-alpine region,<br>electricity production, hydro, reservoir, tropical region,<br>electricity production, hydro, run-of-river |
| Other renewables (tidal and geothermal power) | electricity production, deep geothermal |
| Nuclear | electricity production, nuclear, boiling water reactor,<br>electricity production, nuclear, pressure water reactor, heavy water moderated,<br>electricity production, nuclear, pressure water reactor |
| Coal steam turbine | electricity production, hard coal,<br>electricity production, lignite,<br>electricity production, peat,<br>electricity production, hard coal, conventional,<br>electricity production, hard coal, supercritical |
| Oil steam turbine | electricity production, oil |
| Natural gas open cycle turbine | electricity production, natural gas, conventional power plant |
| Biomass steam turbine | electricity production, wood, future |
| Integrated gasification combined cycle[b] | Electricity, at power plant/hard coal, IGCC, no CCS/2025,<br>Electricity, at power plant/lignite, IGCC, no CCS/2025 |
| Oil combined cycle | electricity production, oil<br>*(Use copy of Oil steam turbine here as Oil combined cycle does not exist in ecoinvent)* |
| Natural gas combined cycle | electricity production, natural gas, combined cycle power plant |
| Biomass combined cycle[b] | Electricity, at BIGCC power plant 450MW, no CCS/2025 |
| Coal with CCS[b] | Electricity, at power plant/hard coal, pre, pipeline 200km, storage 1000m/2025,<br>Electricity, at power plant/lignite, pre, pipeline 200km, storage 1000m/2025,<br>Electricity, at power plant/hard coal, post, pipeline 200km, storage 1000m/2025,<br>Electricity, at power plant/lignite, post, pipeline 200km, storage |

| | |
|---|---|
| | 1000m/2025,<br>Electricity, at power plant/lignite, oxy, pipeline 200km, storage 1000m/2025,<br>Electricity, at power plant/hard coal, oxy, pipeline 200km, storage 1000m/2025 |
| Oil with CCS | Electricity, at power plant/hard coal, pre, pipeline 200km, storage 1000m/2025,<br>Electricity, at power plant/lignite, pre, pipeline 200km, storage 1000m/2025,<br>Electricity, at power plant/hard coal, post, pipeline 200km, storage 1000m/2025,<br>Electricity, at power plant/lignite, post, pipeline 200km, storage 1000m/2025,<br>Electricity, at power plant/lignite, oxy, pipeline 200km, storage 1000m/2025,<br>Electricity, at power plant/hard coal, oxy, pipeline 200km, storage 1000m/2025,<br>Electricity, at power plant/natural gas, pre, pipeline 200km, storage 1000m/2025,<br>Electricity, at power plant/natural gas, post, pipeline 200km, storage 1000m/2025<br>*(the LCI data of oil with CCS is not available, so we just use the dataset of coal and natural gas with CCS as a proxy)* |
| Nature gas with CCS[b] | Electricity, at power plant/natural gas, pre, pipeline 200km, storage 1000m/2025,<br>Electricity, at power plant/natural gas, post, pipeline 200km, storage 1000m/2025 |
| Biomass with CCS[b] | Electricity, at BIGCC power plant 450MW, pre, pipeline 200km, storage 1000m/2025 |
| Coal combined heat and power (CHP) | heat and power co-generation, hard coal,<br>heat and power co-generation, lignite |
| Oil CHP | heat and power co-generation, oil |
| Nature gas CHP | heat and power co-generation, natural gas, combined cycle power plant, 400MW electrical,<br>heat and power co-generation, natural gas, conventional power plant, 100MW electrical,<br>heat and power co-generation, natural gas, 500kW electrical, lean burn |
| Biomass CHP | heat and power co-generation, wood chips, 6667 kW, state-of-the-art 2014,<br>heat and power co-generation, wood chips, 6667 kW |

| | |
|---|---|
| Coal CHP with CCS | Electricity, at power plant/hard coal, pre, pipeline 200km, storage 1000m/2025,<br>Electricity, at power plant/lignite, pre, pipeline 200km, storage 1000m/2025,<br>Electricity, at power plant/hard coal, post, pipeline 200km, storage 1000m/2025,<br>Electricity, at power plant/lignite, post, pipeline 200km, storage 1000m/2025,<br>Electricity, at power plant/lignite, oxy, pipeline 200km, storage 1000m/2025,<br>Electricity, at power plant/hard coal, oxy, pipeline 200km, storage 1000m/2025<br>*(the LCI data of coal CHP with CCS is not available, so we just use the dataset of coal with CCS as a proxy)* |
| Oil CHP with CCS | Electricity, at power plant/hard coal, pre, pipeline 200km, storage 1000m/2025,<br>Electricity, at power plant/lignite, pre, pipeline 200km, storage 1000m/2025,<br>Electricity, at power plant/hard coal, post, pipeline 200km, storage 1000m/2025,<br>Electricity, at power plant/lignite, post, pipeline 200km, storage 1000m/2025,<br>Electricity, at power plant/lignite, oxy, pipeline 200km, storage 1000m/2025,<br>Electricity, at power plant/hard coal, oxy, pipeline 200km, storage 1000m/2025,<br>Electricity, at power plant/natural gas, pre, pipeline 200km, storage 1000m/2025,<br>Electricity, at power plant/natural gas, post, pipeline 200km, storage 1000m/2025<br>*(the LCI data of oil CHP with CCS is not available, so we just use the dataset of coal and natural gas with CCS as a proxy as a proxy)* |
| Natural gas CHP with CCS | Electricity, at power plant/natural gas, pre, pipeline 200km, storage 1000m/2025,<br>Electricity, at power plant/natural gas, post, pipeline 200km, storage 1000m/2025<br>*(the LCI data of natural gas CHP with CCS is not available, so we just use the dataset of coal and natural gas with CCS as a proxy as a proxy)* |
| Biomass CHP with CCS[b] | Electricity, at wood burning power plant 20 MW, truck 25km, post, pipeline 200km, storage 1000m/2025 |

Note:

[a] LCI of wave electricity generation is collected based on an attenuator-type floating oscillating body system wave energy converter with a capacity of 750kW[231]. The LCI data is also summarized in "*1_LCI_wave_electricity.xlsx"* excel file in "LCI_data" folder.

[b] We adopted the LCI of fossil fuel with CCS that is summarized in a previous study[35]. The LCI data is also summarized in "*2_LCI_CCS.xlsx"* excel file in "LCI_data" folder.

## 5. Supplementary Note 5: Limitations

In this study, we modify the background LCI database using IMAGE projections of grid mix, generation efficiency and emissions of thermal power plants (fossil-based sources, biomass, and nuclear), while the renewable sources and their efficiency levels are based on existing available technologies. Technological innovation has been observed for renewable (especially solar[232,233] and wind[234]) and energy storage[235,236] technologies, and they will continue to evolve as they are more widely applied in the energy system. Therefore, to better evaluate the prospective environmental impacts of energy-intensive technologies, such as DACCS, under specific climate contexts, the analysis framework could be expanded to consider the advancement, particularly in material efficiency or circularity of VRE and storage technologies in the background electricity system.

Previous studies looking to the technology learning of DACCS have focused on cost reductions[199,228,237]. Publicly available, empirical studies that reveal how material and energy inputs change as DACCS scales could not be identified. Given this limited data availability, we assume the material and energy inputs of DACCS follow the same learning rates as the associated cost projections. In reality, technology learning rates are likely to vary depending on processes and physical input types[94,238]. Future LCA studies aiming to quantify the effects of technology learning on environmental impacts might be able to rely on more detailed learning data of specific physical inputs. In addition, learning rates of emerging technologies tend to change with technology-readiness-levels (TRL)[239–241]. Prospective analyses of emerging technologies ideally reflect this by applying a multi-factor learning curve approach, differentiating between the varying learning rates at different TRL. The technologies analyzed herein operate at demonstration scale (TRL-7) while we apply a single-factor, constant learning

rate, postulating learning-by-doing improvements at commercial scale (TRL-9). The learning rate at commercial scale is a research frontier and presently unknown. Yet, at the scale of our analysis, a respective differentiation is unlikely to add accuracy or insight. The uncertainty with respect to the specific single learning rate at commercial scale is captured by testing how different learning rates affect our results. Using a single-factor learning curve approach, we thus attribute the cost change and its related material and energy consumption to the cumulative installed capacity of DACCS over time, limiting our capability of revealing the correlation between technology progress and other factors, such as (prior) R&D expenditure[242].

The life cycle impact assessment step relates emissions and resource use to environmental impacts through characterization factors. The framework we adapted here applied global or European scale characterization factors. While location-generic characterization factors are suitable for global impacts such as climate change impact, they may lead to large uncertainty for quantifying non-global impacts, such as acidification[243], eutrophication[244], and ecotoxicity[245], which are typically affected by regional meteorological, hydrological, soil conditions and the sensitivity of ecosystems to emissions. While country-dependent characterization models and factors have been developed for these impact categories, they have not yet been incorporated into the LCA framework applied in this study. Further methodological improvements are needed to enhance the capability of the existing framework for conducting regional impact assessments.

This study shows the environmental impacts of DACCS could have different trajectories depending on the background energy system, so it is important to keep monitoring those environmental metrics or even considering them in the decision-making process. Future research could explore the feasibility of incorporating life cycle environmental metrics into IAMs for better environmental impact assessment. State-of-the art IAMs typically include some

environment-related metrics, such as greenhouse gas emission, land and water use as constraints, but they lack many other environmental impact dimensions. For example, metal consumption could be an important metric given the increasing penetration of renewable and battery storage in the energy system, which are resource intensive. Furthermore, life cycle environmental metrics capture the emissions from all life cycle phases (e.g., construction, transport, operation, and end-of-life, etc.), and IAMs evaluate the interrelationship among different sectors. Therefore, the integration of life cycle environmental metrics and IAMs should carefully allocate the emissions of different life cycle phases to the corresponding sectors/energy carriers in IAM to avoid double counting[48].

6. Supplementary Note 6: Supplementary results

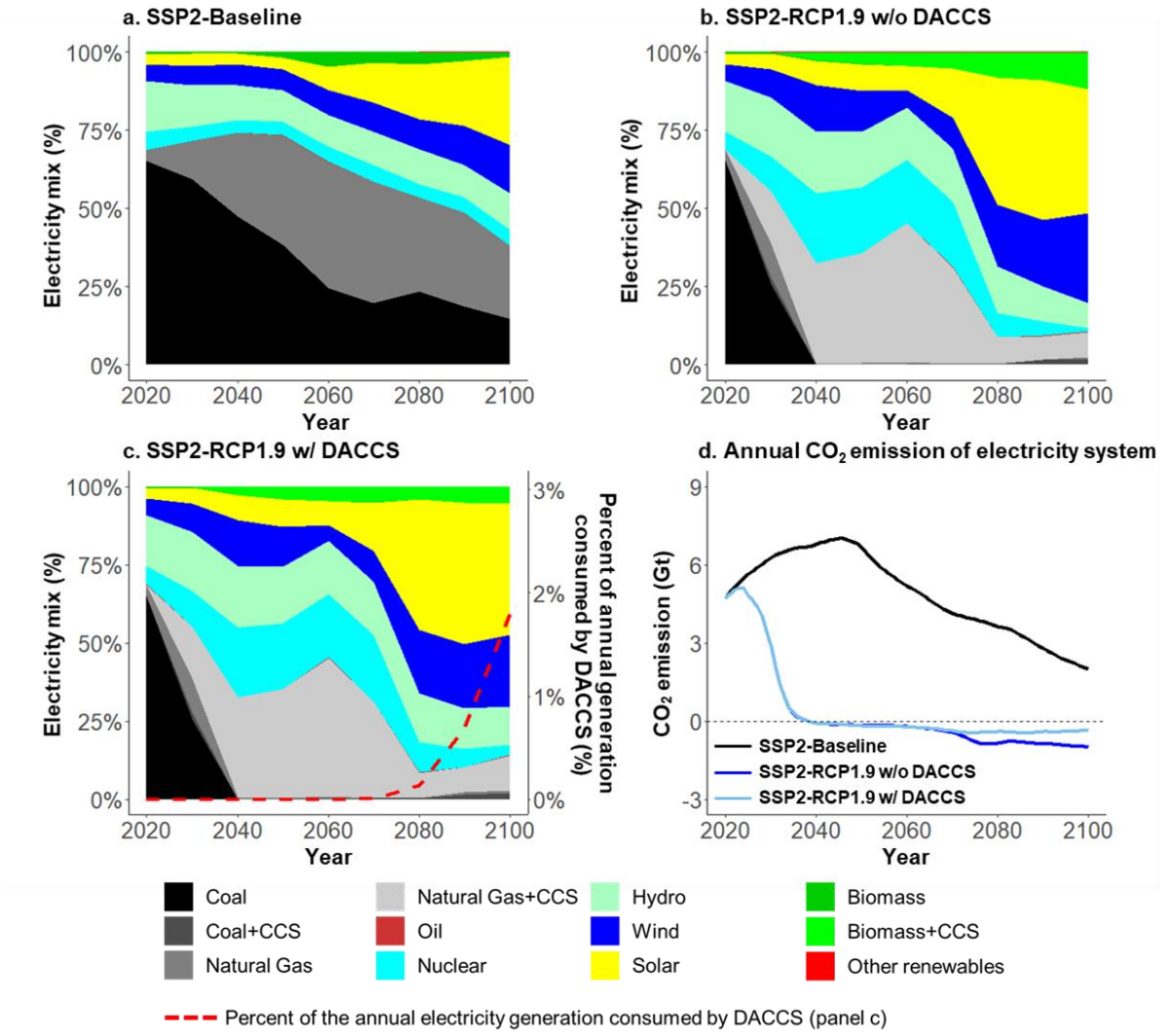


**Supplementary Figure 2. The electricity mix of China under (a) SSP2-baseline, (b) SSP2-RCP1.9 w/ DACCS, (c) SSP2-RCP1.9 w/o DACCS scenarios and (d) the annual $CO_2$ emission of from the electricity system under the three scenarios.** In electricity mix panels (a, b, c), the stacked area represents the market shares of the grid mix. "Solar" includes both solar PV and concentrated solar power (CSP). "Oil" combines both oil with and without CCS as oil with CCS accounts for less than 1% of the grid mix. Other renewables include wave, tidal, and geothermal power. In panel c, the red dash line represents the percent of the annual electricity generation consumed by DACCS, which corresponds to the secondary y axis on the right of this panel.

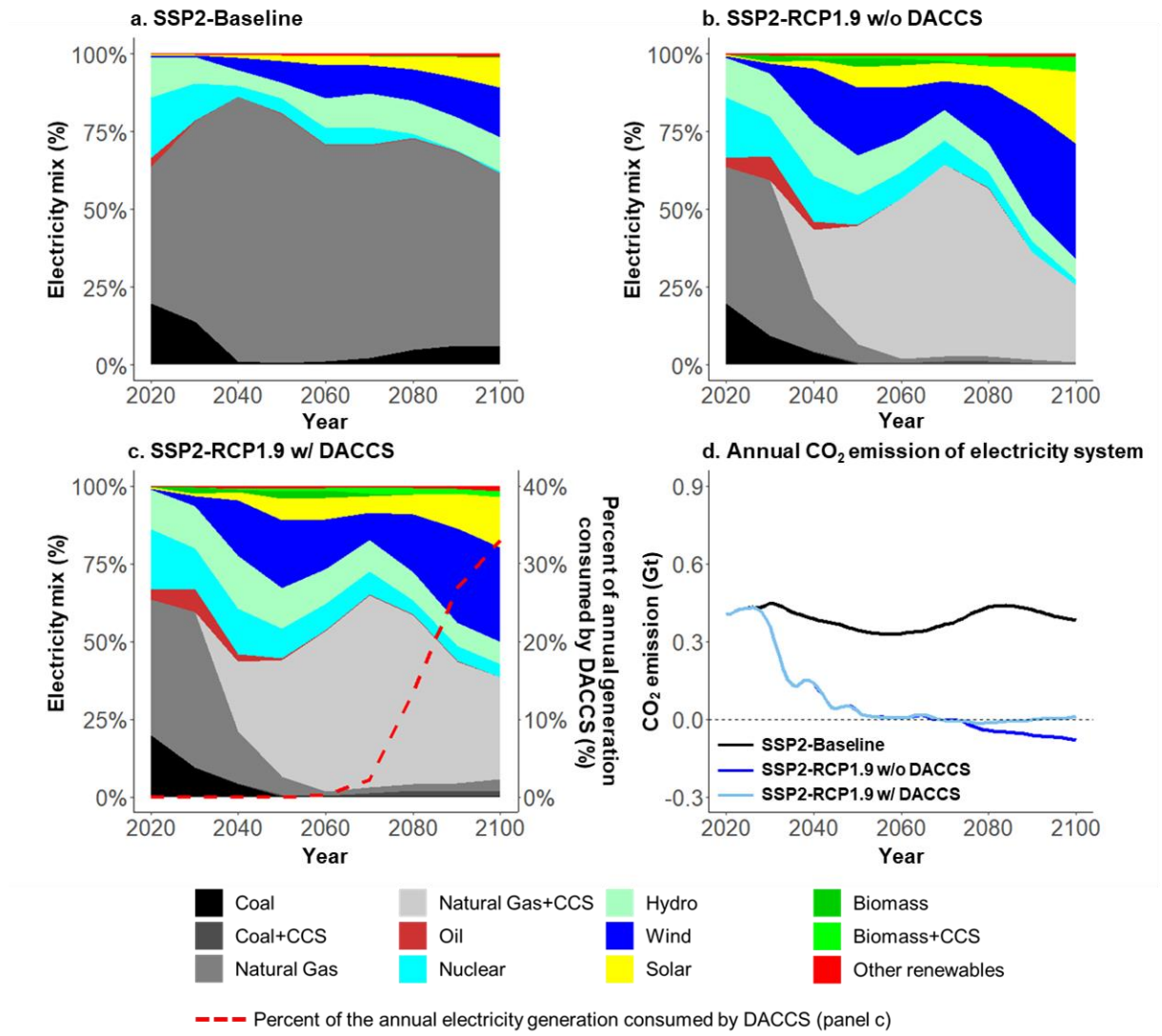


**Supplementary Figure 3. The electricity mix of Russia under (a) SSP2-baseline, (b) SSP2-RCP1.9 w/ DACCS, (c) SSP2-RCP1.9 w/o DACCS scenarios and (d) the annual $CO_2$ emission from the electricity system under the three scenarios.** In electricity mix panels (a, b, c), the stacked area represents the market shares of the grid mix. "Solar" includes both solar PV and concentrated solar power (CSP). "Oil" combines both oil with and without CCS as oil with CCS accounts for less than 1% of the grid mix. Other renewables include wave, tidal, and geothermal power. In panel c, the red dash line represents the percent of the annual electricity generation consumed by DACCS, which corresponds to the secondary y axis on the right of this panel.

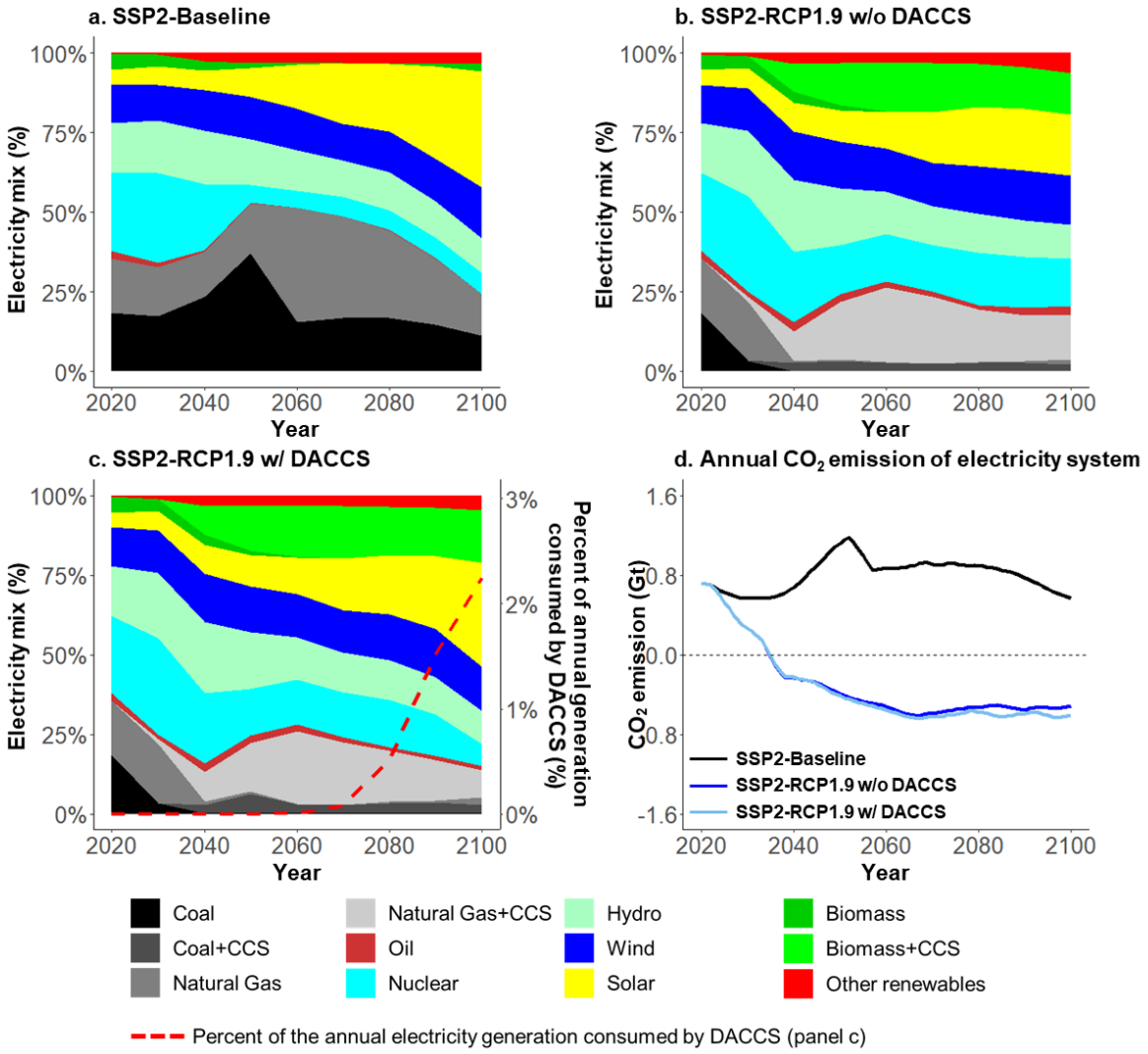


**Supplementary Figure 4. The electricity mix of Western Europe under (a) SSP2-baseline, (b) SSP2-RCP1.9 w/ DACCS, (c) SSP2-RCP1.9 w/o DACCS scenarios and (d) the annual $CO_2$ emission from the electricity system under the three scenarios.** In electricity mix panels (a, b, c), the stacked area represents the market shares of the grid mix. "Solar" includes both solar PV and concentrated solar power (CSP). "Oil" combines both oil with and without CCS as oil with CCS accounts for less than 1% of the grid mix. Other renewables include wave, tidal, and geothermal power. In panel c, the red dash line represents the percent of the annual electricity generation consumed by DACCS, which corresponds to the secondary y axis on the right of this panel.

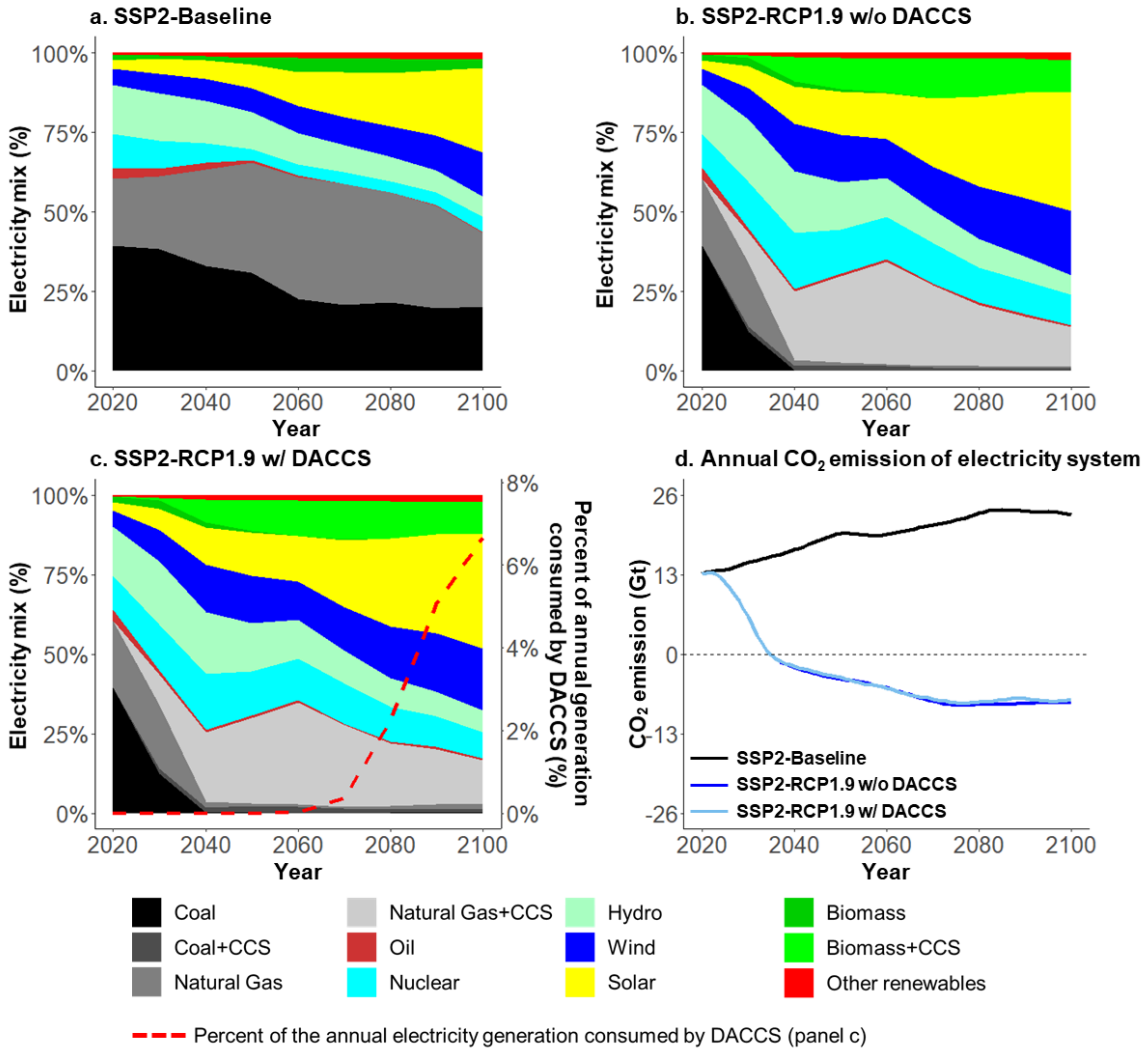


**Supplementary Figure 5. The world electricity mix under (a) SSP2-baseline, (b) SSP2-RCP1.9 w/ DACCS, (c) SSP2-RCP1.9 w/o DACCS scenarios and (d) the annual $CO_2$ emission from the electricity system under the three scenarios.** In electricity mix panels (a, b, c), the stacked area represents the market shares of the grid mix. "Solar" includes both solar PV and concentrated solar power (CSP). "Oil" combines both oil with and without CCS as oil with CCS accounts for less than 1% of the grid mix. Other renewables include wave, tidal, and geothermal power. In panel c, the red dash line represents the percent of the annual electricity generation consumed by DACCS, which corresponds to the secondary y axis on the right of this panel.

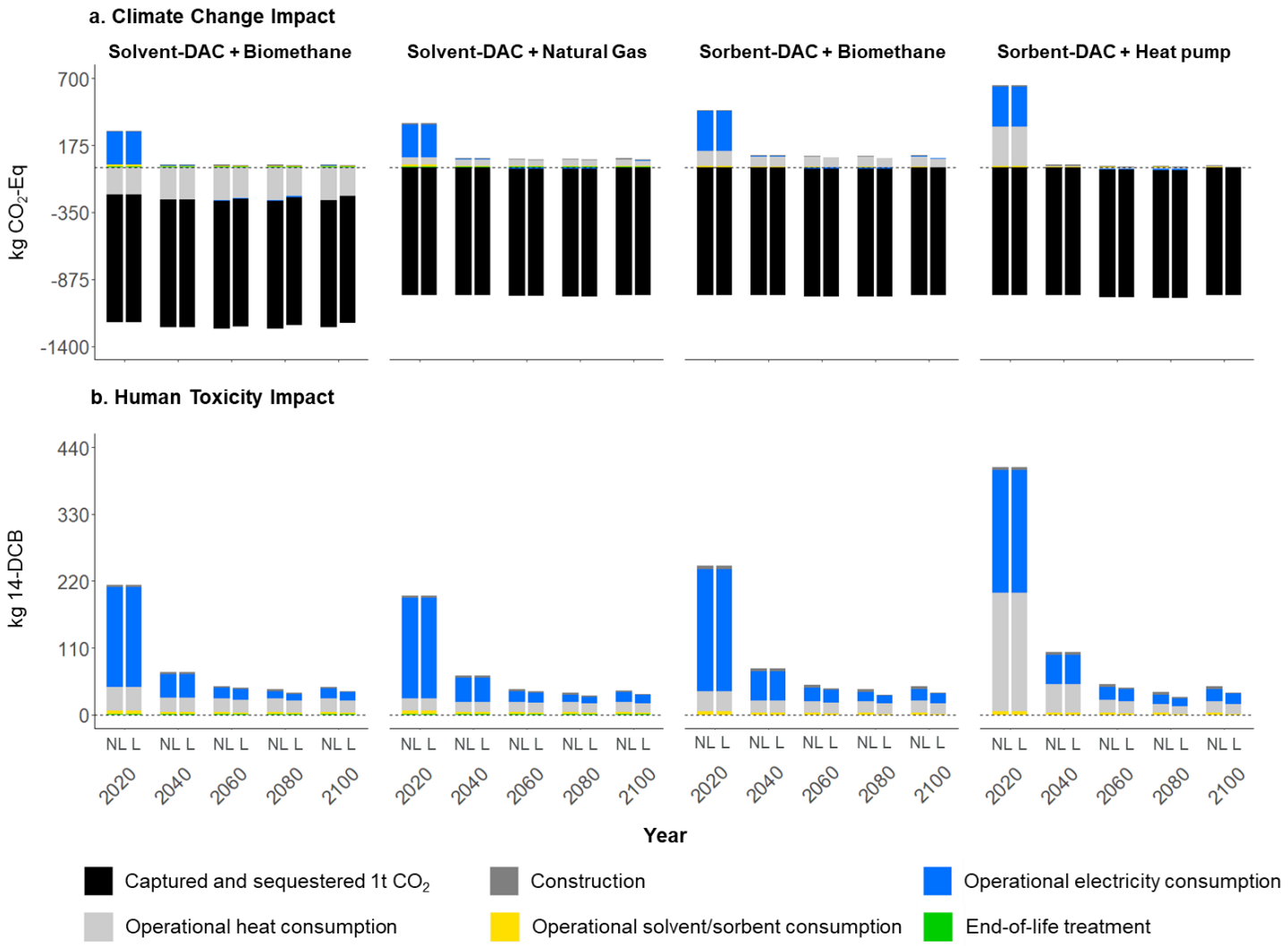


**Figure to be continued**

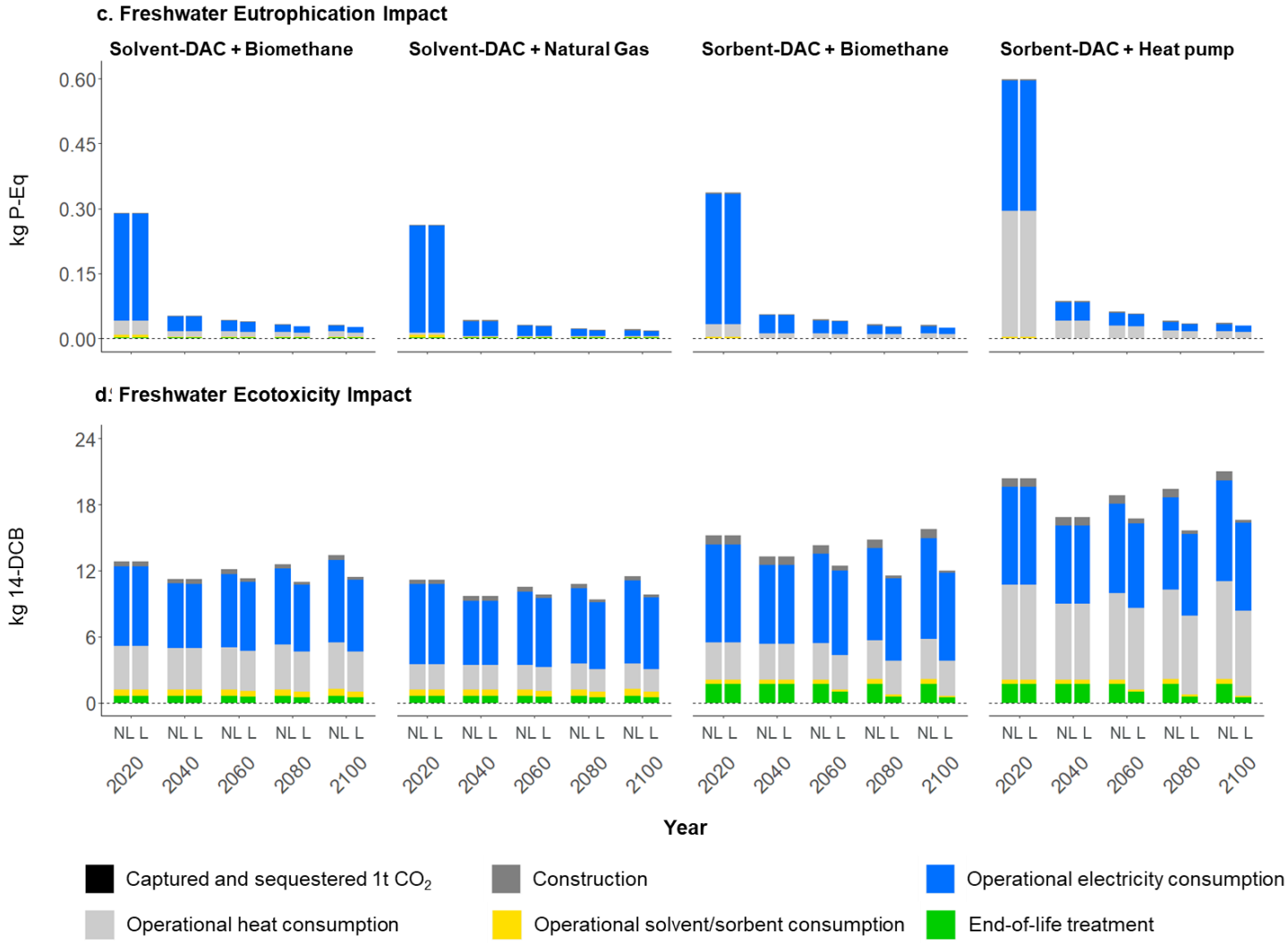


**Figure to be continued**

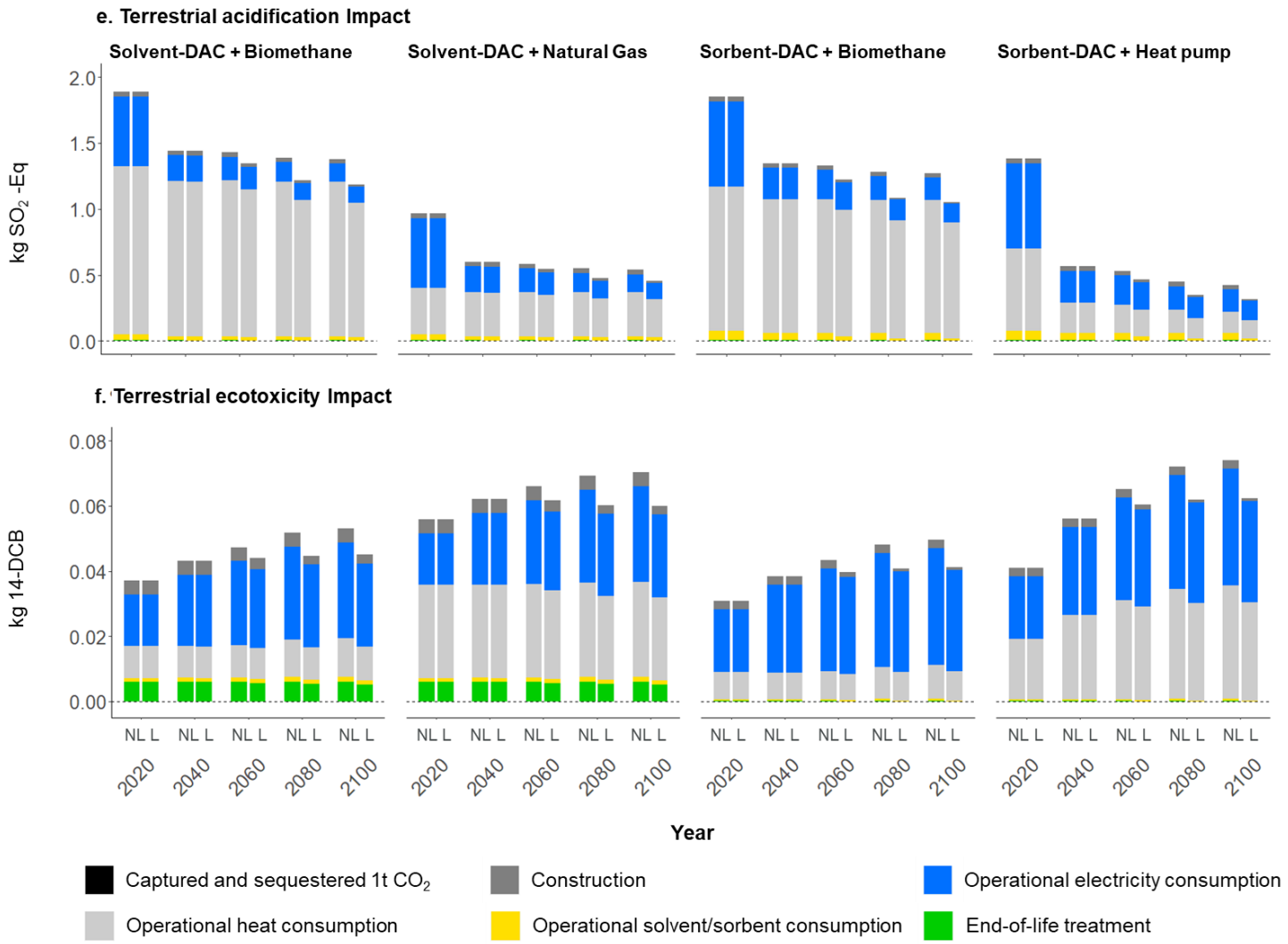


**Figure to be continued**

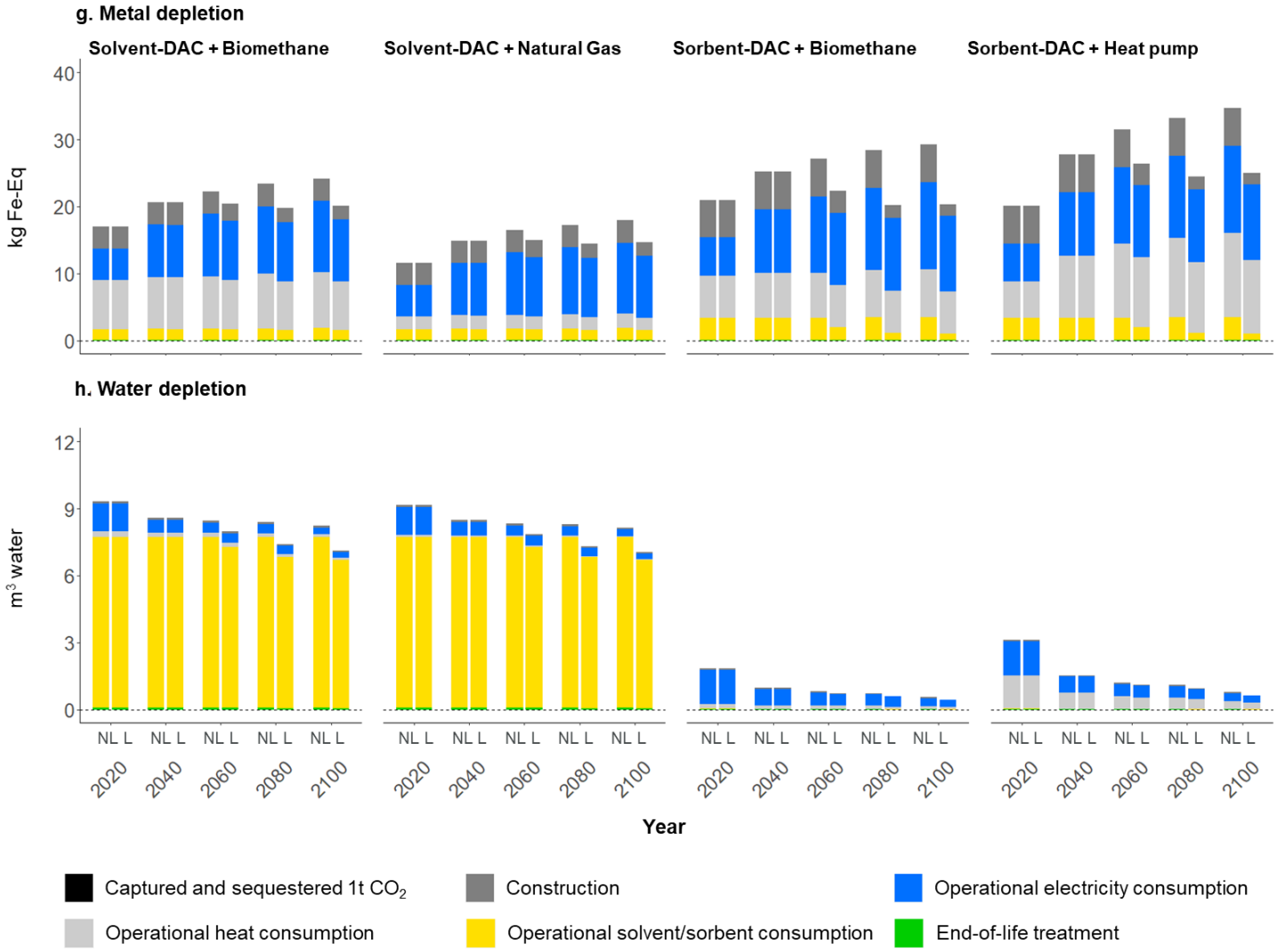


**Supplementary Figure 6. The contribution of different life cycle stages to the total environmental impact (per 1 t atmospheric $CO_2$ captured and sequestered) under SSP2-RCP1.9 w/DAC scenario (US case).** Different colors of the stacked bar represent different life cycle stages. Each year corresponds to two bars representing the results of no technology learning ("NL", on the left) and with technology learning ("L", on the right).

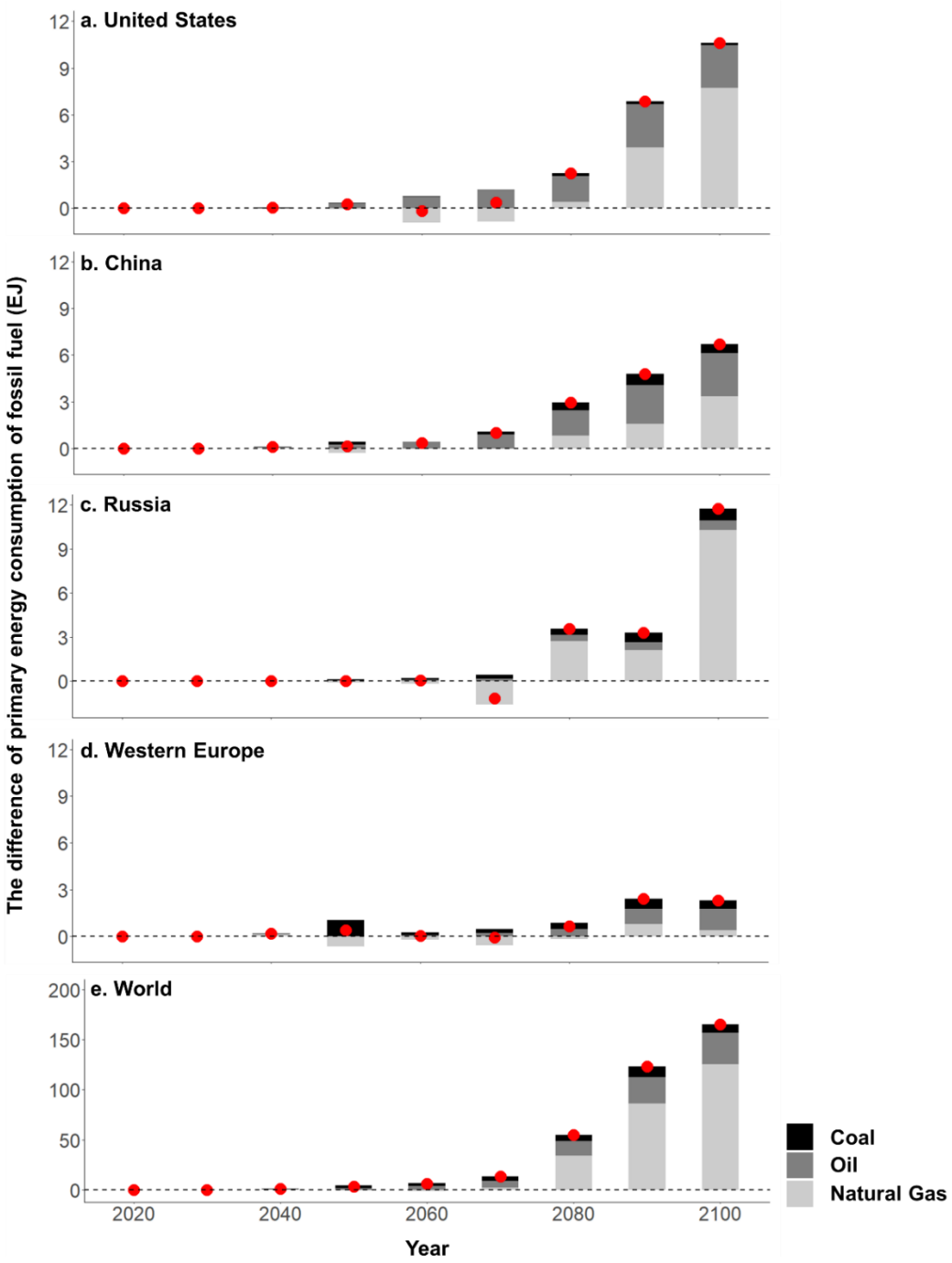


**Supplementary Figure 7. The difference of annual total primary energy consumption of fossil fuels (coal, oil and natural gas) in the United States (a), China (b), Russia (c), Western Europe (d) and the World as a whole (e) between SSP2-RCP1.9 w/o DACCS and SSP2-RCP1.9 w/ DACCS scenarios.** The difference is calculated by subtracting the primary energy consumption under SSP2-RCP1.9 w/o DACCS scenario from that under SSP2-RCP1.9 w/ DACCS scenario. The red dots represent the net difference in each year.

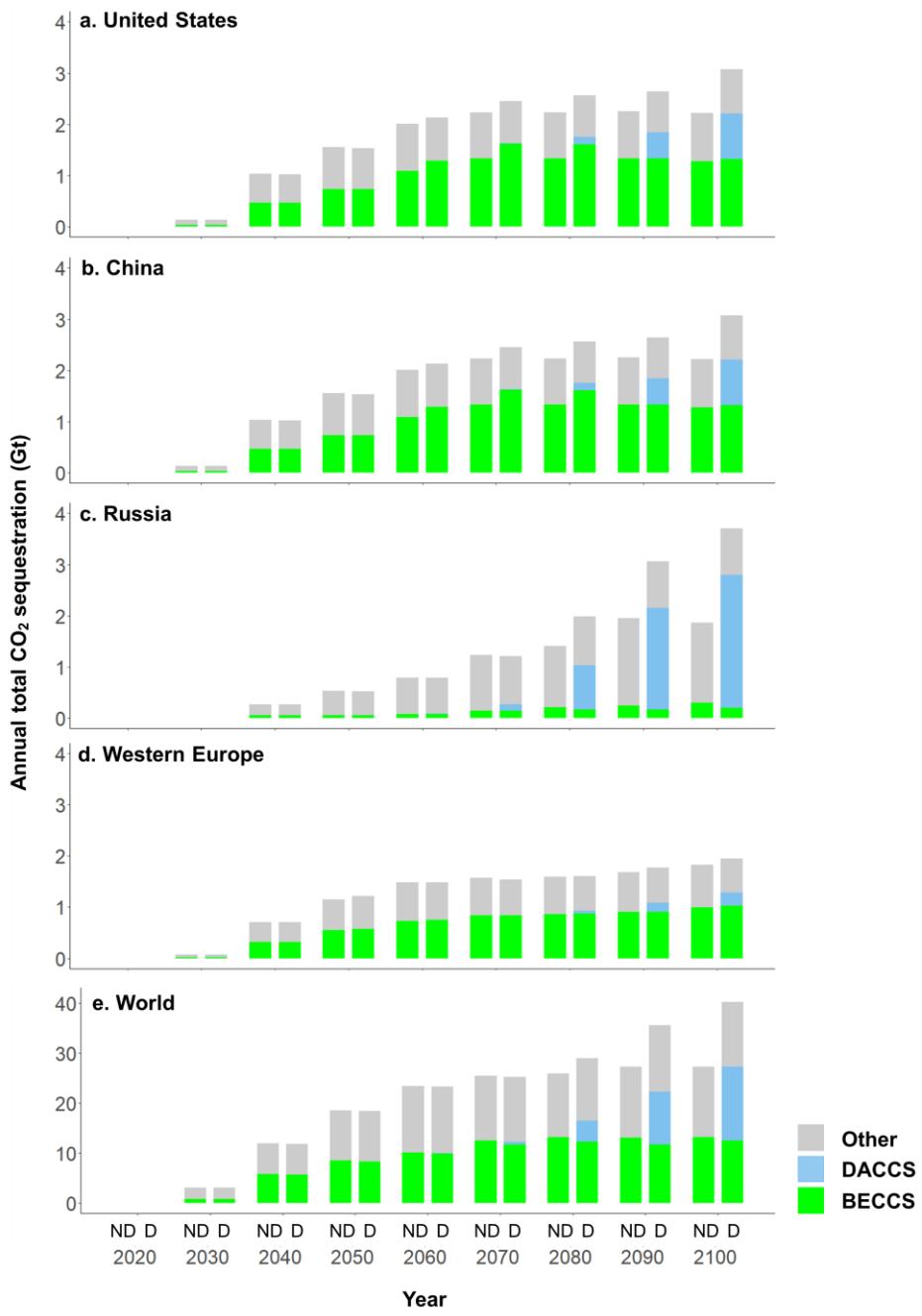


**Supplementary Figure 8. The annual total $CO_2$ sequestration in the United States (a), China (b), Russia (c), Western Europe (d) and the World as a whole (e) under SSP2-RCP1.9 w/o DACCS and SSP2-RCP1.9 w/ DACCS scenarios.** There are two stacked bars for each year. The left bar ("ND") represents the results under SSP2-RCP1.9 w/o DACCS scenario. The right bar ("D") represents the results under SSP2-RCP1.9 w/ DACCS scenario. Different colors in the stacked bars represent different technologies used to sequester $CO_2$. BECCS is bioenergy with carbon capture and storage. DACCS is the direct air carbon capture and storage. Other includes carbon capture and storage (CCS) technologies applied in fossil fuel power plant, hydrogen, and industry sectors.

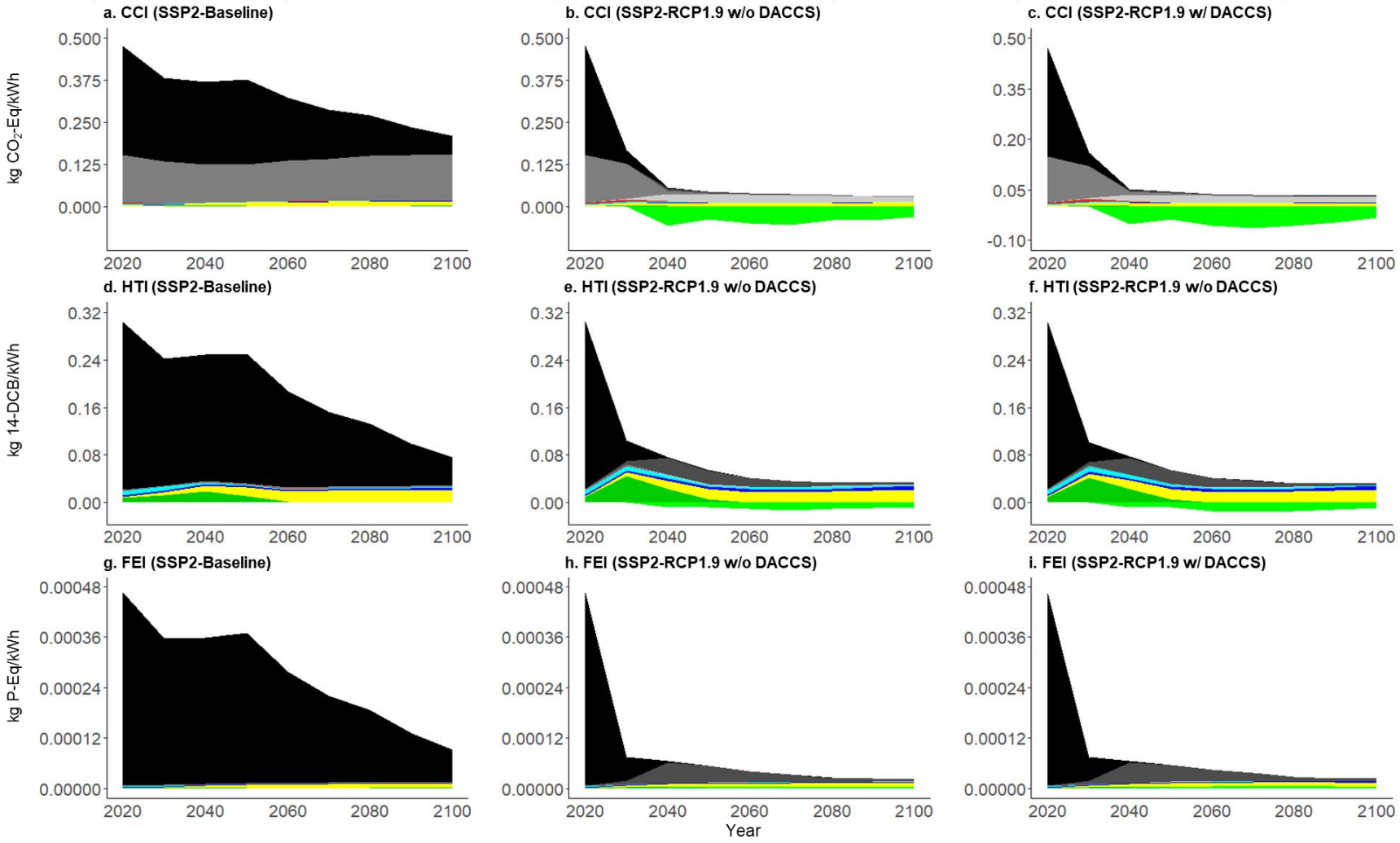


**Figure to be continued**

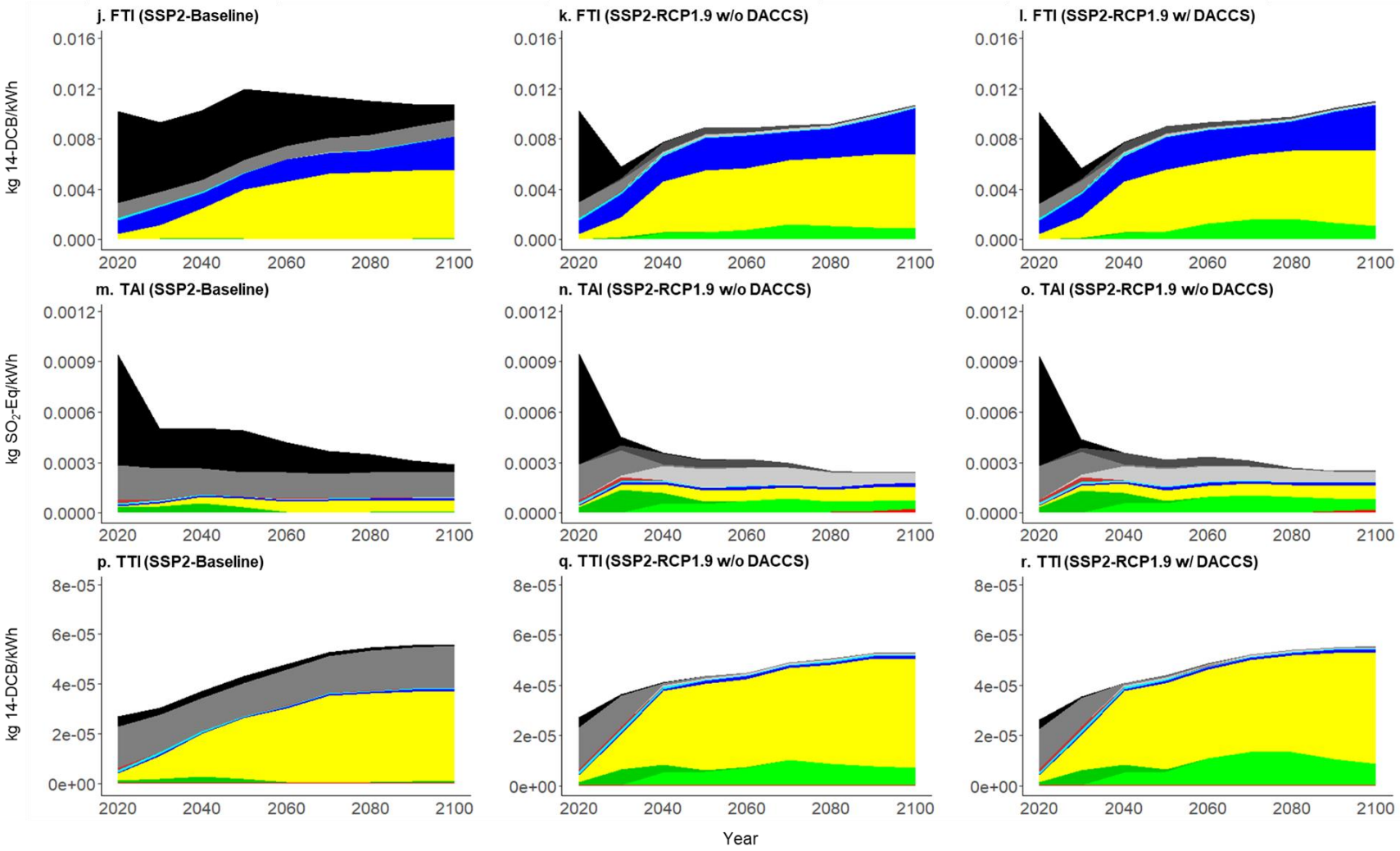


**Figure to be continued**

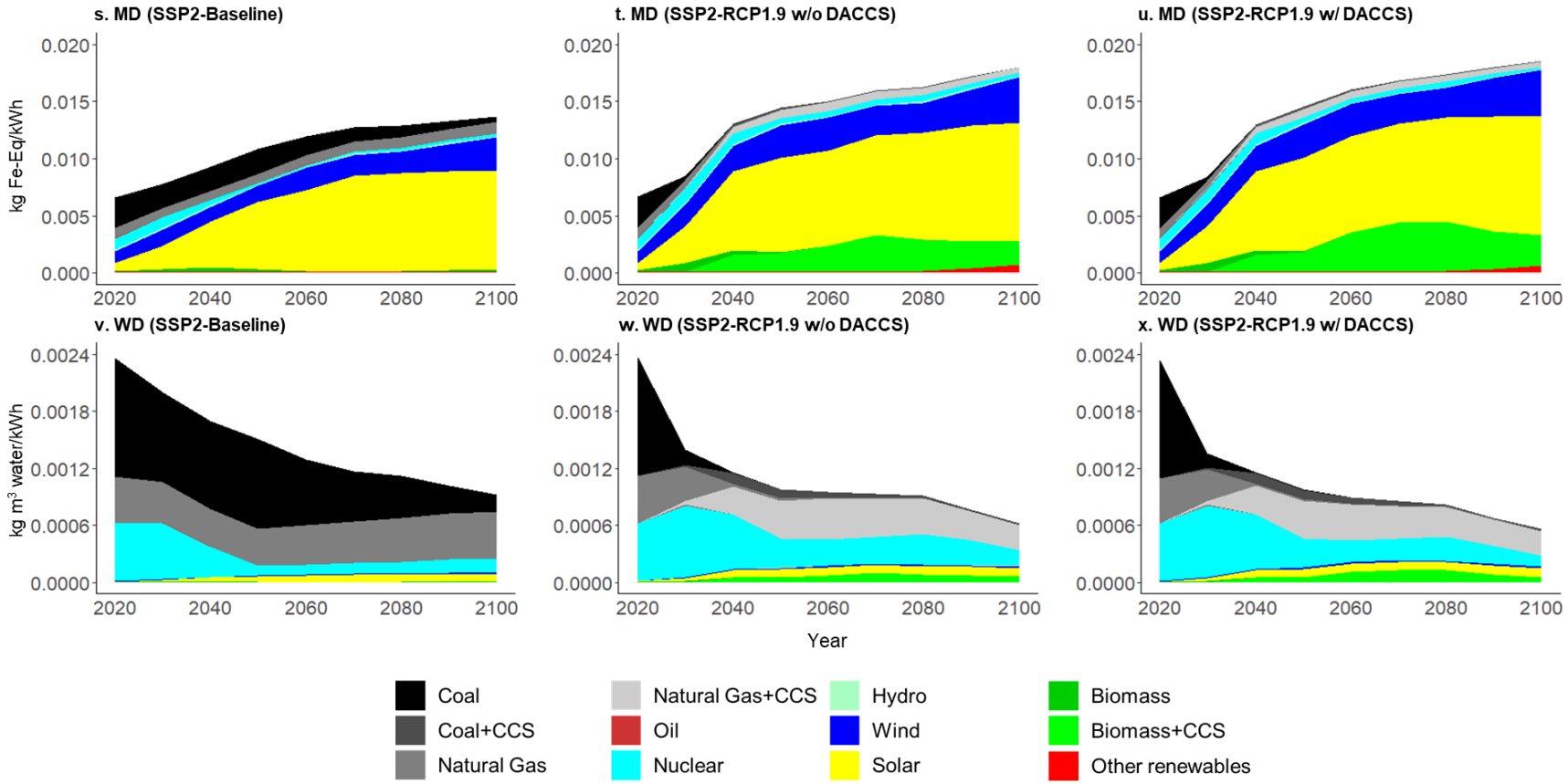


**Supplementary Figure 9. The life cycle environmental impact of 1 kWh US electricity generation from 2020 to 2100 under SSP2-Baseline, SSP2-RCP1.9 w/o DACCS and SSP2-RCP1.9 w/ DACCS scenarios.** The stacked area represents the contribution of different electricity technologies to the total impacts. Impact categories abbreviations: CCI – Climate Change Impact, HTI – Human Toxicity Impact, FEI – Freshwater Eutrophication Impact, FTI – Freshwater Ecotoxicity Impact, TAI – Terrestrial Acidification Impact, TTI – Terrestrial ecotoxicity Impact, MD – Metal depletion, WD – Water depletion.

## V. Summary

The dissertation evaluated the economic and environmental implications of decarbonization actions in the energy system, including energy-efficient transition of lighting technologies, decarbonization of electric power sector, and DACCS. To achieve these research objectives, I linked TEA, LCA, and material flow analysis with scenario analysis and/or system modeling approaches. These methodology integration makes it possible to capture the effects of system interaction and evolution on the performance of decarbonization actions.

In Chapter II, I studied the uses and recycling of critical REOs in the transition to energy-efficient lighting technologies (e.g., fluorescent and LED lightbulbs). The demand for REOs in the lighting sector shows a rapid increase after 1990 and peaked at around 2014 (with 9,000t/yr REO at a medium LED penetration scenario) driven by the global adoption of fluorescent lightbulbs, but this increasing trend decreases after the peak as more efficient LED lightbulbs (that requires significant less REO consumption than fluorescent lightbulbs) penetrated the market and replaced fluorescent lightbulbs. The REO recycling from end-of-life lighting technologies are not economically feasible under 2018 REO prices, even though economy of scale can reduce recycling cost from $7,223/t to $2,496/t (2014 US$) as plant capacity increases from 100 t/yr to 1,500 t/yr, highlighting the improvement of REO recycling rate may need higher REO prices or commensurate policy interventions.

In Chapter III, I quantified the total system cost of the U.S. electric power system under different scenarios based on the capacity expansion and dispatch outputs from a regionally resolved electricity system optimization model. I found pursuing zero $CO_2$ emission by replacing fossil fuel with renewable and other low-carbon energy sources would incur $335–$494 billion

additional cost (5% discount rate and 2020 US$, equivalent to 0.46–0.68 cent/kWh) to the U.S. electricity system during 2020–2050, with regional costs ranging 0.20–1.20 cent/kWh. Additionally, the marginal cost of $CO_2$ abatement increases to as high as \$122/t $CO_2$ for reaching 100% $CO_2$ reduction by 2050, which is higher than the cost lower bounds of BECCS (\$52/t $CO_2$) and DACCS (\$114/t $CO_2$), indicating their potential opportunity to decarbonize the last few percent of $CO_2$ emission from the U.S. electricity system.

In Chapter IV, I evaluated the prospective environmental performance of DACCS. I found decarbonizing the electricity sector improves the sequestration efficiency but increases the terrestrial ecotoxicity (by 33% to 80% depending on technology and heat sources) and metal depletion (by 40% to 73%) levels per tonne of $CO_2$ sequestered from 2020 to 2100. These increases can be reduced by improving the material and energy use efficiencies of DACCS as it scales up. DACCS exhibits regional environmental impact variations, highlighting the importance of smart siting by considering concerning environmental metrics. DACCS deployment aids the achievement of long-term climate targets, its environmental and climate performance however depend on sectoral mitigation actions, and thus DACCS deployment should not suggest a relaxation of sectoral decarbonization targets.

This dissertation provides robust and reliable insights for the low-carbon transition of energy system by evaluating the economic and environmental performances of decarbonization actions in dynamic system contexts. Decarbonization actions in the energy system could lead to economic and environmental trade-offs which should be carefully studied and considered in policy decisions. Future studies and policies may also rely on multi-criterion decision analysis to decide how to implement a variaty of decarbonization actions in energy system based on the optimization of different sustainability dimensions.

# VI. References


1. Nations, U. Paris Agreement to the United Nations Framework Convention on Climate Change. (2015).

2. Intergovernmental Panel on Climate Change. *Climate Change 2014: Mitigation of Climate Change: Working Group III Contribution to the IPCC Fifth Assessment Report*. (Cambridge University Press, 2015). doi:10.1017/CBO9781107415416.

3. IPCC. *Special report on the impacts of global warming of 1.5° C above pre-industrial levels and related global greenhouse gas emission pathways*. (Intergovernmental Panel on Climate Change, 2018).

4. Shukla, P. R. *et al. IPCC, 2022: Climate Change 2022: Mitigation of Climate Change. Contribution of Working Group III to the Sixth Assessment Report of the Intergovernmental Panel on Climate Change*. doi: 10.1017/9781009157926.

5. Rogelj, J. *et al.* Energy system transformations for limiting end-of-century warming to below 1.5 °C. *Nature Climate Change* **5**, 519–527 (2015).

6. Fay, M. *et al. Decarbonizing development: Three steps to a zero-carbon future*. (World Bank Publications, 2015).

7. Williams, J. H. *et al.* Carbon-neutral pathways for the United States. *AGU Advances* **2**, e2020AV000284 (2021).

8. Ray, D. Lazard's Levelized Cost of Energy Analysis—Version 15.0. *Lazard: New York, NY, USA* **20**, (2021).

9. Secretariat, R. *Renewables 2019: Global Status Report, Paris*. (2019).

10. Sepulveda, N. A., Jenkins, J. D., de Sisternes, F. J. & Lester, R. K. The Role of Firm Low-Carbon Electricity Resources in Deep Decarbonization of Power Generation. *Joule* **2**, 2403–2420 (2018).

11. Heptonstall, P. J. & Gross, R. J. K. A systematic review of the costs and impacts of integrating variable renewables into power grids. *Nat Energy* **6**, 72–83 (2021).

12. Lim, S.-R., Kang, D., Ogunseitan, O. A. & Schoenung, J. M. Potential Environmental Impacts from the Metals in Incandescent, Compact Fluorescent Lamp (CFL), and Light-Emitting Diode (LED) Bulbs. *Environmental Science & Technology* **47**, 1040–1047 (2013).

13. Ding, Y. *et al.* Recovery of precious metals from electronic waste and spent catalysts: A review. *Resources, Conservation and Recycling* **141**, 284–298 (2019).

14. Roe, S. *et al.* Contribution of the land sector to a 1.5 °C world. *Nature Climate Change* **9**, 817–828 (2019).

15. Fuhrman, J. *et al.* Food–energy–water implications of negative emissions technologies in a +1.5 °C future. *Nature Climate Change* (2020) doi:10.1038/s41558-020-0876-z.

16. Powell, T. W. R. & Lenton, T. M. Future carbon dioxide removal via biomass energy constrained by agricultural efficiency and dietary trends. *Energy Environ. Sci.* **5**, 8116–8133 (2012).

17. Rehbein, J. A. *et al.* Renewable energy development threatens many globally important biodiversity areas. *Global change biology* **26**, 3040–3051 (2020).

18. Deutz, S. & Bardow, A. Life-cycle assessment of an industrial direct air capture process based on temperature–vacuum swing adsorption. *Nature Energy* **6**, 203–213 (2021).

19. Creutzig, F. *et al.* The mutual dependence of negative emission technologies and energy systems. *Energy & Environmental Science* **12**, 1805–1817 (2019).

20. Marcucci, A., Kypreos, S. & Panos, E. The road to achieving the long-term Paris targets: energy transition and the role of direct air capture. *Climatic Change* **144**, 181–193 (2017).

21. Zimmermann, A. *et al. Techno-Economic Assessment & Life Cycle Assessment Guidelines for CO2 Utilization (Version 1.1)*. (2020).

22. Lai, C. S. & McCulloch, M. D. Levelized cost of electricity for solar photovoltaic and electrical energy storage. *Applied Energy* **190**, 191–203 (2017).

23. Taylor, M., Ralon, P. & Ilas, A. The power to change: solar and wind cost reduction potential to 2025. *International Renewable Energy Agency (IRENA)* (2016).

24. Association, U. E. I. Levelized Costs of New Generation Resources in the Annual Energy Outlook 2022. *US Department of Energy* (2022).

25. Darling, S. B., You, F., Veselka, T. & Velosa, A. Assumptions and the levelized cost of energy for photovoltaics. *Energy Environ. Sci.* **4**, 3133–3139 (2011).

26. CAISO. *What the duck curve tells us about managing a green grid*. (California Independent System Operator Folsom, CA, USA, 2016).

27. Ueckerdt, F., Hirth, L., Luderer, G. & Edenhofer, O. System LCOE: What are the costs of variable renewables? *Energy* **63**, 61–75 (2013).

28. Ela, E., Milligan, M. & Kirby, B. *Operating reserves and variable generation*. (2011).

29. Lucheroni, C. & Mari, C. Optimal Integration of Intermittent Renewables: A System LCOE Stochastic Approach. *Energies* **11**, 549 (2018).

30. Finnveden, G. *et al.* Recent developments in Life Cycle Assessment. *Journal of Environmental Management* **91**, 1–21 (2009).

31. Caduff, M., Huijbregts, M. A. J., Koehler, A., Althaus, H.-J. & Hellweg, S. Scaling Relationships in Life Cycle Assessment. *Journal of Industrial Ecology* **18**, 393–406 (2014).

32. Caduff, M., Huijbregts, M. A. J., Althaus, H.-J., Koehler, A. & Hellweg, S. Wind Power Electricity: The Bigger the Turbine, The Greener the Electricity? *Environ. Sci. Technol.* **46**, 4725–4733 (2012).

33. Caduff, M., Huijbregts, M. A. J., Althaus, H.-J. & Hendriks, A. J. Power-Law Relationships for Estimating Mass, Fuel Consumption and Costs of Energy Conversion Equipments. *Environ. Sci. Technol.* **45**, 751–754 (2011).

34. Bergesen, J. D. & Suh, S. A framework for technological learning in the supply chain: A case study on CdTe photovoltaics. *Applied Energy* **169**, 721–728 (2016).

35. Beltran, A. M. *et al.* When the Background Matters: Using Scenarios from Integrated Assessment Models in Prospective Life Cycle Assessment. *Journal of Industrial Ecology* **24**, 64–79 (2020).

36. Pizzol, M., Sacchi, R., Köhler, S. & Anderson Erjavec, A. Non-linearity in the Life Cycle Assessment of Scalable and Emerging Technologies. *Front. Sustain.* **1**, (2021).

37. Pfenninger, S., Hawkes, A. & Keirstead, J. Energy systems modeling for twenty-first century energy challenges. *Renewable and Sustainable Energy Reviews* **33**, 74–86 (2014).

38. Lopion, P., Markewitz, P., Robinius, M. & Stolten, D. A review of current challenges and trends in energy systems modeling. *Renewable and Sustainable Energy Reviews* **96**, 156–166 (2018).

39. Ringkjøb, H.-K., Haugan, P. M. & Solbrekke, I. M. A review of modelling tools for energy and electricity systems with large shares of variable renewables. *Renewable and Sustainable Energy Reviews* **96**, 440–459 (2018).

40. Lund, H. *et al.* Simulation versus Optimisation: Theoretical Positions in Energy System Modelling. *Energies* **10**, 840 (2017).

41. Mileva, A., Johnston, J., Nelson, J. H. & Kammen, D. M. Power system balancing for deep decarbonization of the electricity sector. *Applied Energy* **162**, 1001–1009 (2016).

42. Cole, W. J. *et al.* Quantifying the challenge of reaching a 100% renewable energy power system for the United States. *Joule* **5**, 1732–1748 (2021).

43. Jacobson, M. Z. *et al.* Impacts of Green New Deal Energy Plans on Grid Stability, Costs, Jobs, Health, and Climate in 143 Countries. *One Earth* **1**, 449–463 (2019).

44. Phadke, A. 2035: Plummeting Solar, Wind and Battery Costs can Accelerate our Clean Electricity Future; Goldman School of Public Policy. *University of California Berkeley: Berkeley, CA, USA* (2020).

45. Arvidsson, R. *et al.* Environmental Assessment of Emerging Technologies: Recommendations for Prospective LCA. *Journal of Industrial Ecology* **22**, 1286–1294 (2018).

46. Luderer, G. *et al.* Environmental co-benefits and adverse side-effects of alternative power sector decarbonization strategies. *Nature Communications* **10**, 5229 (2019).

47. Pehl, M. *et al.* Understanding future emissions from low-carbon power systems by integration of life-cycle assessment and integrated energy modelling. *Nature Energy* **2**, 939–945 (2017).

48. Arvesen, A., Luderer, G., Pehl, M., Bodirsky, B. L. & Hertwich, E. G. Deriving life cycle assessment coefficients for application in integrated assessment modelling. *Environmental Modelling & Software* **99**, 111–125 (2018).

49. De Almeida, A., Zissis, G., Quicheron, M. & Bertoldi, P. Accelerating the deployment of solid state lighting (SSL) in Europe. *Joint Research Center, European Union* (2013).

50. UNEP. *Accelerating the Global Adoption of Energy-Efficient Lighting*. http://united4efficiency.org/resources/accelerating-global-adoption-energy-efficient-lighting/ (2017).

51. Waide, P. *Phase Out of Incandescent Lamps: Implications for International Supply and Demand for Regulatory Compliant Lamps*. https://ideas.repec.org/p/oec/ieaaaa/2010-5-en.html (2010).

52. UNEP. *Achieving the Global Transition to Energy Efficient Lighting Toolkit*. https://www.thegef.org/publications/achieving-global-transition-energy-efficient-lighting-toolkit (2012).

53. Bardsley, N. *et al. Solid-State Lighting R&D Plan-2015*. (2015).

54. Penning, J., Stober, K., Taylor, V. & Yamada, M. Energy Savings Forecast of Solid-State Lighting in General Illumination Applications. *US Department of Energy, Tech. Rep., Sept* (2016).

55. Lim, S.-R., Kang, D., Ogunseitan, O. A. & Schoenung, J. M. Potential Environmental Impacts of Light-Emitting Diodes (LEDs): Metallic Resources, Toxicity, and Hazardous Waste Classification. *Environmental Science & Technology* **45**, 320–327 (2011).

56. UNEP. *Green Paper Policy Options to Accelerate the Global Transition to Advanced Lighting*. https://sustainabledevelopment.un.org/index.php?page=view&type=400&nr=1702&menu=1515 (2014).

57. Bauer, D. *et al.* US Department of Energy Critical Materials Strategy. (2011).

58. Ciacci, L., Vassura, I. & Passarini, F. Shedding Light on the Anthropogenic Europium Cycle in the EU–28. Marking Product Turnover and Energy Progress in the Lighting Sector. *Resources* **7**, 59 (2018).

59. Tan, Q., Li, J. & Zeng, X. Rare Earth Elements Recovery from Waste Fluorescent Lamps: A Review. *Critical Reviews in Environmental Science and Technology* **45**, 749–776 (2015).

60. Wu, Y., Yin, X., Zhang, Q., Wang, W. & Mu, X. The recycling of rare earths from waste tricolor phosphors in fluorescent lamps: A review of processes and technologies. *Resources, Conservation and Recycling* **88**, 21–31 (2014).

61. Wilburn, D. R. *Byproduct Metals and Rare-earth Elements Used in the Production of Light-emitting Diodes: Overview of Principal Sources of Supply and Material Requirements for Selected Markets*. (US Department of the Interior, US Geological Survey, 2012).

62. Setlur, A. A. Phosphors for LED-based Solid-State Lighting. *The Electrochemical Society Interface* 5 (2009).

63. Machacek, E., Richter, J. L., Habib, K. & Klossek, P. Recycling of rare earths from fluorescent lamps: Value analysis of closing-the-loop under demand and supply uncertainties. *Resources, Conservation and Recycling* **104**, 76–93 (2015).

64. Massari, S. & Ruberti, M. Rare earth elements as critical raw materials: Focus on international markets and future strategies. *Resources Policy* **38**, 36–43 (2013).

65. Mancheri, N. A. World trade in rare earths, Chinese export restrictions, and implications. *Resources Policy* **46**, 262–271 (2015).

66. Binnemans, K. *et al.* Rare-Earth Economics: The Balance Problem. *JOM* **65**, 846–848 (2013).

67. Binnemans, K., Jones, P. T., Müller, T. & Yurramendi, L. Rare Earths and the Balance Problem: How to Deal with Changing Markets? *Journal of Sustainable Metallurgy* **4**, 126–146 (2018).

68. Binnemans, K. *et al.* Recycling of rare earths: a critical review. *Journal of Cleaner Production* **51**, 1–22 (2013).

69. Cucchiella, F., D'Adamo, I., Lenny Koh, S. C. & Rosa, P. A profitability assessment of European recycling processes treating printed circuit boards from waste electrical and electronic equipments. *Renewable and Sustainable Energy Reviews* **64**, 749–760 (2016).

70. Solvay. *Loop Life Project*. https://www.solvay.com/en/innovation/open-innovation/european-life-projects/loop-life-project (2014).

71. SudOuest.fr. Closure of the Solvay Rare Earth Recycling Workshop by the End of 2016. https://www.sudouest.fr/2016/01/15/la-rochelle-fermeture-de-l-atelier-de-production-de-solvay-d-ici-fin-2016-2243998-1391.php (2016).

72. Innocenzi, V., De Michelis, I., Ferella, F. & Veglio, F. Rare earths from secondary sources: profitability study. *Advances in environmental research* **5**, 125–140 (2016).

73. Innocenzi, V., De Michelis, I. & Vegliò, F. Design and construction of an industrial mobile plant for WEEE treatment: Investigation on the treatment of fluorescent powders and economic evaluation compared to other e-wastes. *Journal of the Taiwan Institute of Chemical Engineers* **80**, 769–778 (2017).

74. Amato, A. *et al.* Sustainability analysis of innovative technologies for the rare earth elements recovery. *Renewable and Sustainable Energy Reviews* **106**, 41–53 (2019).

75. Melo, M. T. Statistical analysis of metal scrap generation: the case of aluminium in Germany. *Resources, Conservation and Recycling* **26**, 91–113 (1999).

76. Kleijn, R., Huele, R. & Van Der Voet, E. Dynamic substance flow analysis: the delaying mechanism of stocks, with the case of PVC in Sweden. *Ecological Economics* **32**, 241–254 (2000).

77. Brunner, P. H. & Rechberger, H. Practical handbook of material flow analysis. *The International Journal of Life Cycle Assessment* **9**, 337–338 (2004).

78. Müller, D. B. Stock dynamics for forecasting material flows—Case study for housing in The Netherlands. *Ecological Economics* **59**, 142–156 (2006).

79. Hatayama, H., Daigo, I., Matsuno, Y. & Adachi, Y. Outlook of the world steel cycle based on the stock and flow dynamics. *Environmental science & technology* **44**, 6457–6463 (2010).

80. Müller, E., Hilty, L. M., Widmer, R., Schluep, M. & Faulstich, M. Modeling Metal Stocks and Flows: A Review of Dynamic Material Flow Analysis Methods. *Environ. Sci. Technol.* **48**, 2102–2113 (2014).

81. Heidari, M., Majcen, D., van der Lans, N., Floret, I. & Patel, M. K. Analysis of the energy efficiency potential of household lighting in Switzerland using a stock model. *Energy and Buildings* **158**, 536–548 (2018).

82. Van der Voet, E., Kleijn, R., Huele, R., Ishikawa, M. & Verkuijlen, E. Predicting future emissions based on characteristics of stocks. *Ecological Economics* **41**, 223–234 (2002).

83. Song, R., Qin, Y., Suh, S. & Keller, A. A. Dynamic Model for the Stocks and Release Flows of Engineered Nanomaterials. *Environmental Science & Technology* **51**, 12424–12433 (2017).

84. Elshkaki, A., van der Voet, E., Timmermans, V. & Van Holderbeke, M. Dynamic stock modelling: A method for the identification and estimation of future waste streams and emissions based on past production and product stock characteristics. *Energy* **30**, 1353–1363 (2005).

85. Mandil, C. Light's labour's lost: policies for energy-efficient lighting. *Energy world* 14–15 (2006).

86. Ashe, M., Chwastyk, D., de Monasterio, C., Gupta, M. & Pegors, M. US lighting market characterization. *Washington DC.: US Department of Energy, Office of Energy Efficiency and Renewable Energy* (2010).

87. McKinsey & Company. *Lighting the way: perspectives on the global lighting market*. (McKinsey and Company London, 2012).

88. Walk, W. Forecasting quantities of disused household CRT appliances – A regional case study approach and its application to Baden-Württemberg. *Waste Management* **29**, 945–951 (2009).

89. Wang, F., Huisman, J., Stevels, A. & Baldé, C. P. Enhancing e-waste estimates: Improving data quality by multivariate Input–Output Analysis. *Waste Management* **33**, 2397–2407 (2013).

90. Castilloux, R. *Emerging End-Uses of REEs that Could Tranform the Market Prior to 2020*. http://www.techmetalsresearch.com/emerging-new-end-uses-for-rare-earths/ (2014).

91. Argote, L. & Epple, D. Learning Curves in Manufacturing. *Science* **247**, 920–924 (1990).

92. Moore, F. T. Economies of Scale: Some Statistical Evidence. *The Quarterly Journal of Economics* **73**, 232 (1959).

93. Jaber, M. Y. *Learning curves: Theory, models, and applications*. (CRC Press, 2016).

94. Bergesen, J. D. & Suh, S. A framework for technological learning in the supply chain: A case study on CdTe photovoltaics. *Applied Energy* **169**, 721–728 (2016).

95. Wright, T. P. Factors Affecting the Cost of Airplanes. *Journal of the Aeronautical Sciences* **3**, 122–128 (1936).

96. Gruber, H. The learning curve in the production of semiconductor memory chips. *Applied Economics* **24**, 885–894 (1992).

97. Irwin, D. A. & Klenow, P. J. Learning-by-Doing Spillovers in the Semiconductor Industry. *Journal of Political Economy* **102**, 1200–1227 (1994).

98. Hatch, N. W. & Mowery, D. C. Process innovation and learning by doing in semiconductor manufacturing. *Management Science* **44**, 1461–1477 (1998).

99. Kouvaritakis, N., Soria, A. & Isoard, S. Modelling energy technology dynamics: methodology for adaptive expectations models with learning by doing and learning by searching. *International Journal of Global Energy Issues* **14**, 104–115 (2000).

100. McDonald, A. & Schrattenholzer, L. Learning rates for energy technologies. *Energy Policy* **29**, 255–261 (2001).

101. Zeng, X., Mathews, J. A. & Li, J. Urban Mining of E-Waste is Becoming More Cost-Effective Than Virgin Mining. *Environmental Science & Technology* **52**, 4835–4841 (2018).

102. Beolchini, F. *et al.* Urban Miming: A Successful Experience of the EU-FP7 HYDROWEEE Project. *Environmental Engineering and Management Journal* 5 (2013).

103. Strauss, M. L. *The recovery of rare earth oxides fromwaste fluorescent lamps*. (Colorado School of Mines, 2016).

104. U.S. Geological Survey. *Mineral commodity summaries 2019: U.S. Geological Survey*. 200 p https://doi.org/10.3133/70202434. (2019).

105. Binder, K., Heermann, D., Roelofs, L., Mallinckrodt, A. J. & McKay, S. Monte Carlo simulation in statistical physics. *Computers in Physics* **7**, 156–157 (1993).

106. EU Commission. *Report on Critical Raw materials for the EU*. http://www.catalysiscluster.eu/wp/wp-content/uploads/2015/05/2014_Critical-raw-materials-for-the-EU-2014.pdf (2014).

107. Nassar, N. T., Du, X. & Graedel, T. E. Criticality of the Rare Earth Elements. *Journal of Industrial Ecology* **19**, 1044–1054 (2015).

108. Rollat, A., Guyonnet, D., Planchon, M. & Tuduri, J. Prospective analysis of the flows of certain rare earths in Europe at the 2020 horizon. *Waste Management* **49**, 427–436 (2016).

109. OECD. *Extended producer responsibility: A guidance manual for governments*. (Organisation for Economic Co-operation and Development, 2001).

110. Asari, M., Fukui, K. & Sakai, S.-I. Life-cycle flow of mercury and recycling scenario of fluorescent lamps in Japan. *Sci. Total Environ.* **393**, 1–10 (2008).

111. Fan, K.-S., Lin, C.-H. & Chang, T.-C. Management and performance of Taiwan's waste recycling fund. *Journal of the Air & Waste Management Association* **55**, 574–582 (2005).

112. Peng, L., Wang, Y. & Chang, C.-T. Recycling research on spent fluorescent lamps on the basis of extended producer responsibility in China. *Journal of the Air & Waste Management Association* **64**, 1299–1308 (2014).

113. Silveira, G. T. & Chang, S.-Y. Fluorescent lamp recycling initiatives in the United States and a recycling proposal based on extended producer responsibility and product stewardship concepts. *Waste Management & Research* **29**, 656–668 (2011).

114. Richter, J. L. & Koppejan, R. Extended producer responsibility for lamps in Nordic countries: best practices and challenges in closing material loops. *Journal of Cleaner Production* **123**, 167–179 (2016).

115. Williams, J. H. *et al.* The Technology Path to Deep Greenhouse Gas Emissions Cuts by 2050: The Pivotal Role of Electricity. *Science* **335**, 53–59 (2012).

116. Rogelj, J. *et al.* Energy system transformations for limiting end-of-century warming to below 1.5 C. *Nature Climate Change* **5**, 519 (2015).

117. Krey, V., Luderer, G., Clarke, L. & Kriegler, E. Getting from here to there – energy technology transformation pathways in the EMF27 scenarios. *Climatic Change* **123**, 369–382 (2014).

118. Frew, B. A., Becker, S., Dvorak, M. J., Andresen, G. B. & Jacobson, M. Z. Flexibility mechanisms and pathways to a highly renewable US electricity future. *Energy* **101**, 65–78 (2016).

119. Brick, S. & Thernstrom, S. Renewables and decarbonization: Studies of California, Wisconsin and Germany. *The Electricity Journal* **29**, 6–12 (2016).

120. Fernandes, L. & Ferreira, P. Renewable energy scenarios in the Portuguese electricity system. *Energy* **69**, 51–57 (2014).

121. Heal, G. Reflections—What Would It Take to Reduce U.S. Greenhouse Gas Emissions 80 Percent by 2050? *Rev Environ Econ Policy* **11**, 319–335 (2017).

122. Lund, H. & Mathiesen, B. V. Energy system analysis of 100% renewable energy systems—The case of Denmark in years 2030 and 2050. *Energy* **34**, 524–531 (2009).

123. Mathiesen, B. V., Lund, H. & Karlsson, K. 100% Renewable energy systems, climate mitigation and economic growth. *Applied Energy* **88**, 488–501 (2011).

124. MacDonald, A. E. *et al.* Future cost-competitive electricity systems and their impact on US $CO_2$ emissions. *Nature Climate Change* **6**, 526–531 (2016).

125. Jacobson, M. Z. *et al.* 100% clean and renewable wind, water, and sunlight (WWS) all-sector energy roadmaps for the 50 United States. *Energy Environ. Sci.* **8**, 2093–2117 (2015).

126. Jacobson, M. Z. *et al.* 100% Clean and Renewable Wind, Water, and Sunlight All-Sector Energy Roadmaps for 139 Countries of the World. *Joule* **1**, 108–121 (2017).

127. NREL. *LA100: The Los Angeles 100% Renewable Energy Study*. (National Renewable Energy Laboratory Golden, CO, USA, 2020).

128. Jacobson, M. Z., Delucchi, M. A., Cameron, M. A. & Frew, B. A. Low-cost solution to the grid reliability problem with 100% penetration of intermittent wind, water, and solar for all purposes. *Proceedings of the National Academy of Sciences* **112**, 15060–15065 (2015).

129. Iyer, G. *et al.* GCAM-USA analysis of US electric power sector transitions. *Richland, Washington: Pacific Northwest National Laboratory* (2017).

130. Iyer, G. *et al.* Measuring progress from nationally determined contributions to mid-century strategies. *Nature Clim Change* **7**, 871–874 (2017).

131. Larson, E. *Net-zero America: potential pathways, infrastructure, and impacts*. (Princeton University, 2020).

132. Williams, J. H. *et al.* Carbon-Neutral Pathways for the United States. *AGU Advances* **2**, e2020AV000284 (2021).

133. Bistline, J. E. T. & Blanford, G. J. Impact of carbon dioxide removal technologies on deep decarbonization of the electric power sector. *Nat Commun* **12**, 3732 (2021).

134. Brown, P. R. & Botterud, A. The Value of Inter-Regional Coordination and Transmission in Decarbonizing the US Electricity System. *Joule* **5**, 115–134 (2021).

135. Cohen, S. *et al.* Regional Energy Deployment System (ReEDS) Model Documentation: Version 2018. *National Renewable Energy Laboratory* 135 (2019).

136. NREL/ReEDS_OpenAccess. *GitHub* https://github.com/NREL/ReEDS_OpenAccess.

137. Center, B. P. Annual energy outlook 2020. *Energy Information Administration, Washington, DC* (2020).

138. Akar, S. *et al. 2020 Annual Technology Baseline (ATB) Cost and Performance Data for Electricity Generation Technologies*. (2020).

139. U.S. EPA. Technical Support Document:-Technical Update of the Social Cost of Carbon for Regulatory Impact Analysis-Under Executive Order 12866. *Environmental Protection Agency* (2016).

140. Pindyck, R. S. The social cost of carbon revisited. *Journal of Environmental Economics and Management* **94**, 140–160 (2019).

141. Bressler, R. D. The mortality cost of carbon. *Nat Commun* **12**, 4467 (2021).

142. Caldecott, B., Lomax, G. & Workman, M. Stranded carbon assets and negative emissions technologies. (2015).

143. Keith, D. W., Holmes, G., St. Angelo, D. & Heidel, K. A Process for Capturing CO2 from the Atmosphere. *Joule* **2**, 1573–1594 (2018).

144. Jayadev, G., Leibowicz, B. D. & Kutanoglu, E. US electricity infrastructure of the future: Generation and transmission pathways through 2050. *Applied energy* **260**, 114267 (2020).

145. Tapia-Ahumada, K. D., Reilly, J., Yuan, M. & Strzepek, K. Deep Decarbonization of the US Electricity Sector: Is There a Role for Nuclear Power. *Report 338* (2019).

146. Aghahosseini, A., Bogdanov, D., Barbosa, L. S. N. S. & Breyer, C. Analysing the feasibility of powering the Americas with renewable energy and inter-regional grid interconnections by 2030. *Renewable and Sustainable Energy Reviews* **105**, 187–205 (2019).

147. Oyewo, A. S., Aghahosseini, A., Ram, M. & Breyer, C. Transition towards decarbonised power systems and its socio-economic impacts in West Africa. *Renewable Energy* **154**, 1092–1112 (2020).

148. Jenkins, J. D., Luke, M. & Thernstrom, S. Getting to Zero Carbon Emissions in the Electric Power Sector. *Joule* **2**, 2498–2510 (2018).

149. Zappa, W., Junginger, M. & van den Broek, M. Is a 100% renewable European power system feasible by 2050? *Applied Energy* **233–234**, 1027–1050 (2019).

150. Baik, E. *et al.* What is different about different net-zero carbon electricity systems? *Energy and Climate Change* **2**, 100046 (2021).

151. McQueen, N. *et al.* Cost Analysis of Direct Air Capture and Sequestration Coupled to Low-Carbon Thermal Energy in the United States. *Environmental Science & Technology* **54**, 7542–7551 (2020).

152. McLaren, D. A comparative global assessment of potential negative emissions technologies. *Process Safety and Environmental Protection* **90**, 489–500 (2012).

153. Rogelj, J. *et al.* Scenarios towards limiting global mean temperature increase below 1.5 °C. *Nature Climate Change* **8**, 325–332 (2018).

154. Sanz-Pérez, E. S., Murdock, C. R., Didas, S. A. & Jones, C. W. Direct Capture of CO2 from Ambient Air. *Chem. Rev.* **116**, 11840–11876 (2016).

155. Bauer, N. *et al.* Global energy sector emission reductions and bioenergy use: overview of the bioenergy demand phase of the EMF-33 model comparison. *Climatic Change* **163**, 1553–1568 (2020).

156. Smith, P. *et al.* Biophysical and economic limits to negative CO2 emissions. *Nature Clim Change* **6**, 42–50 (2016).

157. Fuss, S. *et al.* Negative emissions—Part 2: Costs, potentials and side effects. *Environmental Research Letters* **13**, 063002 (2018).

158. Stucki, S., Schuler, A. & Constantinescu, M. Coupled CO2 recovery from the atmosphere and water electrolysis: Feasibility of a new process for hydrogen storage. *International Journal of Hydrogen Energy* **20**, 653–663 (1995).

159. Baciocchi, R., Storti, G. & Mazzotti, M. Process design and energy requirements for the capture of carbon dioxide from air. *Chemical Engineering and Processing: Process Intensification* **45**, 1047–1058 (2006).

160. Zeman, F. Energy and Material Balance of CO2 Capture from Ambient Air. *Environ. Sci. Technol.* **41**, 7558–7563 (2007).

161. Keith, D. W., Holmes, G., St. Angelo, D. & Heidel, K. A Process for Capturing CO2 from the Atmosphere. *Joule* **2**, 1573–1594 (2018).

162. Veselovskaya, J. V. *et al.* Direct CO2 capture from ambient air using K2CO3/Al2O3 composite sorbent. *International Journal of Greenhouse Gas Control* **17**, 332–340 (2013).

163. Lu, W., Sculley, J. P., Yuan, D., Krishna, R. & Zhou, H.-C. Carbon dioxide capture from air using amine-grafted porous polymer networks. *The Journal of Physical Chemistry C* **117**, 4057–4061 (2013).

164. Gebald, C., Wurzbacher, J. A., Tingaut, P., Zimmermann, T. & Steinfeld, A. Amine-Based Nanofibrillated Cellulose As Adsorbent for $CO_2$ Capture from Air. *Environ. Sci. Technol.* **45**, 9101–9108 (2011).

165. McDonald, T. M. *et al.* Capture of carbon dioxide from air and flue gas in the alkylamine-appended metal–organic framework mmen-Mg2 (dobpdc). *Journal of the American Chemical Society* **134**, 7056–7065 (2012).

166. Beuttler, C., Charles, L. & Wurzbacher, J. The Role of Direct Air Capture in Mitigation of Anthropogenic Greenhouse Gas Emissions. *Front. Clim.* **1**, (2019).

167. Chen, C. & Tavoni, M. Direct air capture of CO2 and climate stabilization: A model based assessment. *Climatic Change* **118**, 59–72 (2013).

168. Realmonte, G. *et al.* An inter-model assessment of the role of direct air capture in deep mitigation pathways. *Nat Commun* **10**, 3277 (2019).

169. Fuhrman, J. *et al.* The role of direct air capture and negative emissions technologies in the shared socioeconomic pathways towards $\mathplus$1.5 °C and $\mathplus$2 °C futures. *Environ. Res. Lett.* **16**, 114012 (2021).

170. de Jonge, M. M. J., Daemen, J., Loriaux, J. M., Steinmann, Z. J. N. & Huijbregts, M. A. J. Life cycle carbon efficiency of Direct Air Capture systems with strong hydroxide sorbents. *International Journal of Greenhouse Gas Control* **80**, 25–31 (2019).

171. Liu, C. M., Sandhu, N. K., McCoy, S. T. & Bergerson, J. A. A life cycle assessment of greenhouse gas emissions from direct air capture and Fischer–Tropsch fuel production. *Sustainable Energy & Fuels* **4**, 3129–3142 (2020).

172. McQueen, N., Desmond, M. J., Socolow, R. H., Psarras, P. & Wilcox, J. Natural Gas vs. Electricity for Solvent-Based Direct Air Capture. *Front. Clim.* **2**, (2021).

173. Terlouw, T., Treyer, K., Bauer, C. & Mazzotti, M. Life Cycle Assessment of Direct Air Carbon Capture and Storage with Low-Carbon Energy Sources. *Environ. Sci. Technol.* acs.est.1c03263 (2021) doi:10.1021/acs.est.1c03263.

174. Van Vuuren, D. P. *et al.* Energy, land-use and greenhouse gas emissions trajectories under a green growth paradigm. *Global Environmental Change* **42**, 237–250 (2017).

175. Stehfest, E., van Vuuren, D., Bouwman, L. & Kram, T. *Integrated assessment of global environmental change with IMAGE 3.0: Model description and policy applications*. (Netherlands Environmental Assessment Agency (PBL), 2014).

176. Riahi, K. *et al.* The shared socioeconomic pathways and their energy, land use, and greenhouse gas emissions implications: an overview. *Global Environmental Change* **42**, 153–168 (2017).

177. O'Neill, B. C. *et al.* The roads ahead: Narratives for shared socioeconomic pathways describing world futures in the 21st century. *Global Environmental Change* **42**, 169–180 (2017).

178. Van Vuuren, D. P. *et al.* The representative concentration pathways: an overview. *Climatic change* **109**, 5–31 (2011).

179. Tillman, A.-M. Significance of decision-making for LCA methodology. *Environmental Impact Assessment Review* **20**, 113–123 (2000).

180. Hospido, A., Davis, J., Berlin, J. & Sonesson, U. A review of methodological issues affecting LCA of novel food products. *Int J Life Cycle Assess* **15**, 44–52 (2010).

181. Rauner, S. *et al.* Coal-exit health and environmental damage reductions outweigh economic impacts. *Nature Climate Change* (2020) doi:10.1038/s41558-020-0728-x.

182. Mutel, C. Brightway: an open source framework for life cycle assessment. *Journal of Open Source Software* **2**, 236 (2017).

183. Wernet, G. *et al.* The ecoinvent database version 3 (part I): overview and methodology. *The International Journal of Life Cycle Assessment* **21**, 1218–1230 (2016).

184. Mulders, F. M. M., Hettelar, J. M. M. & Van Bergen, F. Assessment of the global fossil fuel reserves and resources for TIMER. *TNO Built Environment and Geosciences, Utrecht, The Netherlands* 98 (2006).

185. Rogner, H.-H. An assessment of world hydrocarbon resources. *Annual review of energy and the environment* **22**, 217–262 (1997).

186. De Vries, B. J., Van Vuuren, D. P. & Hoogwijk, M. M. Renewable energy sources: Their global potential for the first-half of the 21st century at a global level: An integrated approach. *Energy policy* **35**, 2590–2610 (2007).

187. Gernaat, D. E., Bogaart, P. W., van Vuuren, D. P., Biemans, H. & Niessink, R. High-resolution assessment of global technical and economic hydropower potential. *Nature Energy* **2**, 821–828 (2017).

188. Daioglou, V., Doelman, J. C., Wicke, B., Faaij, A. & van Vuuren, D. P. Integrated assessment of biomass supply and demand in climate change mitigation scenarios. *Global Environmental Change* **54**, 88–101 (2019).

189. Soest, H. van *et al.* A Global Roll-out of Nationally Relevant Policies Bridges the Emissions Ga. Preprint at https://doi.org/10.21203/rs.3.rs-126777/v1 (2021).

190. Koelbl, B. S., van den Broek, M. A., Faaij, A. P. C. & van Vuuren, D. P. Uncertainty in Carbon Capture and Storage (CCS) deployment projections: a cross-model comparison exercise. *Climatic Change* **123**, 461–476 (2014).

191. Broehm, M., Strefler, J. & Bauer, N. *Techno-Economic Review of Direct Air Capture Systems for Large Scale Mitigation of Atmospheric CO2*. https://papers.ssrn.com/abstract=2665702 (2015) doi:10.2139/ssrn.2665702.

192. Socolow, R. *et al. Direct air capture of CO2 with chemicals: a technology assessment for the APS Panel on Public Affairs*. (2011).

193. Koornneef, J., van Keulen, T., Faaij, A. & Turkenburg, W. Life cycle assessment of a pulverized coal power plant with post-combustion capture, transport and storage of CO2. *International Journal of Greenhouse Gas Control* **2**, 448–467 (2008).

194. Huijbregts, M. A. *et al.* ReCiPe2016: a harmonised life cycle impact assessment method at midpoint and endpoint level. *The International Journal of Life Cycle Assessment* **22**, 138–147 (2017).

195. Argote, L. & Epple, D. Learning Curves in Manufacturing. *Science* **247**, 920 (1990).

196. Junginger, M. & Louwen, A. *Technological Learning in the Transition to a Low-Carbon Energy System: Conceptual Issues, Empirical Findings, and Use, in Energy Modeling*. (Academic Press, 2019).

197. van der Giesen, C., Cucurachi, S., Guinée, J., Kramer, G. J. & Tukker, A. A critical view on the current application of LCA for new technologies and recommendations for improved practice. *Journal of Cleaner Production* 120904 (2020) doi:https://doi.org/10.1016/j.jclepro.2020.120904.

198. Bergerson, J. A. *et al.* Life cycle assessment of emerging technologies: Evaluation techniques at different stages of market and technical maturity. *Journal of Industrial Ecology* **24**, 11–25 (2020).

199. Baker, S. E. *et al. Getting to neutral: options for negative carbon emissions in California*. (2019).

200. *FACT SHEET: President Biden Sets 2030 Greenhouse Gas Pollution Reduction Target Aimed at Creating Good-Paying Union Jobs and Securing U.S. Leadership on Clean Energy Technologies*. https://www.whitehouse.gov/briefing-room/statements-releases/2021/04/22/fact-sheet-president-biden-sets-2030-greenhouse-gas-pollution-reduction-target-aimed-at-creating-good-paying-union-jobs-and-securing-u-s-leadership-on-clean-energy-technologies/ (2021).

201. Madhu, K., Pauliuk, S., Dhathri, S. & Creutzig, F. Understanding environmental trade-offs and resource demand of direct air capture technologies through comparative life-cycle assessment. *Nat Energy* **6**, 1035–1044 (2021).

202. Carbon Dioxide Emissions Coefficients by Fuel -U.S. Energy Information Administration (EIA). https://www.eia.gov/environment/emissions/co2_vol_mass.php (2021).

203. Kätelhön, A., Bardow, A. & Suh, S. Stochastic Technology Choice Model for Consequential Life Cycle Assessment. *Environmental Science & Technology* **50**, 12575–12583 (2016).

204. Kätelhön, A., von der Assen, N., Suh, S., Jung, J. & Bardow, A. Industry-Cost-Curve Approach for Modeling the Environmental Impact of Introducing New Technologies in Life Cycle Assessment. *Environmental Science & Technology* **49**, 7543–7551 (2015).

205. Qin, Y., Yang, Y., Cucurachi, S. & Suh, S. Non-linearity in marginal LCA: application of spatial optimization model. *Front. Sustain.* **2**, (2021).

206. de Jonge, M. M. J., Daemen, J., Loriaux, J. M., Steinmann, Z. J. N. & Huijbregts, M. A. J. Life cycle carbon efficiency of Direct Air Capture systems with strong hydroxide sorbents. *International Journal of Greenhouse Gas Control* **80**, 25–31 (2019).

207. Keith, D. W., Holmes, G., St. Angelo, D. & Heidel, K. A Process for Capturing CO2 from the Atmosphere. *Joule* **2**, 1573–1594 (2018).

208. Burr, A. & Cheatham, J. *Mechanical Design and Analysis*. (1995).

209. European Cement Research Academy (ECRA). ECRA CCS Project: Report on Phase IV.A (Technical Report). (2016).

210. Sharrcem - Titan Antea Cement. *Scaffolding inside the Pre-heater Cyclones & Calciner*. (2012).

211. American Physical Society (APS). *Direct Air Capture of $CO_2$ with Chemicals*. (2011).

212. Heidel, K. R. & Rossi, R. A. High Temperature Hydrator. (2017).

213. FEECO. Direct-Fired Rotary Kilns. https://feeco.com/rotary-kilns/ (2016).

214. Ebbenis, A. & Carlson, C. Everything You Need to Know on Rotary Kiln Refractory. https://feeco.com/everything-you-need-to-know-on-rotary-kiln-refractory/ (2020).

215. Shaul, S., Rabinovich, E. & Kalman, H. Generalized flow regime diagram of fluidized beds based on the height to bed diameter ratio. *Powder Technology* **228**, 264–271 (2012).

216. Cocco, R., Reddy, S. B. & Knowlton, K. T. *Back to Basics Introduction to Fluidization*. (2014).

217. American Institute of Steel Construction (AISC). *Structural Steel: An Industry Overview*. (2018).

218. Larsen, J., Herndon, W., Analyst, S. & Hiltbrand, G. *Capturing New Jobs: The employment opportunities associated with scale-up of Direct Air Capture (DAC) technology in the US*. (2020).

219. Home Advisor. 2020 Concrete Delivery Costs. https://www.homeadvisor.com/cost/outdoor-living/deliver-concrete/.

220. Wells, E. *Criticial materials requirements for petroleum refining*. (1966).

221. Canadian Fuels Association. *The Economics of Petroleum Refining into fuels and other value added products*. (2013).

222. National Academies of Sciences, E. *Negative emissions technologies and reliable sequestration: a research agenda.* (National Academies Press, 2018).

223. Weather Spark. Average Weather in Midland, Texas, United States, Year Round. https://weatherspark.com/y/4333/Average-Weather-in-Midland-Texas-United-States-Year-Round (2017).

224. Wurzbacher, J. A., Gebald, C. & Steinfeld, A. Separation of CO2 from air by temperature-vacuum swing adsorption using diamine-functionalized silica gel. *Energy Environ. Sci.* **4**, 3584 (2011).

225. Wilcox, J. *Carbon Capture*. (Springer, 2012).

226. Zeman, F. Reducing the cost of ca-based direct air capture of $CO_2$. *Environmental Science and Technology* **48**, 11730–11735 (2014).

227. National Academies of Sciences Engineering and Medicine (NASEM). *Negative Emissions Technologies and Reliable Sequestration: A Research Agenda*. *National Academies Press* (The National Academies Press, 2019).

228. McQueen, N. *et al.* A review of direct air capture (DAC): scaling up commercial technologies and innovating for the future. *Progress in Energy* (2021).

229. Kwon, H. T. *et al.* Aminopolymer-Impregnated Hierarchical Silica Structures: Unexpected Equivalent $CO_2$ Uptake under Simulated Air Capture and Flue Gas Capture Conditions. *Chemistry of Materials* **31**, 5229–5237 (2019).

230. What is direct air capture and storage? | Climeworks. https://climeworks.com/what-is-direct-air-capture-and-storage.

231. Thomson, R. C., Chick, J. P. & Harrison, G. P. An LCA of the Pelamis wave energy converter. *Int J Life Cycle Assess* **24**, 51–63 (2019).

232. Ahmad, L., Khordehgah, N., Malinauskaite, J. & Jouhara, H. Recent advances and applications of solar photovoltaics and thermal technologies. *Energy* **207**, 118254 (2020).

233. Rabaia, M. K. H. *et al.* Environmental impacts of solar energy systems: A review. *Science of The Total Environment* **754**, 141989 (2021).

234. Watson, S. *et al.* Future emerging technologies in the wind power sector: A European perspective. *Renewable and Sustainable Energy Reviews* **113**, 109270 (2019).

235. Aneke, M. & Wang, M. Energy storage technologies and real life applications – A state of the art review. *Applied Energy* **179**, 350–377 (2016).

236. Schmidt, O., Hawkes, A., Gambhir, A. & Staffell, I. The future cost of electrical energy storage based on experience rates. *Nat Energy* **2**, 1–8 (2017).

237. Fasihi, M., Efimova, O. & Breyer, C. Techno-economic assessment of CO2 direct air capture plants. *Journal of Cleaner Production* **224**, 957–980 (2019).

238. Karali, N., Park, W. Y. & McNeil, M. Modeling technological change and its impact on energy savings in the U.S. iron and steel sector. *Applied Energy* **202**, 447–458 (2017).

239. Gross, R. *et al.* Presenting the future: electricity generation cost estimation Methodologies. *UK Energy Research Centre (UKERC): London, UK* (2013).

240. Ferioli, F. & Van der Zwaan, B. C. C. *Learning in times of change: A dynamic explanation for technological progress*. (ACS Publications, 2009).

241. Nemet, G. F. Interim monitoring of cost dynamics for publicly supported energy technologies. *Energy Policy* **37**, 825–835 (2009).

242. Rubin, E. S., Azevedo, I. M. L., Jaramillo, P. & Yeh, S. A review of learning rates for electricity supply technologies. *Energy Policy* **86**, 198–218 (2015).

243. Roy, P.-O. *et al.* Characterization factors for terrestrial acidification at the global scale: A systematic analysis of spatial variability and uncertainty. *Science of The Total Environment* **500–501**, 270–276 (2014).

244. Helmes, R. J. K., Huijbregts, M. A. J., Henderson, A. D. & Jolliet, O. Spatially explicit fate factors of phosphorous emissions to freshwater at the global scale. *Int J Life Cycle Assess* **17**, 646–654 (2012).

245. Dong, Y., Rosenbaum, R. K. & Hauschild, M. Z. Assessment of Metal Toxicity in Marine Ecosystems: Comparative Toxicity Potentials for Nine Cationic Metals in Coastal Seawater. *Environ. Sci. Technol.* **50**, 269–278 (2016).